Inactivation, stabilization and redox regulation of iron-containing proteins

Promotor:	Dr. C. Veeger emeritus hoogleraar in de Biochemie
Co-promotor:	Dr. Ir. W.M.A.M. van Dongen universitair docent, vakgroep Biochemie

Inactivation, stabilization and redox regulation of iron-containing proteins

Johan H. Spee

Proefschrift
ter verkrijging van de graad van doctor
op gezag van de rector magnificus
van de Landbouwuniversiteit Wageningen,
dr. C. M. Karssen,
in het openbaar te verdedigen
op woensdag 10 september 1997
des namiddags te half twee in de Aula

The research described in this thesis was carried out at the Department of Biochemistry, Wageningen Agricultural University, the Netherlands. The investigations were supported by the Netherlands Foundation for Chemical Research (SON), with financial aid from the Netherlands Organization for Scientific Research (NWO).

ISBN 90-5485-753-6

NNO2 201, 2311

Stellingen

1. Haber-Weiss en Fenton reacties spelen een ondergeschikte rol bij de oxidatieve inactivering van heem-eiwitten.

   Hoofdstuk 1 van dit proefschrift.

2. Microperoxidases zijn stabieler in aanwezigheid van H_2O_2 wanneer de peptide-keten langer is, ongeacht of die peptide-keten deel uitmaakt van het microperoxidase.

   D.I. Metelitza, G.S. Arapova, R.A. Vidziunaite, M.V. Demcheva, A.V. Litvinchuck and V.I. Razumas (1994) Co-oxidation of phenol and 4-aminoantipyrine by microperoxidases and microperoxidase-protein complexes, *Biochemistry (Moscow) 9*, 949 - 958

3. Zuurstof oxideert bij relatief lage concentraties het Fe-eiwit zonder het te inactiveren, hierdoor initieert het zelf conformationele bescherming tegen oxidatieve inactivering die plaats vindt bij hogere zuurstof concentraties.

   R.N.F. Thorneley and G.A. Ashby (1989) Oxidation of nitrogenase by dioxygen without inactivation could contribute to high respiration rates of Azotobacter species and facilitate nitrogen fixation in other aerobic environments, *Biochem. J. 261*, 181 - 187

4. De conclusie van Charon et al. dat *enod40* dedifferentiatie en deling van corticale wortelcellen induceert in vlinderbloemigen kan niet uit het door de auteurs beschreven onderzoek worden getrokken.

   C. Charon, C. Johansson, E. Kondorosi, A. Kondorosi and M. Crespi (1997) *enod40* induces dedifferentiation and division of root cortical cells in legumes, *Proc. Natl. Acad. Sci.*, in press

5. Hemoglobine kan, door de katalyse van mono-oxygenase reacties, medicijnen modificeren die gericht zijn tegen pathogene organismen in het bloed, zoals de malaria parasiet *Plasmodium.*

   J.J. Mieyal and D.W. Starke (1994) Hydroxylation and dealkylation reactions catalyzed by hemoglobin, *Meth. Enzymol. 231*, 573 - 599

6. Het gebruik van NITROX (met zuurstof verrijkte luchtmengsels) maakt de duiksport niet veiliger; het gevaar voor stikstof-narcose maakt slechts plaats voor het gevaar voor zuurstof-vergiftiging.

7. Een promotieonderzoek heeft vele dimensies, waaronder één waarin goede hoop spoorloos kan verdwijnen.

8. Persoonlijke problemen kunnen tijdelijk worden opgelost in water.

Stellingen bij het proefschrift
Inactivation, stabilization and redox regulation of iron-containing proteins.

Johan H. Spee
Wageningen, 10 september 1997

I am but mad north-north-west;
when the wind is southerly I know a hawk from a handsaw.

(Hamlet)

aan Gieltje, voor alles.

Contents

Symbols and abbreviations

ADP	adenosine 5'-diphosphate
AlF	all forms of aluminum, fluoride and OH^- coordination
ATP	adenosine 5'-triphosphate
Av1	the tetrameric ($\alpha_2\beta_2$) MoFe protein of *A. vinelandii* nitrogenase
Av1αβ	one of two independently functioning halves of Av1
Av1·[Av2]$_2$	the Av1[Av2(MgADP)$_2$]$_2$ complex of *A. vinelandii* nitrogenase
Av2	the dimeric (γ_2) Fe protein of *A. vinelandii* nitrogenase
Av2 $_{inact.}$	the oxygen-inactivated Fe protein of *A. vinelandii* nitrogenase
A_x	absorbance at x nm
ΔA_x	change in absorbance at x nm
B	magnetic field strength
Δ_{xx}, Δ_{yy}, Δ_{zz}	principal elements of the line-width tensor
D	axial zero-field splitting parameter
Da	Dalton (gram mol^{-1})
DEAE	diethylaminoethyl
DMSO	dimethylsulfoxide
DNA	deoxyribonucleic acid
DTT	dithiothreitol
E	redox potential
E_h	poised redox potential
E_m	midpoint redox potential
EPR	electron paramagnetic resonance
ε_x	molar extinction coefficient at x nm
$\Delta\varepsilon_x$	change in molar extinction at x nm
Fe protein	the iron protein of nitrogenase
FeMoco	the iron-molybdenum-sulfur-homocitrate cofactor of nitrogenase
FeSII	the dimeric (δ_2) FeSII protein from *A. vinelandii*
FeSIIδ	one of two independently functioning halves of FeSII
FKBP	FK506 Binding Protein
g	gravitation
g	g-tensor
g_x, g_y, g_z	principal elements of the g-tensor
h	hour(s)
Hepes	*N*-[2-hydroxyethyl]piperazine-*N'*-[2-ethanesulfonic acid]
HPLC	high performance liquid chromatography
IPTG	isopropyl-β-*D*-thiogalactopyranoside
k	rate constant
kb	kilobase
k_{cat}	turnover number (V_{max} [Enzyme]$^{-1}$)
K_d	dissociation constant
kDa	kiloDalton (10^3 gram mol^{-1})
K_M	Michaelis constant

k_{obs}	observed rate constant
l	liter(s)
M	molar (mol liter^{-1})
min	minute(s)
MoFe protein	the molybdenum-iron protein of nitrogenase
MP#	microperoxidase #
NHE	normal hydrogen electrode
OD_x	optical density at x nm
ox	oxidized
PAGE	polyacrylamide gel electrophoresis
P-cluster	the [8Fe-7S] cluster of nitrogenase
P^0, P^{1+}, P^{2+}	the dithionite reduced, one and two electron oxidized P-cluster
PCR	polymerase chain reaction
P_i	monophosphate
PMS	*N*-methyl-dibenzopyrazine methylsulfate
PPIase	peptidylprolyl *cis-trans* isomerase
psi	pounds per square inch
RBS	ribosome binding site
red	reduced
rpm	rotations per minute
S	electron spin
s	second(s)
SDS	sodium dodecylsulfate
suc-AAPF-pNA	*N*-succinyl-Ala-Ala-Pro-Phe-*p*-nitroanilide
suc-AFPF-pNA	*N*-succinyl-Ala-Phe-Pro-Phe-*p*-nitroanilide
t	time
Tes	2-{[2-hydroxy-1,1-bis(2-hydroxymethyl)ethyl]amino}ethane-sulfonic acid
Tris	2-amino-2-hydroxymethylpropane-1,3-diol
TY	tryptone / yeast extract
v	reaction rate
V_{max}	maximal reaction rate (at infinite substrate concentration)
vol.	volume
χ''	EPR signal intensity (imaginary part of the magnetic susceptibility)
Xaa	any amino acid

Chapter 1

General introduction

1.1 Introduction

The importance of oxygen for biological systems.

Oxygen plays a key role in many of the important processes of life, such as respiration and metabolism, the means by which most organisms derive the energy needed to sustain life. On the basis of the requirement of oxygen for their metabolic processes, living organisms can be divided into two categories: aerobic organisms, that do require oxygen, and anaerobic organisms that do not require oxygen. To obligate anaerobic organisms oxygen is even toxic: they can't survive in its presence. The so called facultative anaerobic organisms fall in both categories: they can adapt their metabolism and live under both aerobic and anaerobic conditions. Both aerobic and anaerobic organisms can be autotrophic, using CO_2 as a carbon source, or heterotrophic, using organic materials, such as carbohydrates, as a carbon source. (for general introductions see [1] or [2])

Anaerobic organisms include photo-autotrophic organisms (such as *Rhodospirillales*) and chemo-autotrophic organisms (such as *Methanobacteriaceae*) in which CO_2 takes over the role that oxygen has in aerobic organisms, as well as a large number of heterotrophic organisms that use other inorganic substrates such as sulfate, nitrate and fumarate instead of oxygen.

Most aerobic organisms, which form the bulk of the biomass on earth, participate in the so called oxygen cycle (see [3] for a general introduction). Aerobic photo-autotrophic organisms, such as plants, algae and cyanobacteria, utilize light energy through photosynthesis to synthesize carbohydrates from CO_2 and H_2O while at the same time releasing O_2 into the atmosphere. Aerobic heterotrophic organisms, such as fungi, most animals and many bacteria, use a complex series of enzyme-catalyzed oxidation and reduction reactions using organic materials such as glucose as the initial reducing agent and O_2 as the terminal oxidizing agent. The end products of metabolism in these organisms are CO_2 and H_2O, which are returned to the atmosphere, thus completing the oxygen cycle. The autotrophes use oxygen in the same way as the heterotrophes do, but in the former organisms oxygen production exceeds oxygen consumption. Aerobic chemo-autotrophic bacteria use chemical energy, through the oxidation of inorganic substrates such as NH_4^+, Fe^{2+}, H_2S and H_2, to synthesize carbohydrates, without oxygen production.

The actual (heterotrophic) oxidation mechanism, called respiration, is not a direct chemical reaction but a series of electron transfers through a number of compounds that accept and release electrons, alternating between a reduced and an oxidized form, known as the 'oxidative phosphorylation' or 'respiratory chain'. Reducing power is generated through the reversible biochemical reactions of substances such as nicotinamide-adenine dinucleotide (NAD), flavins, and cytochromes which can exist in reduced and oxidized

forms. By participating in the respiratory chain, the reduced form is continually regenerated from the oxidized form. In aerobic organisms, the reductant NADH is the initial electron donor in the chain; as the strongest oxidizing agent, oxygen is the final electron acceptor. Its vital role in living organisms is essentially as a substance on which the last link in the chain, cytochrome *c* oxidase, can 'dump' electrons. The respiratory chain is coupled to ATP synthesis, the hydrolysis of which is the driving force for many of the biochemical processes that take place in living organisms [4], but besides the generation of ATP, oxygen is also used in biological systems for other purposes, such as the solubilization and detoxification of aromatic compounds [5] and as a source of oxygen atoms in the biosynthesis of various biomolecules in metabolic pathways [6].

The importance of iron for biological systems.

Iron is an essential mineral nutrient for all living organisms (except for a *Lactobacillus* that appears to maintain high levels of manganese instead of iron [7]), and is the most common transition metal in biology. The processes and reactions in which iron participates are numerous and crucial for the survival of organisms, and include DNA synthesis (ribonucleotide reductase [8]), energy production (cytochromes in the respiratory chain [9]), energy conversion (in connection with photosynthetic reaction centers [10]), oxygen transport (as a part of for instance hemoglobin and myoglobin [11]), oxygenation (detoxification of xenobiotics; e.g. cytochrome *P*-450 [12]), antioxidation (e.g. superoxide dismutase [13]), nitrogen fixation (as a part of all nitrogenase proteins [14]) and many other metabolic processes.

The redox properties of iron are essential for the reactions that are catalyzed by the enzymes that contain this metal. Iron is a transition element, so designated because its ions have partially filled *d*-orbitals, as a consequence of which it can form ions with different valencies. Although iron can exist in many redox states it is found in biological systems mainly as ferrous FeII iron (Fe^{2+}, d^6) and ferric FeIII iron (Fe^{3+}, d^5); in fewer cases as ferryl FeIV iron (Fe^{4+}, d^4). These ions have a maximal coordination number of 6, i.e. six ligands can bind the ion in a complex, but four- and particularly five-coordinate complexes are also encountered (section 1.2 and refs. herein). The possibility to transform from one redox state to the other, and vice versa, accounts for the biological usefulness of iron as an electron donor and acceptor, i.e. as a redox center. The redox potential of the electron transfer to and from the ion depends on the nature and geometry of the ligands that bind the iron to the protein, or to the cofactor that incorporates it, and on the protein environment of the metal-containing center [15, 16]. Ligand substitutions or modification, whether the result of the evolution of the protein, or caused instantaneously by, for instance, substrate-binding or protein-protein interactions (chapter 4 of this thesis) therefore further expands the applicability of iron in biological systems.

In the classification of metal ions in 'hard' and 'soft' acids [17], Fe^{3+} can be considered as almost a 'hard' acid, with a preference for ligands which are 'hard' bases, such as hydroxyl (tyrosine), carboxyl (aspartic acid and glutamic acid) and other oxygen-containing groups; still it does have a biologically affirmed affinity for sulfur ligands such as cysteine and nitrogen ligands such as porphyrin. Fe^{2+} is intermediate between a 'hard' and a 'soft' acid and can accommodate both the oxygen-based 'hard' ligands and 'soft' ligands containing nitrogen and sulfur; examples are histidine, cysteine, methionine, porphyrin and inorganic sulfur. All of the ligands mentioned here are encountered in iron-proteins [18]. In the case when one of the coordination spheres is unoccupied, the possibility exists of binding a sixth non-protein ligand, which may be O_2, H_2O, OH^-, a substrate molecule (e.g. aniline) or an inhibitor molecule (e.g. CO).

Iron in proteins is found in heme groups in which a single iron atom is bound to the N-atoms in the porphyrin of the heme moiety and to, mostly, histidine, methionine and cysteine residues; in iron-sulfur clusters in which the irons are bridged by sulfide and bound to the protein by, mostly, cysteines residues; in oxo-bridged di-iron centers and as a single iron-atom, bound directly to the protein, in which case the iron-binding residues are, for instance, cysteine, tyrosine, histidine and / or aspartate. On this basis, iron-containing proteins can be subdivided into four groups [19]:

I In the first group are the heme proteins, which include oxygen-carriers (like hemoglobin and myoglobin [11]), oxygen activators (like peroxidases [20, 21], cytochrome *c* oxidase [22] and cytochromes *P*-450 [12]) and electron-transfer heme proteins (like cytochromes [23]).

II Proteins that contain iron-sulfur clusters form the second group. Many of these proteins are strictly electron-transport proteins, like rubredoxins [24] and ferredoxins [25, 26]; in other cases electron-transfer is combined with catalytic activity, such as the reduction of N_2 by nitrogenase [27]. Of the iron-sulfur proteins only mitochondrial aconitase is known to have a solely catalytic function: the transformation of citrate to isocitrate in the citric acid cycle [28].

III The third group consists of proteins that directly bind a single iron atom, and includes some dioxygenases [29-31], monooxygenases [32-34] and bacterial superoxide dismutases [35] (all oxygen activators). Strictly speaking rubredoxins also fall into this group (discussed below).

IV Finally, the fourth group is formed by proteins containing oxo-bridged dinuclear iron centers (reviewed in [36]), including hemerythrin, ribonucleotide reductase, purple acid phosphatase and methane monooxygenase.

1.2 Redox enzymes: iron-sulfur and heme proteins.

Proteins that are involved in electron transfer reactions are generally known as redox proteins. Both its capability to bind a specific substrate and the value of its redox potential determine the function of a redox protein in a biological system. In principal, in the living cell, the limits for redox potentials (versus standard hydrogen electrode) are set by the redox couples H_2O / O_2 (+830 mV) and H_2 / H^+ (-420 mV) [37]; there are, nevertheless, proteins with higher and lower physiologically relevant redox potentials, such as CO dehydrogenase, an iron-sulfur-nickel protein with a redox potential of -540 mV [38], and lignin peroxidase, a heme protein for which a redox potential of +1.5 V has been reported for its high-valent iron-oxo intermediate [39]. A common property of all these proteins is the presence of a redox active group. Some contain an organic redox-active cofactor, like flavin or pyrroloquinone, others contain a transition metal, such as copper or iron (previous section), as a part of a cofactor that can accept and donate one or more electrons. Within the scope of this thesis only iron-containing redox proteins that have hemes or iron-sulfur clusters as cofactors will be discussed.

Iron-sulfur proteins.

Four 'basic' types of iron-sulfur clusters can be distinguished, that contain either one, two, three or four iron atoms (reviewed in [40]). Iron-sulfur clusters that have a more complex composition than these basic clusters, such as the clusters found in the nitrogenase MoFe protein, are usually referred to as 'superclusters'. The simplest form is

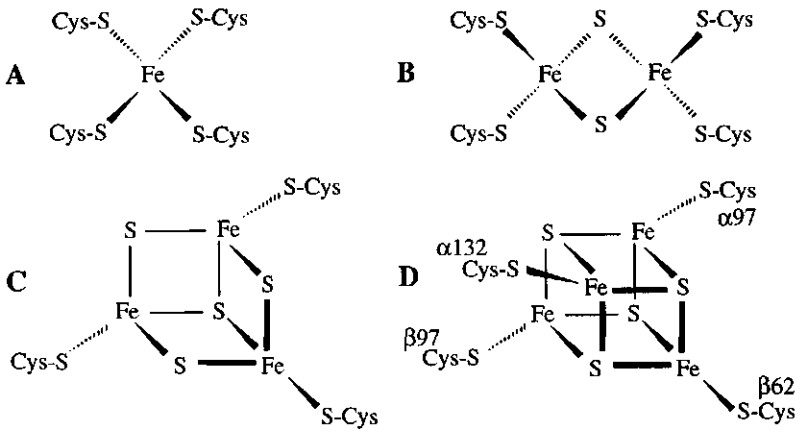

Figure 1

Schematic representation of basic iron-sulfur clusters. A: Rubredoxin-type mononuclear Fe-S cluster. B: Dinuclear [2Fe-2S] cluster. C: [3Fe-4S] partial cubane. D: The [4Fe-4S] cubane cluster of the nitrogenase Fe protein from *A. vinelandii.*

mononuclear iron as found in rubredoxin: a single iron atom tetrahedrally coordinated by the sulfur atoms of four cysteine residues that are part of the protein's peptide chain (Fig. 1A) [24]. Strictly speaking the rubredoxin-type of cluster is not a cofactor since the iron is bound directly, and only, to the protein. The other basic iron-sulfur clusters contain sulfide ions, the so called acid-labile sulfur, that are bound to the iron atoms in different stoichiometries, forming a proper core structure, or cluster, which is linked to cysteine residues [41] or, in some cases, to histidine residues [42] of the peptide chain. Clusters containing two iron atoms, [2Fe-2S], are found in ferredoxins and in many other enzymes, such as the 'Shethna' protein [43] which is a subject of this thesis. In these dinuclear type of clusters the two iron atoms are bridged by two acid-labile sulfur atoms and each iron atom is coordinated to the protein by two cysteine residues (Fig. 1B) [26, 44]. A special case is the [2Fe-2S] cluster in the so called 'Rieske'-type proteins, in which the iron atoms are coordinated by two cysteine residues and two histidine residues [45]. Clusters containing three iron atoms, [3Fe-4S], are also found in ferredoxins [46, 47], sometimes in combination with a separate four-iron [4Fe-4S] cluster, hence the designation 7Fe ferredoxins. A [3Fe-4S] cluster can be thought of as a [4Fe-4S] four-iron cluster with one iron missing (Fig. 1C). The [4Fe-4S] clusters, usually referred to as 'cubanes', have a cubical structure with acid-labile sulfurs on four of the corners of the cubical and iron atoms on the remaining four corners (Fig. 1D); the iron atoms are coordinated to the protein by cysteine residues [48]. Like [2Fe-2S] clusters, [4Fe-4S] clusters are very common in nature; they are found in numerous redox enzymes.

The nitrogenase of *Azotobacter vinelandii*, which is one of the major research subjects of this thesis, catalyzes the reduction of N_2 to NH_3 (see chapters 3 and 4 for the reaction mechanism, [27] for a review). The enzyme complex consists of two dissociable metallo-proteins. The Fe protein is a γ_2 homo-dimer that contains a single [4Fe-4S] cluster, coordinated by four cysteine residues; each of the subunits provides two of these

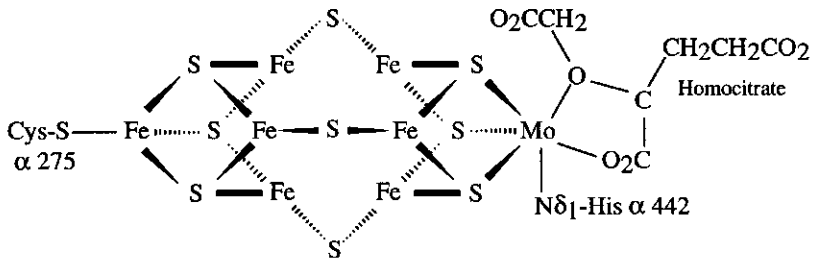

Figure 2

The iron-molybdenum cofactor. Schematic representation of the FeMoco cofactor of the nitrogenase MoFe-protein from *A. vinelandii*. [50]

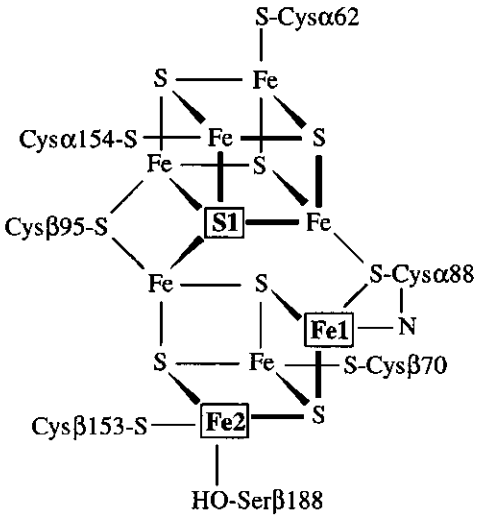

Figure 3

The P-cluster. Schematic representation of the oxidized form of the P-cluster of the nitrogenase MoFe protein from *A. vinelandii*. Upon reduction Fe1 and Fe2 exchange protein coordination by the amide N of Cys α88 and by Ser β188, respectively, for coordination by S1 [50].

residues, so that the [4Fe-4S] cluster bridges the gap between them [49] (Fig. 1D). The second protein, called the MoFe protein is an $\alpha_2\beta_2$ hetero-tetramer that contains two types of superclusters: two P-clusters, [8Fe-7S], and two M-clusters, or FeMoco cofactors, that contain molybdenum and homocitrate besides iron and sulfur. The FeMoco cofactors are presumably the substrate-binding site of the enzyme, i.e. the site where N_2 is bound and reduced to NH_3; the Fe protein provides the MoFe protein with the electrons that are required for this reduction. The structure of the P-cluster depends on its oxidation state. In the oxidized state it can best be described as a [4Fe-4S] cubane and a [4Fe-3S] partial cubane that are connected (Fig. 3) and bound to the α and β subunits, respectively, by six cysteines, serine β188 and the amide N of cysteine α88. Upon reduction of the cluster two Fe atoms (labeled 'Fe1' and 'Fe2' in the figure) of the [4Fe-3S] partial cubane change position and exchange protein coordination by serine β188 (Fe2) and the amide N of cysteine α88 (Fe1) for a ligand supplied by the central sulfur atom labeled 'S1'[50]. The FeMoco cofactors have an even more complex structure (Fig. 2) but can be interpreted, basically, as a dimer of XFe_3S_3 (X being Fe or Mo): partial cubanes linked by three non-protein sulfur ligands. Homocitrate is bound to the molybdenum in the cofactor. At least one cysteine and one histidine residue bind the cofactor to the protein [50].

Heme proteins.

The redox-centers in heme proteins are structurally very different from the iron-sulfur clusters. The heme cofactor consists of a protoporphyrin IX that contains a single iron atom; several heme groups may be present in a single heme protein. As is the case for iron-sulfur clusters, the ligands that bind the heme, and the surrounding peptide chain, largely determine the redox potential of the protein. The iron atom in the heme binds to the four equatorial nitrogens in the center of the protoporphyrin ring; in addition it can form two axial bonds on either side of the heme plane with amino acid residues from the protein chain and with external ligands (as mentioned above). These binding residues are referred to as the fifth and sixth ligand. Three types of hemes are distinguished: the *a*-type heme has a long phytyl 'tail' attached to the protoporphyrin and is found in e.g. cytochrome *c* oxydase; *b*-type hemes, found in e.g. cytochromes *b*, have two vinyl-groups attached to the porphyrin and are comparable to the heme in Fig. 4, except for the two thioether linkages that are formed between the vinyl-groups and cysteines residues in the protein, which are characteristic for the *c*-type hemes that are found in cytochromes *c*.

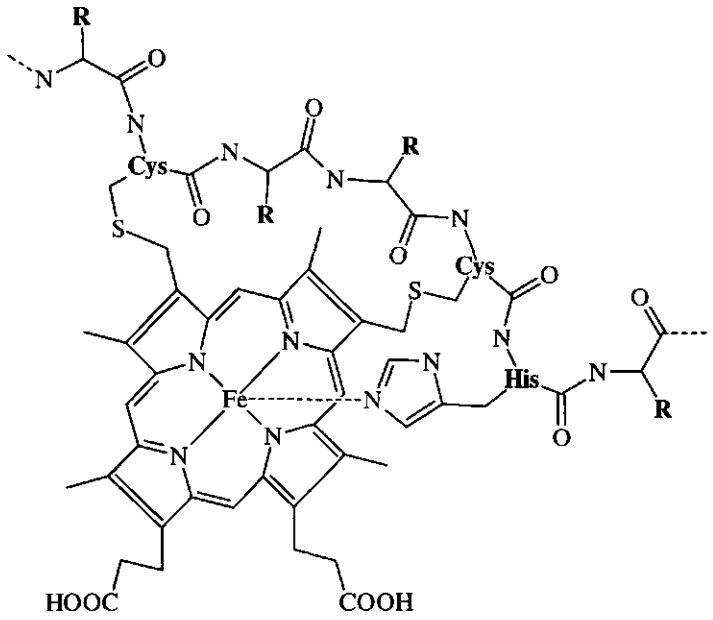

Figure 4

Schematic representation of a *c*-type heme. The N atoms in the porphyrin are the four equatorial ligands for the iron in its center. The axially coordinated histidine is the fifth ligand. In some proteins a sixth ligand is coordinated axially from the other side of the heme plane.

Cytochromes are typically classified on the basis of the heme type that is contained in the protein. The *c*-type cytochromes, one of the subjects of this thesis, are divided into three classes [51, 52]. The class I cytochromes *c*, found in a variety of eukaryotes and prokaryotes, contain axial histidine and methionine ligands. In class II cytochromes *c'*, found in photosynthetic bacteria, the heme is five-coordinate with only a histidine as the fifth ligand. Class III cytochromes c_3, found in a restricted class of sulfate-reducing bacteria, contain four hemes, each coordinated by two histidines.

The so called microperoxidases, that are the topic of chapter 2 of this thesis, are mini-enzymes that can be prepared by proteolytic digestion of cytochromes *c* [53]. As a consequence of the thioether links in cytochromes *c*, a short residual peptide chain remains bound to the heme after digestion. This peptide contains the motif Cys-$(Xaa)_2$-Cys-His, which includes the two heme-binding cysteines and histidine, the fifth ligand. The molecule shown in Fig. 4 can, in fact, be seen as a microperoxidase. Lack of a specific substrate-binding site enables these mini-enzymes to use a variety of substrates. They are able to catalyze peroxidase-type reactions as well as cytochrome *P*-450-type reactions and are used, as a model system, to study the catalytic mechanism of these reactions [54-56]. Cytochromes *P*-450, that contain a single five-coordinate *b*-type heme with cysteine as the fifth ligand, constitute a family of enzymes that play a key role in the oxidative and peroxidative biotransformation of a large variety of xenobiotic chemicals (detoxification) [5]. By using hydrogen peroxide in the oxidation of various organic and inorganic substrates, peroxidases function as antioxidants [20]. Peroxidases, for which the X-ray structures have been determined, contain a single five-coordinate *b*-type heme with histidine as the fifth ligand [57], or tyrosine, in the case of catalase [58].

1.3 The deleterious properties of oxygen.

Oxygen toxicity.

Although the oxidative power of oxygen can be controlled and efficiently converted to a form (ATP) that can be stored and subsequently used, aerobic metabolism has its disadvantages as well. The interior of a cell is a reducing environment, and many of the components are thermodynamically capable of reacting directly with dioxygen, thus bypassing, or damaging, the enzymes that control the beneficial reactions of dioxygen or other metabolic processes. Nitrogenase is an example of an enzyme that is particularly sensitive to oxygen-inactivation [59-61] (chapter 3 of this thesis). Although these reactions are generally slow and activation is often required, in aerobic cells reactions take place that produce small but significant amounts of partially reduced forms of dioxygen, especially superoxide anion ($O_2^{\bullet -}$), hydroxyl radical ($HO^{\bullet}$) and hydrogen

peroxide (H_2O_2) (Fig. 5) [18]; in addition to these reduced forms, also the chemically or photo-activated singlet $^1O_2$, represents a reactive, toxic form of oxygen [62]. All of these oxygen-species can carry out deleterious reactions with lipids, DNA and proteins being the major targets [63]. It is unknown how dioxygen initiates the sequence of chemical reactions that attack the biological targets in vivo; there is, however, no question that superoxide anion and hydrogen peroxide are formed during the normal course of aerobic metabolism [64, 65].

Superoxide anion can cause damage to proteins by itself [66], but the most commonly proposed mechanism for superoxide anion toxicity in relation to proteins containing transition metals is the so called 'Site Specific Haber-Weiss Reaction', which involves conversion of superoxide anion to oxygen and the generation of destructive hydroxyl radicals [67, 68] (Fig. 6). This mechanism is based on the idea that most reducing agents in the cell are too bulky to come into close proximity of sequestered oxidized metal ions, such as copper and iron, that are bound to proteins. Superoxide

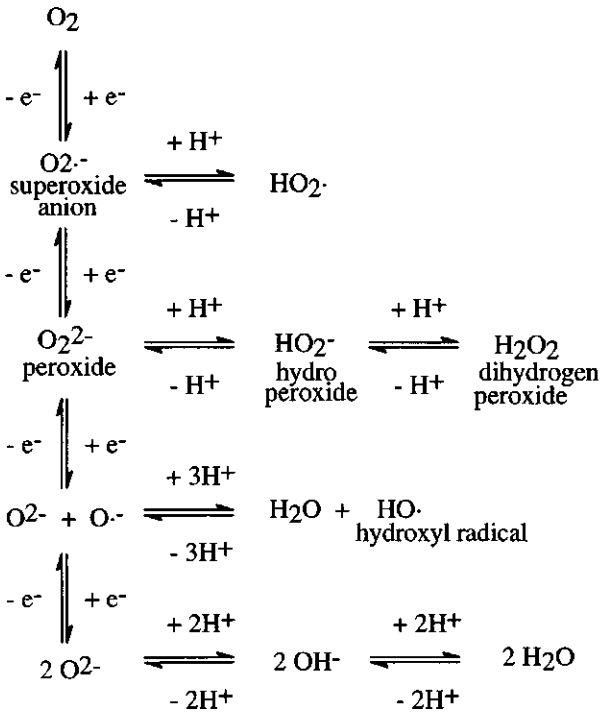

Figure 5

Formation of reactive oxygen species. Some of the reactions through which toxic intermediates can be formed from molecular oxygen. [18]

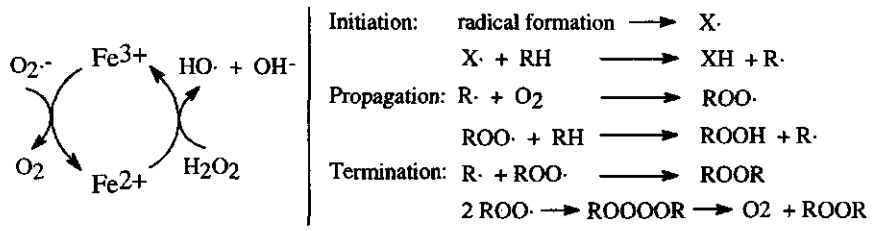

Figure 6

Left: **The Haber-Weiss reaction** ($Fe^{3+} \rightarrow Fe^{2+}$) **and the Fenton reaction** ($Fe^{2+} \rightarrow Fe^{3+}$).
Right: **The free-radical autoxidation mechanism.** R is any organic substrate. Not all possible oxidation products, such as ROH and others, are shown. HO•, formed through the Fenton reaction, on the left, can act as an initiator for this chain reaction. [79]

anion, however, in addition to being a powerful reducing agent, is very small and could penetrate the protein to reach these metal ions and reduce them. The reduced metal ions could then react with hydrogen peroxide (the Fenton reaction [69]), generating the hydroxyl radical, an extremely powerful and indiscriminate oxidant, which would immediately attack at a site near the location of the bound metal ion, thus damaging the protein or the metal-containing cofactor. In addition to this, the hydroxyl radical is an effective initiator of free-radical autoxidation reactions [70] in which dioxygen reacts with an organic substrate radical (Fig. 6). The highly reactive free radicals, produced by this mechanism, will indiscriminately react with vulnerable sites on enzymes, substrates and other cell components, causing serious damage. Oxygen free-radical attack on proteins yields many possible products [71 and refs. herein]: HO•, and possibly RO• intermediates of free-radical autoxidation, can cause cross-links within the protein or with other proteins; HO• and O_2•$^-$ can modify amino acid residues, especially methionine, tryptophan, histidine and cysteine; HO• in combination with O_2 can cause lesions, presumably by hydrolysis of peptide-bonds, especially those of proline residues, which may result in fragmentation of the protein; finally free radicals can cause specific disintegration of metal-containing cofactors (section 1.4). The consequence of these radical modifications is often inactivation of the enzyme.

Protection mechanisms.

In vivo, enzymatic and nonenzymatic antioxidants (scavengers) neutralize the harmful oxygen species (Fig. 7). Superoxide anion, for example, can be scavenged by superoxide dismutase (SOD), an enzyme present in all aerobic organisms, which catalyzes the conversion of two of these radicals into hydrogen peroxide and dioxygen [13]. Hydrogen peroxide formed by superoxide dismutase, and by the uncatalyzed reaction of hydroperoxy radicals, is scavenged by catalase, a heme protein that catalyzes the conver-

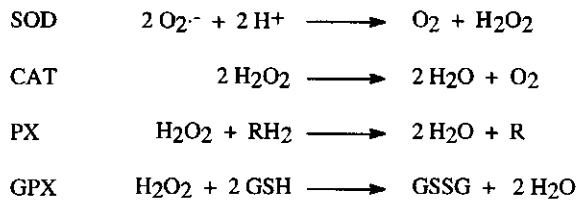

Figure 7

Reactions of enzymatic scavengers. SOD: superoxide dismutase; CAT: catalase; PX: peroxidase; GPX: glutathion peroxidase. R is an organic or inorganic substrate, GSH is glutathion (γ-Glu-Cys-Gly).

sion of hydrogen peroxide into water and dioxygen; peroxidases catalyze an analogous reaction in which H_2O_2 is reduced to water by various reducing substrates [20].
Examples of nonenzymatic oxidant scavengers are ascorbic acid (vitamin C) and α-tocopherol (vitamin E) [72]. Glutathion (GSH) can act as a nonenzymatic scavenger by itself or as the substrate of glutathion peroxidase, an enzymatic scavenger [73]. Finally, metal chelating proteins, such as ferritin, transferrin and lactoferrin, prevent the (not site-specific) Haber-Weiss reaction catalyzed by trace amounts of unsequestered, oxidized metal ions in the cell, an thus may, in this respect, also be considered to be a part of the group of nonenzymatic antioxidants [74, 75].

1.4 Inactivation of iron-containing proteins.

The reactions described above, which cause oxidative damage, are perfectly valid in vitro; in aqueous solutions the presence of both dioxygen and iron-proteins will result in the formation of superoxide anion. Oxy-hemoglobin and oxy-myoglobin are known to undergo a slow, spontaneous redox reaction in which the heme-iron is oxidized to the ferric form and the oxygen is reduced to superoxide anion [76, 77]. Also reduced ferredoxins, which contain iron-sulfur clusters, are subject to spontaneous oxidation which produces superoxide anion [78]. Once formed, superoxide anion will rapidly disproportionate in aqueous solution (except at very high pH) to form hydrogen peroxide and dioxygen [79]. Superoxide anion, hydrogen peroxide and trace amounts of free FeIII will result in Haber-Weiss and Fenton reactions that produce hydroxyl radicals. Furthermore, site-specific Haber-Weiss and Fenton chemistry can take place at the iron-containing centers in the proteins [80].

In the case of iron-sulfur and heme proteins site-specific damage can result in loss of the integrity of the iron-containing cofactor in the protein: free radicals will react with the metal-binding center, rather than escape from the site of their generation [80]. As

explained above, the amino acid residues, that are especially prone to modification by HO• and O_2•$^-$ (methionine, tryptophan, histidine and cysteine [81]) are all encountered as ligands in iron-proteins, but also the iron itself and the acid-labile sulfur atoms in iron-sulfur proteins may be involved in the disintegration of the cofactor [82].

It should be noted, however, that many iron-containing proteins are not affected by dioxygen and that oxidative inactivation does not always involve Haber-Weiss and Fenton reactions. In the case of iron-sulfur proteins, inactivation probably does involve Haber-Weiss and Fenton chemistry, but inactivation of heme proteins by oxygen seems to require the formation of high-valent FeIV-oxo compounds during catalysis, which by themselves, or through the generation of free radicals, cause degradation of the heme moiety. Both types of oxidative inactivation are discussed below.

Oxidative inactivation of iron-sulfur proteins

It was already noted decades ago that under non-reducing conditions, i.e. in the presence of oxidizing substances, some iron-sulfur proteins can be very unstable [83]. Wang and colleagues [60] demonstrated that after 1 minute exposure to 20% oxygen in argon the activity of the nitrogenase Fe protein from *A. vinelandii* was reduced to less than 20%. The authors also noticed loss of Fe from the protein which indicates that its [4Fe-4S] cluster is destroyed in the inactivation process. Although the actual mechanism of cluster disintegration is uncertain, it has been speculated that loss of electrons from the cluster, beyond a certain point, results in partial free radical formation at the bridging sulfurs and cysteine ligands, which is then followed by coupling reactions between free radicals and hydrolytic degradation of the oxidized center by solvent [82]. Upon oxidation of aconitase, its active [4Fe-4S] cluster is rapidly transformed to the inactive [3Fe-4S] form (a normal, reversible process for this enzyme), followed by a slower, total destruction of the cluster [84]; also a polysulfide-containing degradation product is formed [85]. Research on synthetic clusters has further confirmed that iron-sulfur clusters are easily destroyed by oxidation [86].

Recent studies on the in vivo inactivation of [4Fe-4S] containing dehydratases showed that superoxide anion can act as a potent oxidant of the iron-sulfur cluster; also in this case FeII was released from the cluster [87, 88]. Since superoxide anion acts as an oxidant towards ferrous iron in the cluster, rather than as a reductant towards ferric iron, at least in vivo, this inactivation does not occur through a Haber-Weiss-type of reaction.

$$O_2^{\cdot -} + 2H^+ + [2FeII\text{-}2FeIII\text{-}4S] \longrightarrow [FeII\text{-}3FeIII\text{-}4S] + H_2O_2$$

$$[FeII\text{-}3FeIII\text{-}4S] \longrightarrow [3FeIII\text{-}4S] + FeII$$

Figure 8

Oxidation of an [4Fe-4S] cluster by superoxide anion, according to Liochev [89].

The hypothetical, alternative reaction mechanism proposed by Liochev [89] is shown in Fig. 8. The product of this mechanism, H_2O_2, will next react normally according to the Fenton reaction with the FeII that is released from the cluster; consequently, also through this mechanism, HO• radicals are formed.

Iron-sulfur clusters are commonly found not only in anaerobic organisms, but also in aerobic organisms. Not all protein-bound iron-sulfur clusters are inactivated by oxygen. Those proteins that contain stable iron-sulfur clusters tend to share the common feature that the cluster is bound to a region of the protein that is inaccessible to solvent and oxidants. Recent studies on a bacterial [4Fe-4S] HiPIP protein from *Chromatium vinosum* have shown that modification of the binding pocket of the cluster, to become more hydrophilic, results in destabilization of the cluster, probably because oxidants dissolved in aqueous solution can gain access to the cluster [90]. This hypothesis is sustained by the fact that crystal structures of two of the oxygen-sensitive iron-sulfur proteins that were used as examples above, the nitrogenase Fe protein [49] and aconitase [91], show that the cluster is positioned on the surface of these proteins, i.e. exposed to the solvent. Furthermore, it has been demonstrated that in synthetic iron-sulfur clusters the polarity of the surrounding group is important to the stability of the cluster [86]. Evidence is given in chapter 3 of this thesis that complex formation of the nitrogenase Fe protein with the nitrogenase MoFe protein results in stabilization of the [4Fe-4S] cluster in the Fe protein. This may be the result of shielding of the cluster from the solvent solution or of stabilization of the cluster by the protein environment of the complex.

A final remark must be made about the fact that, in some cases, the interaction of oxygen with iron-sulfur clusters is not deleterious but even functional to an organism. It appears that at least in one situation, the FNR protein of *E. coli*, the loss of the integrity of the cluster in the presence of oxygen is the key to the sensing of oxygen levels (reviewed in [82]). Other proteins, which contain oxo-bridged iron centers, can even use oxygen as a substrate, such as methane monooxygenase [92] and ribonucleotide reductase [93].

Formation of FeIV-oxo compounds in heme proteins.

Interactions of oxygen with heme proteins are in general not destructive, and oxygen, or one of its partially reduced forms (see Fig. 5), is used as a substrate by many of the enzymes that contain a heme cofactor. For those heme proteins that do not interact with oxygen, such as the electron-transporting cytochromes *c*, X-ray structures show that the heme-iron is in some cases five-, but more often six-coordinate and buried in the interior of the protein, almost completely surrounded by the polypeptide chain, in an essentially hydrophobic environment [94]. In itself this does, however, not explain why these proteins are not inactivated by oxygen: the other heme proteins, oxygen carriers

and oxygen activators, possess an unoccupied sixth coordination site, situated within a pocket that is usually referred to as 'hydrophobic', but that has in fact a polar site around the central iron [79], often occupied by a water molecule, where dioxygen or hydrogen peroxide can bind, or where, in the case of cytochrome *P*-450, even iron-carbon or iron-nitrogen bonds with the substrate can be formed. In microperoxidases the protein environment is absent and the heme completely exposed to the solvent. Nevertheless, also these proteins are stable in the presence of oxygen. Apparently, different from what was observed for iron-sulfur proteins, the hydrophylicity of the heme-binding pocket, and consequently its accessibility for oxygen, does not make heme proteins susceptible to inactivation by oxygen. It seems therefore that oxygen, by itself, is not capable of causing damage to heme proteins. This may change, however, when the heme protein becomes catalytically active.

It is a well established fact that, in vitro, heme proteins possess various enzymatic activities, such as cytochrome *P*-450 [95] and peroxidase activities [96, 97]. In contrast to their stability in the presence of oxygen, hydrogen peroxide is known to cause oxidative damage to many heme proteins, including hemoglobins, myoglobins and cytochromes *c* [98-101], microperoxidases [102] and hemin [103]. Is seems therefore that oxidative inactivation of heme proteins requires the formation of reactive intermediates such as those formed during the catalysis of hydrogen peroxide-dependent reactions.

In the initial 'resting' state the heme-iron in oxygen activating enzymes is predominantly FeIII, probably with water as the sixth ligand (Fig 9). In the activated state (compound I and II) iron is present in the FeIV, ferryl, form. Microperoxidases, cytochromes *P*-450 and heme peroxidases go through these reactive intermediate states with such unusually high oxidation levels of the iron center [104-106]. In (micro)-peroxidases FeIV-oxo complexes can be formed by heterolytic or homolytic splicing of hydrogen peroxide; heterolytic splicing yields compound I, homolytic splicing yields compound II (Fig. 9). For the peroxidase reaction under physiological conditions, it is believed that the oxidation proceeds in one-electron steps, i.e. compound I is formed through heterolytic splicing of hydrogen peroxide and subsequent abstraction of an electron from the substrate yields compound II [20, 107, 108]. Formation of an FeIV-oxo compound in cytochrome *P*-450 involves reduction, by an external electron donor, of the FeII-O_2 compound in this enzyme, followed by heterolytic cleavage of the O-O bond, which yields H_2O and the FeIV-oxo compound I homologue (Fig. 9) [109, 110] (In cytochrome *P*-450 this compound has not yet been fully characterized, hence the designation 'homologue'). It is often assumed that the formation of a reactive FeIV-oxo heme group is, by itself, sufficient to initiate inactivation of heme proteins. This raises the question how cytochrome *P*-450 and peroxidases control the reaction mechanism of the oxy-heme group, favoring catalysis over inactivation.

The cysteine axial ligand in cytochrome *P*-450 is a strong electron donor and could therefore be responsible for the stabilization of the FeIV-oxo group [111]. In peroxidases the histidyl imidazole may deprotonate to form an imidazolate bond with the iron [112], or may be strongly hydrogen-bonded to the protein [113], thus serving a similar stabilizing function for the FeIV-oxo compounds. Compared to the cysteine ligand of the cytochrome *P*-450 system, however, histidine is certainly a weaker electron donor, which possibly effects a shift of the radical density from the iron-oxo compound to the porphyrin π system, as opposed to a shift to the sulfur of the cysteine ligand [114]. This difference in delocalization of valence electrons may contribute to the different reactivities for these enzymes [115]. But also the protein environments must be respon-

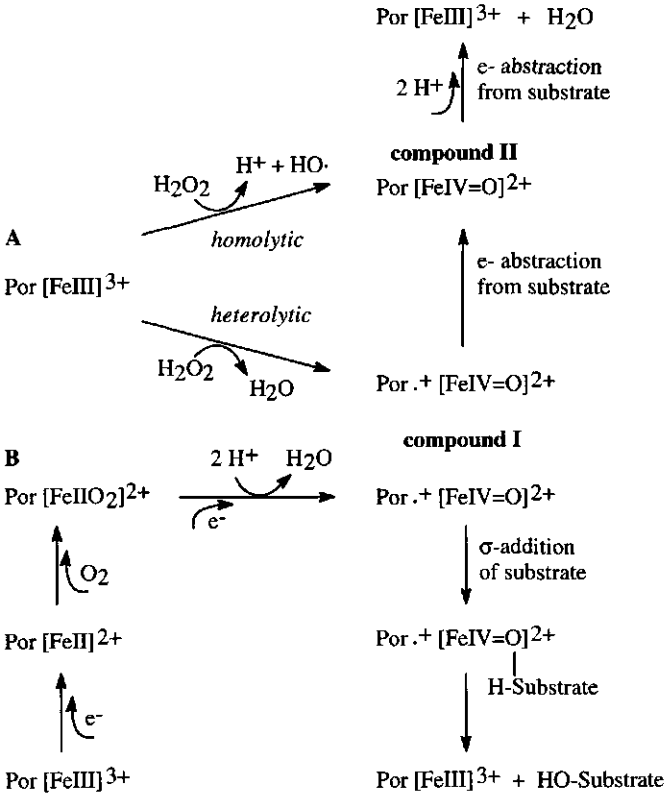

Figure 9

Catalytic mechanisms of microperoxidases and cytochrome *P*-450. A: Formation of compounds I and II and substrate oxidation in peroxidases. B: formation of the FeIV-oxo compound and substrate oxidation in cytochrome *P*-450. σ-addition occurs with aromatic substrates, but cytochrome *P*-450 can also catalyze other reactions. Note that the configuration of the FeIV-oxo compound in cytochrome *P*-450 is speculative, since it has not yet been fully characterized.

sible for such different reactivities: in cytochrome *P*-450 oxygen is transferred directly from the heme-iron to the substrate ('cage reaction'), while in peroxidases the protein environment does not allow the substrate to approach the heme-iron and electrons are abstracted from the substrate at the heme-*edge*. The substrate then reacts further in a non-catalyzed fashion with, for instance, solvent molecules, which may lead to the typical 'escape' of free radicals [101, 116].

Microperoxidases have both cytochrome P-450 features (the heme-iron is accessible to the substrate) and peroxidase features (the fifth ligand is histidine). The microperoxidase-catalyzed *para*-hydroxylation of aniline proceeds through a cytochrome *P*-450-type of σ-addition mechanism [117]. This mechanism involves the formation of a reaction intermediate in which the oxygen of compound I, formed as in peroxidases, is bound to the substrate, as in cytochrome *P*-450; upon dissociation of this intermediate, oxygen is transferred to aniline to form the hydroxylated product and the enzyme returns to its FeIII resting state (Fig. 9). Typical peroxidase reactions, which involve formation of compound II through electron abstraction, can also be catalyzed by microperoxidases (e.g. [54, 118]). However, the reactive FeIV-oxo compounds I or II can not be stabilized by a cysteine ligand, as was suggested for cytochrome *P*-450. Furthermore, the absence of the protein environment in microperoxidases, excludes the stabilization of the histidine ligand by hydrogen bonds, as in peroxidases, or any other form of control of the reaction. This may account for the rapid inactivation of these enzymes.

The hemes in myoglobin and hemoglobin are structurally comparable to those of peroxidases and cytochromes *P*-450. However, iron is present as FeII in the deoxy-form and to some degree as FeIII (in a semi FeIII-superoxo complex) in the oxy-form (proposed in [119]). In all cytochrome hemes the iron can alternate only between the reduced FeII and oxidized FeIII states and reactive FeIV-containing hemes are not found [120]. The catalytic properties of these proteins in the presence of hydrogen peroxide, however, indicate that under these conditions FeIV-oxo compounds can be formed; literature provides evidence for this [121-124]. This may explain why hydrogen peroxide causes oxidative damage to cytochromes, hemoglobins and myoglobins. In the presence of dioxygen formation of an FeIV-oxo compound from the FeIII-O_2 heme in hemoglobins and myoglobins is possible, but requires the presence of an external reductant, capable of donating an additional electron to the system to enable O-O bond cleavage, as for cytochrome *P*-450 [95]. Absence of such a reductant may be an important reason for the in vitro stability of hemoglobins and myoglobins in the presence of oxygen. Cytochromes are also capable of accepting electrons from external reductants; the shielding of the heme-iron from solvent and oxygen, by the hydrophobic pocket and / or its two axial amino acid ligands, may be the key to the stability of these proteins: when oxygen cannot bind to the heme-iron a reactive FeIV-oxo complex can not be formed.

Oxidative Inactivation of heme proteins.

Although the formation of FeIV-oxo compounds during catalytic activity seems to play an important role in the inactivation of heme proteins, the mechanisms of inactivation are largely unidentified. Several possible mechanisms are mentioned in literature:

I Oxidation of the fifth ligand (histidine), to form arginine, may occur, as has been observed for copper-histidinyl complexes [125]. Although oxidation of histidine, that is not coordinated to the heme-iron, has been reported in peroxide-treated myoglobin [126, 127], there is no conclusive evidence for the involvement of this process in inactivation.

II There is kinetic evidence for a 'substrate-involved' inactivation during the oxidation of various substrates by H_2O_2, using microperoxidase 8 as a catalyst [54]. Bleaching of the catalyst during substrate-involved inactivation is observed [54], and it has been suggested that the process proceeds through disintegration of the heme moiety of the microperoxidase [128], but other than that the mechanism remains unexplained.

III Metelitza et al. [129] report that microperoxidases can tolerate much higher concentration of hydrogen peroxide when equimolar amounts of human serum albumin or monoclonal antibodies against porphyrin are added to the reaction mixture. The authors ascribe this stabilization to the protection of the heme against destruction by free radicals.

IV The *meso* positions of the porphyrin ring play a central role in some of the proposed mechanisms for the degradation of hemes: oxidation at these positions and subsequent hydrolysis results in cleavage of the porphyrin (Fig. 10). For hemin the preferred site of oxidative attack appears to be the α-double bond [103], causing opening of the ring and loss of iron [99]. It has been proposed that H_2O_2 attack on cytochrome *c* also leads to opening of the porphyrin α-double bond [130]. Porphyrins are, as stated before, relatively resistant to oxidative damage and, like oxygen, hydrogen peroxide itself is not a sufficiently strong oxidant to cause cleavage of the α-methene bridge. The heme group must activate H_2O_2 to an oxygen species which is a much more powerful oxidant [98, 131]. Singlet oxygen, superoxide anion or free HO• radicals do not seem to be involved in the degradation of the heme of cytochrome *c*, since scavengers of these activated oxygen species have no effect on the degradation rate [130]. This points at a role for the FeIV-oxo compound in this degradation mechanism. A bound, reactive oxygen of this type could be shielded from large scavenger molecules, and could thus, unimpeded, carry out its attack on the porphyrin ring.

Microperoxidases lack such a shielding protein environment. Still, no effect of scavengers on the catalytic activity of microperoxidase 8 has been observed [117]. The P-450-type of σ-addition in the hydroxylation of aniline, mentioned above, was observed for microperoxidase 8 in the presence of ascorbic acid; this scavenger inhibits the

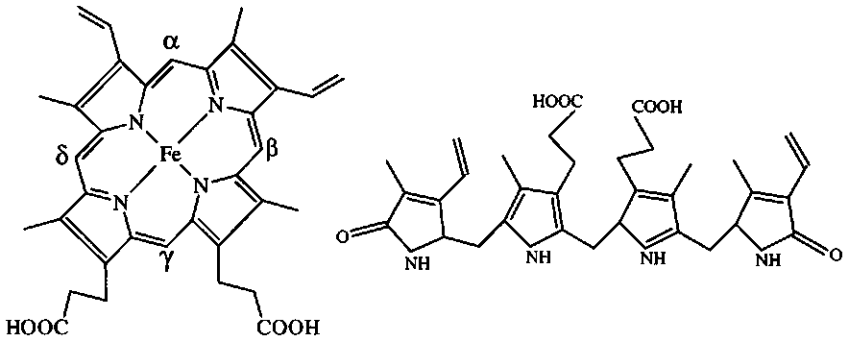

Figure 10

Degradation of heme. Left: Heme. α,β,γ and δ indicate the positions of the *meso* H-atoms. Right: The product of oxidative cleavage of heme at the α position: Biliverdin IX α. [103]

peroxidative pathway (electron abstraction, see Fig. 9) by reducing the oxidized substrate, rather than by scavenging compound II [117]. Therefore both compounds I and II are formed in the absence as well as in the presence of ascorbic acid. Possibly the oxidative attack on the α-methene bridge in the porphyrin, mediated by these FeIV-oxo compounds, proceeds very fast, and may thus escape reduction by scavengers.

V The meso positions in the porphyrin ring are also believed to be the sites where cross-linking can occur between peroxide-treated myoglobins [122]. The cross-links are probably formed by tyrosine residues, which has also been reported for the formation of cross-links in peroxide-treated leghemoglobin [132]. It is suggested that oxidation of a histidine yields a radical that is eventually transferred to a tyrosine residue. The tyrosine radical may next form a *meso* adduct with the porphyrin by a mechanism analogous to that for *meso* addition of radicals to the heme of horse-radish peroxidase [105, 133]: the radicals bind to a *meso* carbon of compound II with concomitant reduction of the iron from the ferryl to the ferric state. Elimination of a proton yields the *meso* adduct. The resulting oxidized FeIII heme has spectral properties that differ markedly from normal FeIII hemes and can not be reduced by dithionite or ascorbic acid, precluding any role for this adduct in redox reactions [122, 132].

Since the microperoxidases investigated in this thesis do not contain tyrosine residues, inactivation of these enzymes in this way can be ruled out. In earlier publications, however, it has been suggested that also the oxidized histidine can bind covalently to the heme [126, 127]. In the microperoxidases discussed here the only histidine is the fifth ligand, which is of vital importance for catalysis. Oxidation and subsequent *meso* adduction of this ligand to the porphyrin ring would undoubtedly result in inactivation of the enzyme.

VI An inactivation mechanism that specifically depends on the absence of a protective environment of the heme, and also involves the formation of FeIV-oxo compounds, is the formation of μ-oxo dimers (Fig. 11). Simple FeII-porphyrin complexes can react with O_2 to form FeIII-O_2^- complexes. These complexes can react rapidly with other FeII porphyrins, unless sterically prevented by the protein environment, to form binuclear peroxo-bridged complexes. These peroxo complexes are stable at low temperature, but when the temperature is raised the O-O bond cleaves and two equivalents of an FeIV-oxo compound II homologue are formed. Subsequent reactions between the FeIV-oxo complex and the FeII porphyrin complex produce the binuclear μ-oxo porphyrin dimer [134]. However, the formation of μ-oxo dimers probably does not play an important role in the inactivation of microperoxidases: amino acid residues of other microperoxidase molecules, or added substrate, may occupy the sixth coordination site and thus hinder the dimerization mechanism. Furthermore, the aerobically prepared microperoxidases contain predominantly FeIII heme, whereas μ-oxo dimerization requires FeII heme. Finally, the fact that it has been demonstrated that, at least at micromolar concentrations, microperoxidase 8 is essentially monomeric in aerobic aqueous solution [135] also argues against μ-oxo dimerization of microperoxidases.

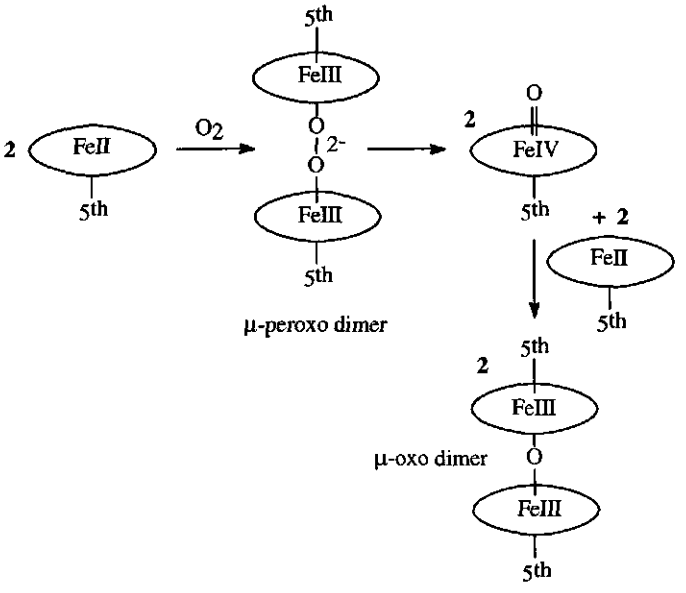

Figure 11

Formation of μ-oxo dimers from FeII porphyrin complexes. Ovals indicate the porphyrin ring; the 5th ligand is histidine in microperoxidases. [18]

1.5 Outline of this thesis.

The original goal set at the beginning of the research resulting in this thesis was the elucidation of the mechanism of biosynthesis of iron-sulfur clusters in iron-sulfur proteins. As a subject the nitrogenase Fe protein from *Azotobacter vinelandii* was chosen because the genes involved in the maturation of this protein, and possibly in the biosynthesis of the [4Fe-4S] clusters, had been identified previously (*nifM*, *nifS*, *nifU*) [136]. Soon after the start of the project the role of NifS as a cysteine desulfurase in the biosynthesis of the [4Fe-4S] clusters was elucidated by the group of Dr. D.R. Dean (Virginia Tech) [137, 138]. Also the investigation of NifU turned out to be in an advanced stage [139]. Our investigation of NifM is presented in chapter 5. The research did not result in a clue to the function of this protein, but did confirm the role of NifM in the maturation of the nitrogenase Fe protein. For the subsequent research a new goal was chosen, which is reflected in the title of this thesis.

Microperoxidases are so-called mini-enzymes, prepared by proteolytic digestion of cytochromes *c* [53]. Lack of a specific substrate-binding site enables these mini-enzymes to use a wide variety of substrates. They are able to catalyze peroxidase-like reactions [54, 118], as well as cytochrome *P*-450-like reactions, [55, 56]. A major drawback for the application of microperoxidases, for instance in industrial conversions, is their limited stability under reaction conditions: these enzymes are rapidly inactivated by hydrogen peroxide. Chapter 2 describes the preparation of microperoxidases, with increasing lengths of the peptide attached to the heme-moiety, by proteolytic digestion of horse-heart cytochrome *c* (microperoxidase 6, 8 and 11) and of cytochrome c_{550} from *Thiobacillus versutus* (microperoxidase 17). The kinetic properties of the different microperoxidases were analyzed with respect to their capability to catalyze the hydrogen peroxide-dependent *para*-hydroxylation of aniline, as well as the influence of the attached peptide chain on the stability.

Nitrogenase proteins are inactivated when they are exposed to oxygen (section 1.4) [59-61]. *Azotobacter vinelandii* produces a small protein, the FeSII protein, that can bind to nitrogenase, rendering it temporarily oxygen resistant [140]. In chapter 3 the mechanism by which the FeSII protein offers protection for the nitrogenase Fe protein against inactivation by oxygen is investigated. Based on the results a model that describes the reactions that are involved in this process, and a possible spatial organization of the nitrogenase-FeSII complex, that plays a key role in the protection of nitrogenase, are presented.

Nitrogenase catalyzed reduction of N_2 to NH_3 requires the association of the nitrogenase Fe protein with the nitrogenase MoFe protein, MgATP dependent electron transfer from the Fe protein to the MoFe protein and on-enzyme MgATP hydrolysis

followed by dissociation of the Fe-MoFe complex [141]. Aluminum fluoride plus MgATP or MgADP inhibits nitrogenase by stabilizing the protein-protein complex of an intermediate of the on-enzyme MgATP hydrolysis reaction [142]. Chapter 4 reports on the redox properties, obtained by redox titration and electron paramagnetic resonance (EPR) spectroscopy of the AlF-MgADP stabilized transition state complex of *Azotobacter vinelandii* nitrogenase. A possible mechanism of MgATP hydrolysis-driven electron transport within the nitrogenase protein complex, based on the results, is discussed.

References

1 Schlegel, H.G. (1993) *General microbiology*, 2nd edn., Cambridge University Press, London

2 Madigan, M.T., Martinko, J.M. and Parker, J. (1997) *Biology of microorganisms*, 8th edn., pp. 473 - 531, Prentice Hall International, London

3 Stryer, L. (1988) *Biochemistry*, 3rd edn., pp. 313 - 544, Freeman And Company, New York

4 Atkins, D.E. (1977) *Cellular energy metabolism and its regulation*, Academic Press, New York.

5 Guengerich, F.P. (1993) *American Scientist 81*, 440 - 447

6 Malstrom, B.G. (1982) *Annu. Rev. Biochem. 51*, 21 - 59

7 Neilands, J.B. (1974) in: *Microbial iron metabolism* (Neilands, J.B., Ed.) pp. 3 - 34, Academic Press, New York

8 Thelander, L. And Reichard, P. (1979) *Annu. Rev. Biochem. 48*, 133 - 158

9 Ferguson-Miller, S., Brantigan, D.L and Margoliash, E. (1979) in: *The porphyrins. Vol. VII* (Dolphin, D., Ed.) pp. 149, Marcel Dekker, New York.

10 Deisenhofer, J., Epp, O., Miki, K., Huber, R. and Michel, H. (1985) *Nature 318*, 618 - 624

11 Fermi, G. and Perutz, M.F. (1981) *Atlas of molecular structures in biology 2: Haemoglobin and myoglobin*, Clarendon Press, Oxford

12 Hasemann, C.A., Kurumbail, R.G., Buddupali, S.S., Petersen, J.A. and Deisenhofer, J. (1995) *Structure 15*, 41 - 62

13 Fridovich, I. (1986) *Advan. Enzymol. 58*, 61 - 97

14 Smith, B.E. and Eady, R.R. (1991) *Eur. J. Biochem. 205*, 1 - 15

15 Williams, R.J.P. (1982) *Pure Apl. Chem. 54*, 1889 - 1904

16 Hawker, P.N. and Twigg, M.V. (1987) in: *Comprehensive inorganic chemistry* (Wilkinson, G., Gillard, R.D. and McCleverty, J.A., Eds.) Pergamon Press, Oxford

17 Pearson, R.G. (1963) *J. Am. Chem. Soc. 85*, 3533 - 3539

18 Kaim,W. and Schwederski, B. (1994) *Bioinorganic chemistry: Inorganic elements in the chemistry of life*, Wiley & Sons, New York

19 Crighton, R.R. (1991) *Inorganic chemistry of iron metabolism*, Ellis Horwood, New York

20 Dunford, H.B. (1982) *Adv. Inorg. Biochem. 4*, 41 - 68

21 Dawson, J.H. (1988) *Science 240*, 433 - 439

22 Steffens, C.G.M., Soulimane, T., Wolff, G. and Buse, G. (1993) *Eur. J. Biochem. 213*, 1149 - 1157
23 Dickerson, R.E. (1972) *Sci. Amer. 226*, 58 -72
24 Wattenpaugh, K.D., Sieker, L.C. and Jensen, L.H. (1979) *J. Mol. Biol. 131*, 509 - 522
25 Matsubara, H. and Saeki, K. (1992) *Adv. Inorg. Chem. 38*, 223 - 280
26 Fukuyama, K, Hase, T, Matsumoto, S., Tsukihara, T., Katsube, Y., Tanaka, N., Kakudo, M., Wada, K. and Matsubara, H. (1980) *Nature 286*, 522 - 524
27 Howard, J.B. and Rees, D.C. (1994) *Annu. Rev. Biochem. 63*, 235 - 264
28 Kennedy, M.C., West, M., Telser, J., Emptage, M.H., Beinert, H. and Hoffmann, B.M. (1987) *Proc. Natl. Acad. Sci. USA 84*, 8854 - 8858
29 Ohlendorf, D.H., Weber, P.C. and Lipscomb, J.D. (1987) *J. Mol. Biol. 195*, 225 - 227
30 Kivirikko, K.I. and Myllyla, R. (1987) *Meth. Enzymol. 144*, 96 - 114
31 Hanauske-Abel, H.M. and Guntzler, V. (1982) *J. Theor. Biol. 94*, 421 - 455
32 Nozaki, M. (1974) in: *Molecular mechanisms of oxygen activation* (Hayaishi, O., Ed.) pp. 135 - 167, Academic Press, New York.
33 Pistorius, E.K., Axelrod, B. and Palmer, G. (1976) *J. Biol. Chem 251*, 7144 - 7148
34 Weisner, R., Hausdorf, G., Anton, M. and Rapoport, S. (1983) *Biomed. Biochim. Acta 42*, 431 - 436
35 Carlioz, A., Ludwig, M.L., Stallings, W.C., Fee, J.A., Steinman, H.M. and Touati, D. (1988) *J. Biol. Chem. 263*, 1555 - 1562
36 Lippard, S.J. (1988) *Angew. Chem. 27*, 344 - 361
37 Frausto da Silva, J.J.R., and Williams, R.J.P. (1991) *The biological chemistry of the elements*, Oxford University Press, Oxford.
38 Ragsdale, S.W and Riordan, C.G. (1996) *J. Biol. Inorg. Chem. 1*, 489 - 493
39 Kersten, P.J., Kalyanaraman, B., Hammel, K.E., Reinhammer, B. and Kirk, T.K. (1990) *Biochem.J. 268*, 475 - 480
40 Armstrong, W.H. (1988) *ACS Symp. Ser. 372*, 1 -27
41 Cammack, R.C. (1992) in: *Advances in inorganic chemistry, vol 38: Iron-Sulfur proteins*, (Cammack, R.C. and Sykes, A.G, Eds.) pp. 281 - 322, Academic Press, San Diego, Ca.
42 Link, T.A., Hagen, W.R., Pierik, A.J., Assman, C. and Von Jagow, G. (1992) *Eur. J. Biochem. 208*, 685 - 691
43 Moshiri, F., Crouse, B.R., Johnson, M.K. and Maier, R.J. (1995) *Biochemistry 34*, 12973 - 12982
44 Tsukihara,T., Fukuyama, K, Tahara, K., Katrube, Y., Matsu-ura, Y., Taneka, N., Kaludo, M., Wada, K. and Matsubara, H. (1978) *J. Biochem. 84*, 1645 - 1647
45 Iwata, S., Sanyovits, M., Link, T.A. and Michel, H. (1996) *Structure 4*, 567 - 579
46 Stout, G.H., Turley, S., Sieker, L.C. and Jensen, L.H. (1988) *Proc. Natl. Acad. Sci. USA 85*, 1020 - 1022
47 Stout, C.D. (1988) *J. Biol. Chem. 263*, 9256 - 9260
48 Adman, E.T., Sieker, L.C. and Jensen, L.H. (1973) *J. Biol. Chem. 248*, 3987 - 3996
49 Georgiades, M.M., Komiya, H., Chakrabarti, P., Woo, D., Kornuc, J.J and Rees, D.C. (1992) *Science 257*, 1653 - 1659
50 Peters, J.W., Stowell, M.H.B., Soltis, M., Finnegan, M.G., Johnson, M.K. and Rees, D.C. (1997) *Biochemistry 36*, 1181 - 1187
51 Palmer, G. and Reedijk. J. (1991) *Eur. J. Biochem. 200*, 599 - 611
52 Amber, R.P. (1980) in: *From cyclotrons to cytochromes* (Robinson, A.B. and Kaplan, N.D., Eds.) pp. 263 - 279, Academic Press, New York

53 Harbury, H.A., Cronin, J.R., Franger, M.W., Hettinger, T.P., Murphy, A., Meyer, A.J. and Vinogradov, S.N. (1965) *Proc. Natl. Acad. Sci. USA 54*, 1658 - 1664
54 Cunningham, I.D., Bachelor, J.L. and Pratt, J.M. (1991) *J. Chem. Soc. Perkin Trans. 2*, 1839 - 1843
55 Rusvai, E., Vegh, M., Kramer, M., Horvath, I. (1988) *Biochem. Pharmacol. 37*, 4574 - 4577.
56 Nakamura, S., Mashino, T., Hirobe, M. (1992) *Tetrahedron Lett. 33*, 5409 - 5412.
57 Poulos, T.L. and Kraut, J. (1980) *J. Biol. Chem.* 225, 8199 - 8205
58 Fita, I. and Rossmann, M.G. (1985) *J. Mol. Biol. 185*, 21 - 37
59 Veeger, C., Laane, G., Scherings, G., Matz, L, Haaker, H. and Van Zeeland-Wolbers, L. (1980) in: *Nitrogen Fixation* (Newton W.E. and Orme-Johnson W.H. Eds.) vol. I, pp. 111-137, University Park Press, Baltimore.
60 Wang, Z.C., Burns, A. and Watt, G.D. (1985) *Biochemistry 24*, 214-221
61 Robson, R.L. (1979) *Biochem. J. 181*, 569 - 575.
62 Foote, C.S. (1982) in: *Pathology of oxygen* (Autor, A.P., Ed.) pp. 21 - 44, Academic Press, New York
63 Halliwell, B. and Gutteridge, J.M.C. (1989) *Free radicals in biology and medicine*, 2nd edn., Clarendon Press
64 Imlay, J.A. and Fridovic, I. (1991) *J. Biol. Chem. 266*, 6957 - 6965
65 Fridovich, I. (1978) *Science 201*, 875 - 880
66 Fridovich, I. (1986) *Arch. Biochem. Biophys. 247*, 1 - 11
67 Korbashi, P. (1989) *J. Biol. Chem. 264*, 8479 - 8482
68 Stadtmann, E.R. (1990) *Free Rad. Biol. Med. 9*, 315 - 325
69 Sutton, H.C. and Winterbourn, C.C. (1989) *Free Rad. Biol. Med. 6*, 53 - 60
70 Sheldon, R.A. and Kochi, J.K. (1981) *Metal-catalyzed oxydations of organic compounds*, Academic Press, New York
71 Wolff, S.P., Garner, A. and Dean, R.T. (1986) *Trends. Biol. Sci. 11*, 27 - 31
72 Machlin, L.J. and Bendich, A. (1987) *FASEB J. 1*, 441 - 445
73 Meister, A. and Anderson, M.E. (1983) *Annu. Rev. Biochem. 52*, 711 - 760
74 Winterbourn, C.C. (1981) *Biochem. J. 198*, 125 - 131
75 Buege, J.A. and Aust, S.D. (1978) *Meth. Enzymol. 52*, 302 - 310
76 Gotoh, T. and Shikama, K. (1976) *J. Biochem. 80*, 397 - 399
77 Misra, H.P. and Fridovich, I. (1972) *J. Biol. Chem. 247*, 6960 - 6962
78 Misra, H.P. and Fridovich, I. (1971) *J. Biol. Chem. 246*, 6886 - 6890
79 Bertini, I., Gray, H.B, Lippard, S. and Valentine, J. (1994) *Bioinorganic chemistry*, University Science Books, Mill Valley, California
80 Floyd, R.A. (1990) *FASEB J. 4*, 2587 - 2597
81 Many articles in: (1984) *Meth. Enzymol. 105*
82 Rouault, T.A. and Klausner, R.D. (1996) *Trends. Biol. Sci. 21*, 174 - 177
83 Petering, D., Fee., J.A. and Palmer G. (1971) *J.Biol. Chem. 246*, 643 - 653
84 Kennedy, M.C., Emptage, M.H., Dreyer, J.L. and Beinert, H. (1983) *J. Biol. Chem. 258*, 11098 - 11105
85 Kennedy, M.C. and Beinert, H. (1988) *J. Biol. Chem. 263*, 8194 - 8198
86 Ciurli, S., Carrié, M., Weigel, J.A., Carney, M.J., Stack, T.D.P., Papoefthymiou, G.C. and Holm, R.A. (1990) *J. Am. Chem. Soc. 112*, 2654 - 2664
87 Flint, D.H., Tuminello, J.F. and Emptage, M.H. (1993) *J. Biol. Chem. 268*, 22369 - 22376
88 Liochev, S.I. and Fridovich, I. (1994) *Free Rad. Biol. Med. 16*, 29 - 33
89 Liochev, S.I. (1996) *Free Rad. Res. 25*, 369 - 384

90 Agarwal, A., Li, D. and Cowan, J.A. (1995) *Proc. Natl. Acad. Sci. USA 92*, 9440 - 9444
91 Robbins, A.H. and Stout, C.D. (1989) *Proc. Natl. Acad. Sci. USA 86*, 3639 - 3643
92 Green, J. and Dalton, H. (1989) *J. Biol. Chem. 264*, 17698 - 17703
93 Reichard, P. and Ehrenberg, A. (1983) *Science 221*, 514 - 519
94 Meyer, T.E and Kamen, M.D. (1982) *Adv. Prot. Chem. 35*, 105 - 212
95 Mieyal, J.J. and Starke, D.W. (1994) *Meth. Enzymol. 231*, 573 - 599
96 Everse, J., Johnson, M.C. and Marini, M.A. (1994) *Meth. Enzymol. 231*, 547 - 561
97 Adams, P.A. and Louw, J. (1995) *J. Chem. Soc. Perkin Trans. 2*, 1683 - 1690
98 Rice, R.H., Lee, Y.M. and Brown, W.D. (1983) *Arch. Biochem. Biophys. 221*, 417 - 427
99 Brown, S.P., Hatzikonstantinou, H. and Herries, D.G. (1978) *Biochem. J. 174*, 901 - 907
100 Ortiz de Montellano, P.R., Choe, S.Y., Depillis, G. and Catalano, E.C. (1987) *J. Biol. Chem. 262*, 11641 - 11646
101 Ortiz de Montellano, P.R. (1992) *Annu. Rev. Pharmacol. Toxicol. 32*, 89 - 107
102 Spee, J.H., Boersma, M.G., Veeger, C., Samyn, B., Van Beeumen, J., Warmerdam, G., Canters, G.W., Van Dongen, W.M.A.M. and Rietjens, I.M.C.M. (1996) *Eur. J. Biochem. 241*, 215 - 220.
103 Bonnett, R and McDonagh, A.F. (1973) *J. Chem. Soc. Perkin Trans 1*, 881 - 888
104 Cunningham, I.D. and Snare, G.R. (1992) *J. Chem. Soc. Perkin Trans. 2*, 2019 - 2023
105 Ortiz de Montellano, P.R. (1987) *Acc. Chem. Res. 20*, 289 - 294
106 Groves, J.T. and Watanabe, Y. (1988) *J. Am. Chem. Soc. 110*, 8443 - 8452
107 George, P. (1952) *Nature 169*, 612 - 613
108 Everse, J., Everse, K.E. and Grisham, M.B. (1991) *Peroxidases in chemistry and biology*, CRC Press
109 Larroque, C., Lange, R., Maurin, L., Bienvenue, A. and Van Lier, J.E. (1990) *Arch. Biochem. Biophys. 282*, 198 - 201
110 Guengerich, F.P., and MacDonald, T.L. (1990) *FASEB J. 4*, 2453 - 2459
111 Champion, P.M. (1989) *J. Am. Chem. Soc 111*, 3433 - 3434
112 Quinn, R, Nappa, M. and Valentine, J.S (1982) *J. Am. Chem. Soc. 104*, 2588 - 2595
113 Quinn, R. (1984) *J. Am. Chem. Soc. 106*, 4136 - 4144
114 Rietjens. I.M.C.M, Osman, A.M., Veeger, C., Zakharieva, O., Antony, J., Grodzicki, M. and Trautwein, A.X. (1996) *J. Biol. Inorg. Chem. 1*, 372 - 376
115 Weiss, R., Mandon, D., Wolter, T., Trautwein, A.X., Munther, M., Eckhard, B., Gold, A., Jayaraj, K. and Terner, J. (1996) *J. Biol. Inorg. Chem. 1*, 377 - 383.
116 Poulos, T.L. (1995) *Curr. Opin. Struct. Biol. 5*, 767 - 774
117 Osman, A.M., Koerts, J., Boersma, M.G., Boeren, S., Veeger, C. and Rietjens, I.M.C.M. (1996) *Eur. J. Biochem. 240*, 232 - 238
118 Baldwin, D.A., Marques, M. and Pratt, J.M. (1987) *Proc. Natl. Acad. Sci. USA 54*, 1658 - 1664
119 Vaska, L. (1976) *Acc. Chem. Res. 9*, 175 - 183
120 Williams, R.J.P. (1985) *Eur. J. Biochem. 150*, 231 - 248
121 Brittain, T., Little, R.H., Greenwood, C. and Watmough, N.J. (1996) *FEBS Lett. 399*, 21 - 25
122 Catalano, C.E., Choe, Y.S. and Ortiz de Montellano, P.R. (1989) *J. Biol. Chem. 18*, 10534 - 10541
123 Aviram, I., Wittenberg, B.A. and Wittenberg, J.B. (1978) *J. Biol. Chem. 253*, 5685 - 5689
124 Giulivi, C. and Cadenas, E. (1994) *Meth. Enzymol. 233*, 189 - 202

125 Cooper, B., Creeth, J.M. and Donald, A.S.R. (1985) *Biochem. J. 228*, 615 - 626
126 King, N.K. and Winfield, M. E. (1963) *J. Biol. Chem. 238*, 1520 - 1528
127 Fox, J.B., Nicholas, R.A., Ackerman, S.A. and Swift, C.E. (1974) *Biochemistry 13*, 5178 - 5186
128 Wiseman, J.S., Nichols, J.S and Kolpak, M.X. (1982) *J. Biol. Chem. 257*, 6328 - 6332
129 Metelitza, D.I., Arapova, G.S., Vidziunaite, R.A., Demcheva, M.V., Litvinchuck, A.V. and Razumas, V.I. (1994) *Biochemistry (Moscow) 9*, 949 - 958
130 Florence, T.M. (1985) *J. Inorg. Biochem. 23*, 131 - 141
131 Cadenas, E., Boveris, A. and Chance, B. (1980) *Biochem. J. 187*, 131 - 140
132 Moreau, S, Davies, M.J. and Puppo, A. (1995) *Biochim. Biophys. Acta 1251*, 17 - 22
133 Artor, M.A. and Ortiz de Montellano, P.R. (1987) *J. Biol. Chem. 262*, 1542 - 1551 and 14954 - 14960
134 Balch, A.L. (1984) *J. Am. Chem. Soc. 106*, 7779 - 7785
135 Aron, J., Baldwin, D.A., Marques, J. and Pratt, J.M. (1987) *J. Inorg. Chem. 30*, 203 - 208
136 Jacobson, M.R., Cash, V.L., Weiss, M.C., Laird, N.F., Newton, W.E. and Dean, D.R. (1989) *Mol. Gen. Genet. 219*, 49 - 57.
137 Zheng, L., White, R.H., Cash, V.L., Jack, R.F. and Dean, D.R. (1993) *Proc. Natl. Acad. Sci. U.S. 90*, 2754 - 2758.
138 Zheng, L., White, R.H., Cash, V.L. and Dean, D.R. (1994) *Biochemistry 33*, 4714 - 4720
139 Fu, W., Jack, R.F., Morgan, T.V., Dean, D.R. and Johnson, M.K. (1994) *Biochemistry 33*, 13455 - 13463.
140 Shethna, Y.I, DerVartanian, D.V. and Beinert, H. (1968) *Biochem. Biophys. Res. Comm. 31*, 862 - 867.
141 Lowe, D.J. and Thorneley, R.N.F. (1984) *Biochem. J. 224*, 877 - 886
142 Duyvis, M.G, Wassink, H. and Haaker, H. (1994) *Eur. J. Biochem. 225*, 881 - 890

Chapter 2

The influence of the peptide chain on the kinetics and stability of microperoxidases.

Johan H. SPEE, Marelle G. BOERSMA, Cees VEEGER, Bart SAMYN, Jozef VAN BEEUMEN, Gertrüd WARMERDAM, Gerard W. CANTERS, Walter M.A.M. VAN DONGEN and Ivonne M.C.M. RIETJENS

Abstract

Microperoxidases with increasing lengths of the peptide attached to the heme moiety have been isolated after proteolytic digestion of horse-heart cytochrome *c* (microperoxidases 6, 8 and 11) and of cytochrome c_{550} from *Thiobacillus versutus* (microperoxidase 17). The different microperoxidases catalyze the hydrogen peroxide-dependent *para*-hydroxylation of aniline relatively efficiently but are rapidly inactivated under turnover conditions. The horse-heart cytochrome *c* derived microperoxidases have identical values for V_{max} but showed a decrease of the K_M for aniline and a higher stability when the attached peptide is longer. The kinetic constants obtained for microperoxidase 17 differ markedly from the microperoxidases derived from horse-heart cytochrome *c*. Possible factors underlying the observed differences are discussed.

Introduction

Microperoxidases are so-called mini-enzymes, prepared by proteolytic digestion of cytochromes *c* [1]. They consist of a protoporphyrin IX covalently bound to a short residual peptide chain that contains the motif Cys-$(Xaa)_2$-Cys-His. The protoporphyrin is covalently bound through thioether links to the cysteine side chains. The histidine, which is usually referred to as the fifth ligand, is axially coordinated to the heme-iron. The amino acid that serves as a sixth ligand for the heme-iron in the cytochromes (His or Met) is absent as a result of the proteolytic digestion.

Lack of a specific substrate-binding site enables these mini-enzymes to use a wide variety of substrates. They are able to catalyze peroxidase-like reactions, such as the oxidation of *o*-dianisidine [2-5] as well as cytochrome *P*-450-like reactions, such as the *para*-hydroxylation of aniline [6] and the demethylation of *N*-methylaniline [7]. A major drawback for the application of microperoxidases in, for instance, industrial conversions, is their limited stability under turnover conditions: these enzymes are rapidly inactivated by hydrogen peroxide.

Up to now, only microperoxidases derived from horse-heart cytochrome *c*, namely microperoxidase 8, 9, 11 and 50, with polypeptide chains of 8, 9, 11 and 50 amino acids, respectively, have been described [6-8]. The present study was designed to investigate whether the composition of the peptide chain of the microperoxidases plays a role in the catalytic efficiency. For this purpose microperoxidases with different chain lengths were prepared from horse-heart cytochrome *c*, namely microperoxidase 8,

microperoxidase 11 and the novel microperoxidase 6. Furthermore, also a novel microperoxidase 17, which has an essentially different amino acid composition around the heme site, was prepared from cytochrome c_{550} from *Thiobacillus versutus* produced in *Escherichia coli*.

Microperoxidases 6, 8, 11 and 17 were investigated and compared with respect to the *para*-hydroxylation of aniline. The results demonstrate significant differences in kinetic properties and stability.

Materials and methods

Preparation of microperoxidases.

Microperoxidase 11 was prepared by digestion of horse-heart cytochrome *c* (Boehringer Mannheim) with pepsin (Sigma) essentially as described in the literature [9]. Microperoxidase 8 was prepared by digestion of the purified microperoxidase 11 with trypsin (Sigma) [9].

Microperoxidase 6 was prepared by digestion of microperoxidase 8 with carboxypeptidase Y (Boehringer Mannheim). To microperoxidase 8 (3.5 ml 225 µM enzyme in 75 mM sodium acetate, pH 5.0), carboxypeptidase Y (0.5 mg in 0.5 ml H_2O) was added and the mixture was incubated at 25°C for 7 h.

Microperoxidase 17 was prepared by digestion of cytochrome c_{550} from *T. versutus* with trypsin. Cytochrome c_{550} from *T. versutus* was produced in *E. coli*, from the cloned gene under semi-anaerobic conditions and purified essentially as described previously [10]. Cytochrome c_{550} (9 mg in 375 µl 100 mM Tris/HCl, pH 8.0) was digested for 20 h at 37°C with 9 mg trypsin.

To follow the course of the protease digestions, samples of 20 or 50 µl were taken at different time-points. After inactivation of the proteases by addition of phenylmethylsulfonyl fluoride (PMSF) to a final concentration of 5 mM, the samples were analyzed by reverse-phase chromatography as described in the next section. Digestions were continued to completion, i.e. until no further changes were detected in the elution pattern of the peptides.

Purification and analysis of microperoxidase preparations.

Microperoxidases 6 and 17 were purified from the digestion-mixtures using an 18 mm x 350 mm Biogel P6-Fine (Bio-Rad) column, equilibrated with 50 mM KP_i, pH 7.5, at a flow rate of 0.25 ml min^{-1}. 2-ml portions of the digestion mixture were applied to the column and the microperoxidases were eluted at 0.15 ml min^{-1}. The eluate was moni-

tored for the absorbance at 395 nm to detect heme-containing peptides. Microperoxidases 8 and 11 were purified likewise on a larger scale. Peak fractions were collected and the purity of the microperoxidases was checked by HPLC analysis, as described below. The heme content of the final preparations was determined, in duplicate, essentially as described previously [9]. The A_{423} / A_{280} ratio of the preparations was above 3.0.

For HPLC analysis, a Baker Bond WPC4 (250 mm x 4.6 mm) reverse-phase column was used in combination with a Waters TM 600 HPLC controller. Peptides were eluted at a flow rate of 1 ml min^{-1} with a 50-ml linear gradient from 0% to 50% acetonitrile in 0.1% trifluoroacetic acid. Elution was continued for another 5 min with 50% acetonitrile in 0.1% trifluoroacetic acid. The eluate was monitored at 214 nm (using an Isco V4 detector) for detection of peptides and at 395 nm (using an Applied Biosystems 757 detector) for the detection of porphyrin.

Characterization of microperoxidases.

Microperoxidases 8 and 11 have been characterized previously [9]. Microperoxidase 6 was characterized by determination of the amino acids that were removed from microperoxidase 8 by proteolytic digestion using a Biotronic LC 6000E analyzer. At the end of the incubation period, 20 µl 30 % (mass / vol.) sulfosalicylic acid and 100 µl 1 M acetic acid were added to 100 µl digestion mixture. After centrifugation (1 min, 23000 g) the supernatant fluid was used for quantitative determination of the free amino acids.

Microperoxidase 17 was characterized by sequence analysis and mass spectrometry. Sequence analysis was performed on the model 476A pulsed liquid phase sequenator, with on-line Pth-Xaa analysis, on a 120A analyzer (Applied Biosystems). Sequencing reagents and solvents were obtained from the same firm. For mass spectrometry, the peptides were subjected to matrix-assisted laser desorption ionization time-of-flight (MALDI-TOF) analysis. Samples of 1 µl were mixed with 1 µl 50 mM α-cyano-4-hydroxycinnamic acid (Sigma) in water/acetonitrile/trifluoroacetic acid (60 : 39.9 : 0.1, by vol.) and applied onto the multi-sample target. The samples were analyzed on a VG Tofspec (Fisons) equipped with a Nitrogen laser.

Assay for the *para*-hydroxylation of aniline.

Assays of the H_2O_2-dependent hydroxylation of aniline were according to a modification of the standard procedure of Brodie and Axelrod [11]. KP_i buffer (274 µl, 0.2 M, pH 7.6) was preincubated in glass tubes in a 37°C water bath. After 5 min, ascorbic acid (35 µl of a 3.5 mg ml^{-1} stock; final concentration 1.8 mM), aniline (3.5 µl 20-120 mM aniline in DMSO; final concentration 0.2-12 mM) and the appropriate microperoxidase (20 µl of a 87.5 µM stock; final concentration 5 µM) were added. 30 s later, the hydroxylation reaction was started with H_2O_2 (17.5 µl of a 50 mM stock; final concen-

tration 2.5 mM.). The incubations were always kept in a 37°C water bath and constantly stirred; these conditions were also maintained during the additions. After the required incubation time (5-60 s), the reactions were stopped by adding 100 µl 20% (mass / vol.) trichloroacetic acid. After 15 min at room temperature, precipitated protein was removed by centrifugation (1 min, 23000 g). The *para*-hydroxylated aniline produced in the assay was determined after quantitative conversion to the colored indophenol. To this end, 45 µl of phenol reagent [5% (mass / vol.) phenol in 2.5 M NaOH] and 90 µl 2.5 M Na_2CO_3 were added to the supernatant containing the hydroxylated aniline. The test-tubes were shaken at 250 rpm at room temperature for 1-3 h, until the maximum absorbance at 630 nm was observed. Concentrations were calculated using a molar extinction coefficient of $\varepsilon_{630} = 30.5\ mM^{-1}\ cm^{-1}$.

The addition of ascorbic acid to the incubation mixture is an important modification of the standard assay described by Brodie and Axelrod [11]: it efficiently blocks all peroxidase-type of reactions catalyzed by the microperoxidases, but does not affect the hydroxylation of aniline [12].

Stopped-flow spectroscopy.

For the analysis of the degradation of microperoxidase 8 by H_2O_2 on a 10 s timescale a Hi-Tech SF-51 stopped-flow spectrophotometer (Salisbury, Wiltshire, UK) equipped with a data acquisition and analysis system was used. One syringe contained 5 mM H_2O_2 in 0.2 M KP_i, pH 7.6; the other syringe contained 3.6 mM ascorbic acid, 0.8 or 24 mM aniline and 10 µM microperoxidase 8 in the same buffer. The mixing ratio was 1:1. For each of four separately prepared mixtures, four traces were recorded observing the disappearance of the Soret band. These traces could be analyzed by fitting the data to a single-exponential curve.

```
MP6          *C-A-Q-C-H-T*
MP8          *C-A-Q-C-H-T-V-E*
MP11  *V-Q-K-C-A-Q-C-H-T-V-E*
MP17         *C-K*A-C-H-M-V-Q-A-P-D-G-T-D-I-V-K*
```

Figure 1

Amino acid sequences of the microperoxidases. * indicate cleavage sites after proteolytic digestion. Note that microperoxidase 17 has a cleavage site between the heme-binding cysteines.

Results and discussion

Preparation and characterization of microperoxidases.

Microperoxidase 17. Cytochrome c_{550} from *T. versutus* was purified from a recombinant *E. coli* strain, which contained the cloned gene [10], to greater than 95% purity. The A_{525}/A_{280} ratio was 0.41. After digestion with trypsin for 24 h almost all of the cytochrome c_{550} had been digested, but several different heme-containing products could still be observed (Fig. 2A). The fraction with the highest absorbance at 395 nm was isolated by means of gel-filtration on an 18 mm x 350 mm Biogel P6-Fine (Bio-Rad) column. Based on HPLC analysis, the final preparation was estimated to be over 95% pure (Fig. 2B). The purified heme-containing microperoxidase was subjected to N-terminal sequence analysis yielding the sequence {(Cys) / Ala}{(Cys) + Lys} His Met Val Gln. This indicates that the microperoxidase contains two peptide chains: a dipeptide and a larger peptide. Apparently proteolytic cleavage has occurred between lysine-36 and alanine-37, but both peptides remain covalently bound to the heme by the liganding cysteine residues.

The mass of the microperoxidase was determined by matrix-assisted laser desorption mass spectrometry. The experimentally obtained mass, 2451.3 Da, closely corresponds to the sum of the masses of peptides Cys35 - Lys36 and Ala37 - Lys51 (1834.2 Da total), plus the mass of the heme group (616.5 Da). An additional mass of 2487.8 Da that was found can be attributed to the potassium salt of the microperoxidase. This novel microperoxidase has been designated microperoxidase 17.

Microperoxidase 6. HPLC analysis of samples taken during the digestion of microperoxidase 8 with carboxypeptidase Y clearly shows the disappearance of microperoxidase 8 and the formation of one intermediate and one final product (Fig. 3A). Analysis of the free amino acids present in the digestion mixture indicates that this is the result of the consecutive removal of the two C-terminal amino acids of microperoxidase 8, glutamate and valine, which make up the C-terminus of microperoxidase 8 (Fig. 1). Together these two amino acids constituted over 95 % of the total amount of amino acids detected in the digestion mixture after completion of the digestion. Digestion of 10 nmole of microperoxidase 8 yielded 9.3 nmole glutamate and 9.5 nmole valine. Since no other (intermediate) products were observed after completion of the digestion (Fig. 3A) and since no significant amounts of threonine or histidine (respectively the third and fourth C-terminal amino acid in microperoxidase 8) were found in the mixture, the final product can be identified as microperoxidase 6 (Fig. 1). Fig. 3B shows the HPLC analysis of the final preparation, i.e. after gel-filtration. Based on these results, the purity was estimated to be over 95%.

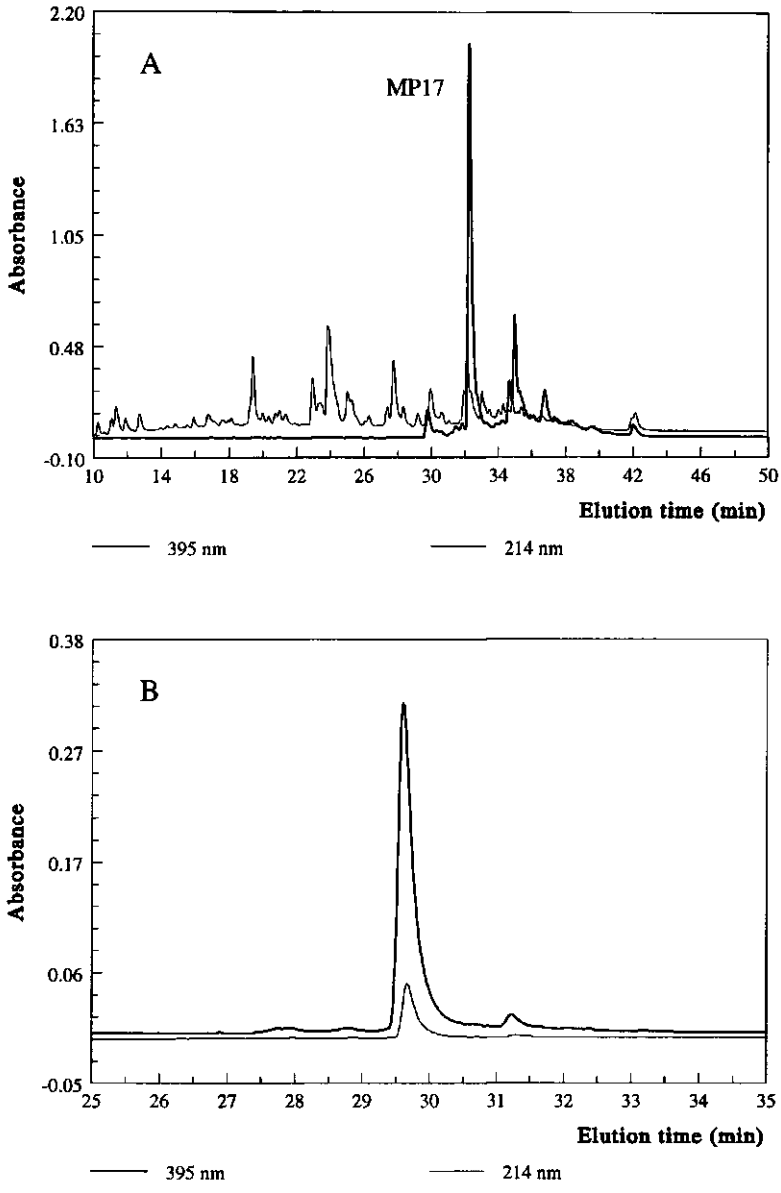

Figure 2

Preparation of microperoxidase 17. Analysis by HPLC of peptides obtained after a 24-h digestion of *T. versutus* cytochrome c_{550} with trypsin (A) and of the final preparation of MP17 after purification on Biogel P6 (B).

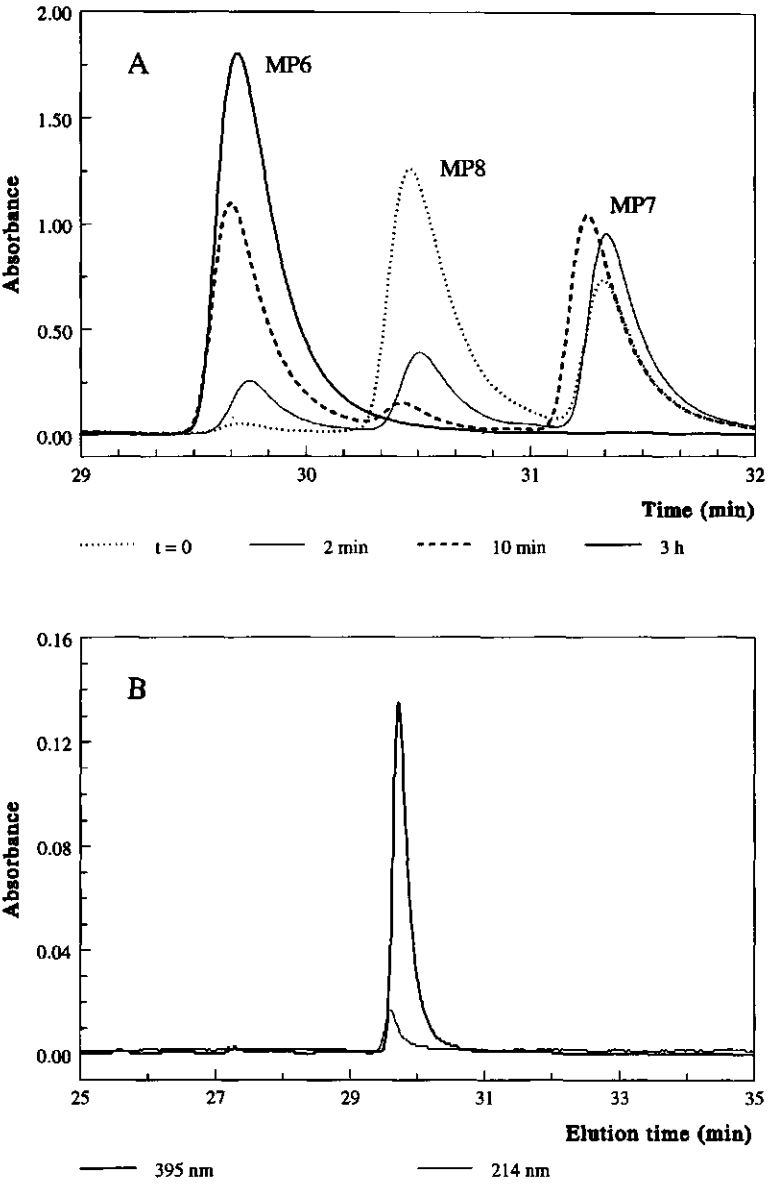

Figure 3

Preparation of microperoxidase 6. Analysis by HPLC of peptides at several time-points during the digestion of microperoxidase 8 with carboxypeptidase Y (A) and of the final preparation of microperoxidase 6 obtained after purification by gel-filtration (B).

Catalytic activities of the different microperoxidases.

Figs. 4 and 5 compare the yields of *p*-hydroxyaniline obtained with the different microperoxidases in the hydroxylation assay of aniline at varying concentrations of H_2O_2 and aniline, respectively. The reaction time in the experiments in Figs. 4 and 5 was 60 s.

In the experiment in Fig. 4, the H_2O_2 concentration was varied at a saturating concentration of the second substrate, aniline (12 mM). It is immediately obvious from visual inspection of the data in Fig. 4 that the reaction does not follow Michaelis-Menten kinetics. With all microperoxidases, optimal product yields are obtained at a H_2O_2 concentration of 2.5 - 3.5 mM; at higher concentrations, product yields decrease again. The major reason for deviation of Michaelis-Menten kinetics lies in the rapid inactivation of the microperoxidases during the time-course of the reaction (compare Figs. 6A and 6B) due to oxidative damage. Fig. 4 indicates that inactivation is faster at higher H_2O_2 concentrations.

Product yields obtained with the different microperoxidases under conditions of varying aniline concentrations at a fixed concentration of H_2O_2 (2.5 mM) are shown in Fig. 5. Although the data can be fitted perfectly with the Michaelis-Menten equation, it

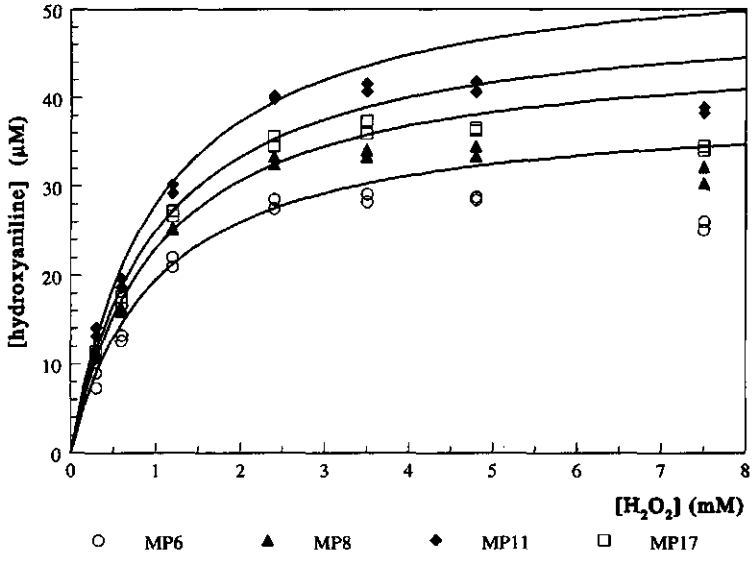

Figure 4

Hydroxylation of aniline with the different microperoxidases as a function of the H_2O_2 concentration. Reaction time 60 s; 12 mM aniline; 5 μM microperoxidase. In order to demonstrate the deviation of Michaelis-Menten kinetics, data-points obtained for the four lowest peroxide concentrations were fitted with the Michaelis-Menten equation.

should be emphasized that this equation may not be used to calculate apparent K_M and V_{max} values. This is obvious from inspection of Figs. 6A and 6B, which demonstrate the time-course of the hydroxylation reaction at high (12 mM) and low (0.4 mM) aniline concentrations, respectively. It is apparent from Fig. 6 that the reaction rates are not constant but decrease rapidly due to inactivation of the peroxidases.

Although the experiments in Figs. 4 and 5 do not allow a kinetic description of the hydroxylation of aniline by the different microperoxidases, they do show that the size of the attached polypeptide influences the yield of the hydroxylated product. Comparing the three microperoxidases derived from horse-heart cytochrome *c* shows increasing product yields in the order MP6 → MP8 → MP11. This effect is most pronounced at low substrate concentrations: at 0.4 mM aniline, microperoxidase 11 yields almost 3 times more hydroxylated product than microperoxidase 6 (Fig. 6B).

The activity of microperoxidase 17 from *T. versutus* cytochrome c_{550} is similar to that of microperoxidase 8. This indicates that not only the size of the attached peptide, but also its amino acid composition influences the efficiency of the reaction.

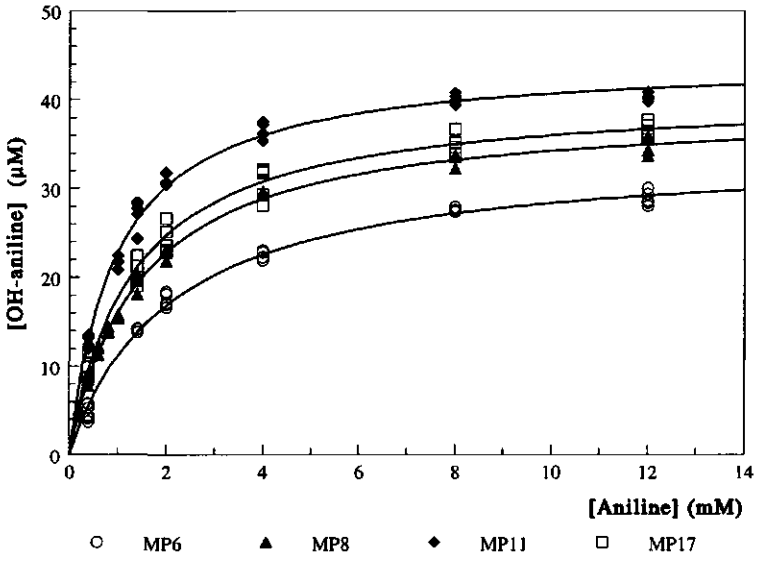

Figure 5

Hydroxylation of aniline with the different microperoxidases as a function of the aniline concentration. Reaction time 60 s; 2.5 mM H_2O_2; 5 μM microperoxidase. Data-points were fitted with the Michaelis-Menten equation; see the text for the validity of this fitting.

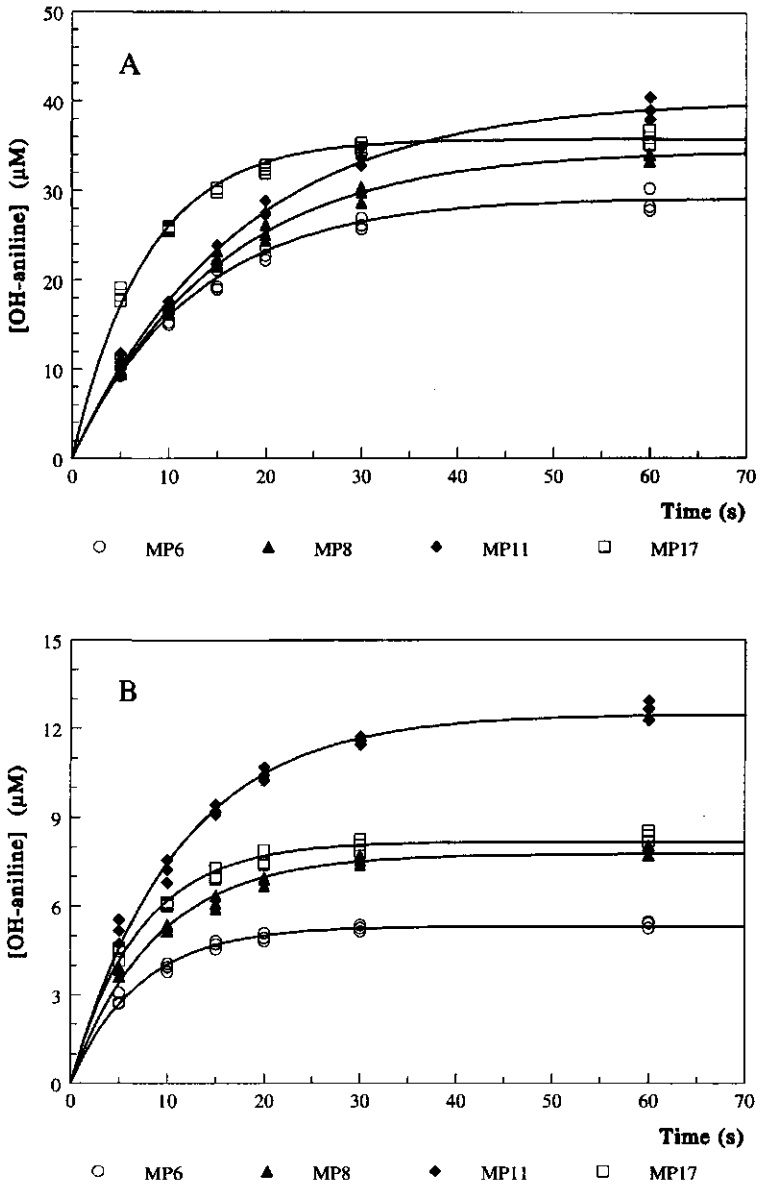

Figure 6

Time-course of the hydroxylation of aniline with the different microperoxidases. A: 12 mM aniline. B: 0.4 mM aniline. All samples: 2.5 mM H_2O_2 and 5 µM microperoxidase. Data in (A) and (B) were fitted with equations (1) and (3) in the Results section, respectively.

A full kinetic description of the microperoxidase-catalyzed hydroxylation of aniline should not only include kinetics for two-substrate reactions, but also the kinetics of inactivation. In a first approach to calculate apparent K_M and V_{max} values we used the data in Figs. 6A and 6B, that show the time-course of the hydroxylation catalyzed by the respective microperoxidases at high (12 mM) and low (0.4 mM) aniline concentrations and a fixed H_2O_2 concentration (2.5 mM). At 12 mM aniline (well above the K_M), the initial rate of the reactions approaches V_{max}. It is obvious from Fig. 6A that the three microperoxidases from horse-heart cytochrome *c* have similar initial rates under these conditions; the initial rate of the reaction catalyzed by microperoxidase 17 from *T. versutus* cytochrome c_{550}, however, is approximately two times faster.

The data in Fig. 6A ([aniline] >> K_M) were fitted assuming:

$$v = V_{max}\, e^{-kt}$$

with v being the actual rate at time t after the start of the incubation, and k the apparent first-order rate constant for inactivation of the microperoxidase. After integration we get:

$$[P]_t = (V_{max} / k)\,(1 - e^{-kt}) \qquad (1)$$

with $[P]_t$ being the concentration of the formed product at time t and $V_{max} / k = [P]_{max}$, the maximal product concentration at infinite time. Using equation (1) to fit the data resulted in values for k and $[P]_{max}$, from which V_{max} was then calculated.

It should be emphasized that this equation does not imply that the inactivation of the microperoxidases is a first-order process. The rate of inactivation is dependent on the concentrations of both H_2O_2 (which causes the inactivation) and aniline (which protects against inactivation; see below), according to a mechanism not yet fully understood. Therefore, equation (1) gives only a first approximation of the kinetics of the inactivation; k can be expected to be dependent on both the H_2O_2 and aniline concentrations and should therefore only be used to compare different microperoxidases under similar conditions. Application of equation (1) to fit the data-points in Fig. 6A results in the values for V_{max} and k given in Table I. The three microperoxidases derived from horse-heart cytochrome *c* have similar V_{max} values for the hydroxylation of aniline, but the apparent rate constant for inactivation increases slightly from microperoxidase 11 to microperoxidase 6. Microperoxidase 17, which is derived from *T. versutus* cytochrome c_{550}, has a twofold higher V_{max} for the reaction, but also a much higher rate constant for inactivation.

Fig. 6B shows the *para*-hydroxylation of aniline by the different microperoxidases at low aniline concentration (0.4 mM). The data-points in Fig. 6B were fitted with the use of the Michaelis-Menten equation, again corrected for single exponential

decrease of the enzyme activity:

$$v = \{(V_{max}\,[S]) / (K_M + [S])\}\, e^{-kt}$$

After integration we get:

$$[P]_t = \{[S] / (K_M + [S])\}\, (V_{max} / k)\, (1 - e^{-kt}) \qquad (2)$$

which can also be written as:

$$[P]_t = [P]_{max}\, (1 - e^{-kt}) \qquad (3)$$

Fitting the data to equation (3) gave the values for the apparent rate constant for inactivation at this aniline concentration (Table I) and for the maximal product concentration, $[P]_{max}$. With these data and the values for V_{max} obtained from Fig. 6A. the K_M values were then calculated from equation (2).

Inspection of the results, summarized in Table I, leads to the following conclusions: for the microperoxidases derived from horse-heart cytochrome *c*, an increase in the size of the attached polypeptide results in a decrease of the apparent K_M for aniline, together with an increase in stability. microperoxidase 11 has a twofold lower K_M for aniline and a 35% lower apparent rate constant for inactivation compared to microperoxidase 6. The microperoxidase derived from the *T. versutus* cytochrome has a higher K_M than those derived from horse-heart cytochrome and a rate constant for inactivation comparable to microperoxidase 6.

	Incubation time variable **[aniline] = 12 mM.**		Incubation time variable **[aniline] = 0.4 mM.**		
	V_0 (V_{max}) ($\mu M\ s^{-1}$)	k (s^{-1})	K_M (mM)	V_0 ($\mu M\ s^{-1}$)	k (s^{-1})
MP6	**2.28** ± 0.04	**0.079** ± 0.004	**0.82** ± 0.04	**0.75** ± 0.02	**0.141** ± 0.007
MP8	**2.35** ± 0.03	**0.069** ± 0.002	**0.63** ± 0.04	**0.89** ± 0.02	**0.115** ± 0.005
MP11	**2.28** ± 0.04	**0.056** ± 0.002	**0.41** ± 0.05	**1.14** ± 0.03	**0.091** ± 0.004
MP17	**4.47** ± 0.04	**0.132** ± 0.004	**1.33** ± 0.03	**1.14** ± 0.02	**0.141** ± 0.006

Table I **Kinetic parameters of the microperoxidases, with 95% confidence intervals.** *k* indicates a pseudo first-order rate of inactivation at 2.5 mM hydrogen peroxide.

The apparent rate constants for inactivation of the microperoxidases at low substrate concentration are always higher than those at high substrate concentration, which indicates that the substrate protects the microperoxidase against inactivation (Table I). An explanation of this observation is that hydroxylation of the substrate competes with side reactions of the intermediate iron-(per)oxo complex that inactivate the microperoxidase (such as the production of highly oxidative hydroxyl or superoxide radicals, the irreversible oxidation of the catalyst to μ-oxo dimers or the abstraction of H-atoms from the meso-positions of the porphyrin). Although equations (1) and (2) serve our purposes well for the moment, a more accurate description of the kinetics of inactivation should also account for the dependence on the concentration of both substrates. When observing the horse-heart cytochrome *c*-derived microperoxidases, the influence of the aniline concentration on protection against inactivation (the ratio of the k values at 0.4 mM and at 12 mM aniline in Table I) decreases with the length of the peptide chain, i.e. in terms of stability, microperoxidases with a longer peptide chain benefit less from a higher aniline concentration. Of all microperoxidases investigated here the stability of microperoxidase 17 is least dependent on the aniline concentration.

Stopped-flow analysis of the degradation of microperoxidase 8 by H_2O_2 in the presence of aniline and ascorbic acid on a 10 s time-scale yielded k values of 0.118 s^{-1} (±0.008) at 0.4 mM aniline and 0.080 s^{-1} (±0.005) at 12 mM aniline. These k values for the degradation of microperoxidase 8 are consistent with the k values for the inhibition of microperoxidase 8 as determined on a 1-min time-scale by the kinetic experiments, also with respect to the dependence of these processes on the aniline concentration (Table I). From this it can be concluded that investigation of the inactivation of microperoxidases on a seconds time-scale would not result in a better understanding of this process.

Conclusions.

The present study indicates that microperoxidases are relatively efficient catalysts. Specificity constants for the hydroxylation of aniline (k_{cat} / K_M), for the microperoxidases used in this study, vary in the range 550 - 1200 M^{-1} s^{-1}.

The kinetic parameters for the microperoxidases derived from horse-heart cytochrome *c* (microperoxidases 6, 8 and 11) show that the increase of the size of the peptide chain attached to the heme moiety has no effect on the V_{max} for the hydroxylation of aniline, but does result in 50% decrease of the K_M. Obviously, a larger size of the attached peptide chain in these microperoxidases creates an environment around the heme-iron that is more suitable for the fairly hydrophobic substrate, but does not influence the actual rate of hydroxylation. Microperoxidase 17, which is derived from *T. versutus* cytochrome c_{550}, has a twofold higher V_{max} in this reaction, but the K_M is lower than that of the microperoxidases derived from horse-heart cytochrome *c*.

A major drawback for the application of microperoxidases is their limited stability under turnover conditions. Comparing the rate constants for inactivation of the three microperoxidases derived from horse-heart cytochrome *c* indicates that the size of the attached peptide protects against inactivation, but a much higher stability under turnover conditions is required to make microperoxidases attractive for industrial application. To understand the mechanism of protection of the microperoxidase by the peptide, it is necessary to obtain information on the mechanism of inactivation. This work is currently in progress. One possibility is that the peptide chain serves as scavenger for hydroxyl or superoxide radicals produced during the reaction; another is that the peptide chain forms a physical barrier for the irreversible dimerization to the inactive μ-oxo dimer. The peptide chain could also act as an alternative source of H-atoms and thus reduce the inactivation of the enzyme by H-atom abstraction from the *meso*-positions of the porphyrin by the iron-oxo species.

The kinetic constants derived for the reaction catalyzed by microperoxidase 17, the microperoxidase derived from *T. versutus* cytochrome c_{550}, are remarkably different from those of the microperoxidases derived from horse-heart cytochrome *c*. Values for V_{max}, K_M and the rate constant for inactivation are approximately 2-, 3-, and 1.5-fold higher than those for the largest cytochrome *c*-derived microperoxidases, microperoxidase 11. One of the reasons for the higher catalytic rate constant of microperoxidase 17 may be the nick in the peptide chain, between the two cysteine residues, which form the thioether bonds with the porphyrin, caused by the digestion with trypsin. This may allow the ligating histidine, which is proximal to the second cysteine (Fig. 1), to take a slightly altered position towards the heme-iron, changing its electronic configuration and reactivity. Further research will have to provide conclusive evidence for this, possibly by means of site-directed mutagenesis of the cleavage site. The fact that microperoxidase 17 was prepared from a cloned bacterial cytochrome *c* makes this approach possible.

Acknowledgments

The present research was financially supported by the EC Human Capital and Mobility grant MASIMO no. ERBCHRXCT, by the Biotech grant no. BIO2-CT942052, by the Concerted Research Action no. 12052293 of the Flemish Ministry of Scientific Research and by the Netherlands Foundation for Chemical Research (SON) with financial aid from the Netherlands Organization for Scientific Research (NWO).

References

1 Harbury, H.A., Cronin, J.R., Franger, M.W., Hettinger, T.P., Murphy, A.J., Meyer, Y.P. and Vinogradov, S.N. (1965) *Proc. Natl. Acad. Sci. (USA) 54*, 1658-1664.

2 Baldwin, D.A., Marques, M. and Pratt, J.M. (1987) *J. Inorg. Biochem. 30*, 203-217.

3 Traylor, T.G. and Xu, F. (1990) *J. Am. Chem. Soc. 112*, 178-186.

4 Adams, P.A. (1990) *J. Chem. Soc. Perkin Trans. 2*, 1407-1414.

5 Cunningham, I.D., Bachelor, J.L. and Pratt, J.M. (1991) *J. Chem. Soc. Perkin Trans. 2*, 1839-1843.

6 Rusvai, E., Vegh, M., Kramer, M. and Horvath, I. (1988) *Biochem. Pharmacol. 37*, 4574-4577.

7 Nakamura, S., Mashino, T. and Hirobe, M. (1992) *Tetrahedron lett. 33*, 5409-5412.

8 Adams, P.A., De Milton, R.C. and Silver, J. (1994) *BioMetals 7*, 217-220.

9 Aron, J., Baldwin, D.A., Marques, M., Pratt, J.M. and Adams, P.A. (1986) *J. Inorg. Biochem. 27*, 227-243.

10 Ubbink, M., Van Beeumen, J. and Canters, G.W. (1993) *J. Bacteriol. 174*, 3707-3714.

11 Brodie, B.B. and Axelrod, J. (1948) *J. Pharmacol. Exp. Ther. 94*, 22-28.

12 Osman, A.M., Koerts, J., Boersma, M.G., Boeren, S., Veeger, C. and Rietjens, I.M.C.M. (1996) *Eur. J. Biochem. 240*, 232-238.

Chapter 3

Protection of the nitrogenase Fe protein from *Azotobacter vinelandii* against oxygen-inactivation by complex formation with the MoFe protein.

Johan H. SPEE, Hans WASSINK, Walter M.A.M. VAN DONGEN and Huub HAAKER

Abstract

Nitrogenase consists of two metalloproteins, the Fe protein and the MoFe protein. The purified Fe protein is extremely susceptible to inactivation by oxygen. In a solution exposed to air its half-live of inactivation is about 30 seconds. In crude extracts prepared from *Azotobacter* species, the Fe protein is more resistant to oxygen-inactivation as a result of complex formation with the MoFe protein and a [2Fe-2S] protein, called the FeSII protein. The mechanism by which these proteins offer protection against inactivation by oxygen was investigated. It is shown that binding of the Fe protein to the MoFe protein decreases its oxygen sensitivity. A further decrease of the oxygen sensitivity was brought about by stabilization of the Fe protein-MoFe protein complex by the FeSII protein or by aluminum fluoride and MgADP.

Kinetic evidence is presented that the three-component protein complex, formed by the Fe protein, the MoFe protein and the FeSII protein, can exist in at least two stoichiometries: one FeSII protein binds one or two MoFe protein-Fe protein complexes.

A model which quantitatively describes the experimental data is presented. This model takes into account 1: the protection against oxygen-inactivation of the Fe protein offered by the MoFe protein; 2: the stabilization of the MoFe protein-Fe protein complex by the FeSII protein; 3: the different stoichiometries of the three-component protein complexes and 4: the kinetics of reduction and dissociation of these complexes. In the present study evidence is obtained supporting the model in which the specific protein environment of the [4Fe-4S] cluster of the Fe protein in the Fe protein-MoFe protein complex is the basis for the preservation of the integrity of the cluster under oxidative conditions.

Introduction

Nitrogenase catalyzes the MgATP-dependent reduction of N_2 to NH_3. The enzyme consists of two component proteins. The homodimeric (γ_2) iron protein (Fe protein) contains a single [4Fe-4S] cluster which is coordinated by two cysteine residues from each subunit [1]. The heterotetrameric ($\alpha_2\beta_2$) molybdenum-iron protein (MoFe protein), contains two unique iron-molybdenum-sulfur-homocitrate cofactors (FeMoco) [2] that are the proposed sites for binding and reduction of N_2 [3, 4] plus two unique [8Fe-7S] clusters (P-clusters) [5, 6] which are believed to accept an electron from the Fe protein before transferring it to the FeMoco substrate binding-site.

A kinetic mechanism for nitrogenase catalysis has been described by Lowe and Thorneley [7] and has recently been extended by Duyvis et al. [8-10] and by Lowe et al. [11]. The model consists of two coupled cycles: the Fe protein cycle and the MoFe protein cycle. In the Fe protein cycle, the reduced Fe protein associates with the MoFe protein forming a two-component protein complex. The MoFe protein has two independent binding sites for the Fe protein, one per αβ-dimer. Binding of MgATP to the Fe protein induces electron transfer from the Fe protein to the MoFe protein followed by on-enzyme hydrolysis of MgATP. Next the oxidized Fe protein, with MgADP bound, dissociates from the MoFe protein. With dithionite as the reductant, this dissociation is the rate-limiting step [12]. Finally, the free Fe protein is reduced and MgADP is replaced by MgATP. The MoFe protein cycle describes the stepwise reduction of the MoFe protein by eight consecutive electron transfer steps from the Fe protein, followed by the reduction of N_2 to NH_3, which requires six electrons, and the production of H_2 from two protons and two electrons.

Both nitrogenase proteins are inactivated when they are exposed to oxygen. In vitro studies with *Azotobacter* nitrogenase proteins indicated that especially the Fe protein is prone to inactivation by oxygen [13-15]. Wang and colleagues [14] demonstrated that the MoFe protein from *A. vinelandii* still retained about 90% of its activity after a 1 min exposure to 20% oxygen in argon, whereas under the same conditions the activity of the Fe protein was reduced to less than 20%. The authors noticed loss of Fe from the Fe protein which indicates that its [4Fe-4S] clusters are destroyed in the inactivation process.

Consequently, aerobic diazotrophic bacteria have to protect their nitrogenases from rapid and irreversible inactivation by oxygen but at the same time require oxygen to provide sufficient ATP to sustain nitrogen fixation. This requirement of ATP, produced by means of oxygen-dependent respiratory metabolism, on the one side and the oxygen instability of nitrogenases on the other side is known as the 'oxygen problem' [16, 17]. The nitrogen fixing soil bacterium *A. vinelandii* deals with this problem in two different ways. At high oxygen concentrations it produces a terminal oxidase, cytochrome *d*, with a high V_{max}. Cytochrome *d* effectively prevents the accumulation of intracellular oxygen and subsequent inactivation of nitrogenase [18]. In addition to this so called respiratory protection *A. vinelandii* has a second strategy known as conformational protection. The bacterium produces a small iron-sulfur protein, known as the FeSII- or Shethna protein [19]. The FeSII protein has been isolated as a homodimeric (δ_2) protein containing one [2Fe-2S] cluster per subunit. Under non-reducing conditions and in the presence of Mg^{2+} the FeSII protein associates with the Fe protein and MoFe protein, thus forming a three-component protein complex in which the Fe protein is protected against oxygen-inactivation [13, 14, 20, 21]. The stoichiometry of the three-component protein complex

as isolated from *A. vinelandii* is approximately one FeSII protein (δ_2), one MoFe protein ($\alpha_2\beta_2$) and two Fe proteins (γ_2) [20]. The oxygen tolerant three-component protein complex can be reconstituted in vitro by mixing the anaerobically oxidized forms of the MoFe protein, the Fe protein and the FeSII protein in the presence of $MgCl_2$ [14, 22]. This reconstituted complex dissociates upon reduction with dithionite making the nitrogenase proteins again sensitive to oxygen-inactivation [22].

It has been demonstrated recently [23, 24] that the Fe protein-MoFe protein complex can be stabilized with aluminum fluoride and MgADP, resulting in a very stable nitrogenase complex which has been proposed to represent the transition state for ATP-hydrolysis and subsequent electron transfer. The structure of this AlF-MgADP stabilized complex has been solved recently [25]: it has the subunit composition $(\alpha\beta\gamma_2)_2$; one Fe protein γ_2 dimer per $\alpha\beta$-subunit pair of the MoFe protein, i.e. two Fe protein dimers are bound to one MoFe protein heterotetramer.

In the present study we investigated the kinetics of oxygen-inactivation of the Fe protein under different conditions (all in the presence of MgADP and $MgCl_2$). 1: without addition of the MoFe or FeSII proteins; 2: in the presence of only the MoFe protein, i.e. the Fe protein mainly bound to the MoFe protein; 3: in the AlF-MgADP stabilized two-component protein complex and 4: in the presence of the MoFe protein plus different amounts of FeSII protein, i.e. the Fe protein mainly in a three-component protein complex. The kinetics of the reduction of the three-component protein complex was investigated by means of stopped flow spectrophotometry. Based on the results obtained with these experiments a model is proposed in which stabilization of the Fe protein-MoFe protein complex by the FeSII protein prevents the oxidative degradation of the [4Fe-4S] cluster of the Fe protein.

Materials and methods

Purification of the FeSII protein.

The *A. vinelandii* FeSII protein was overexpressed in *E. coli* W3110 harboring the plasmid pAVFeSII and purified, essentially as described by Moshiri et al. [26]. In all purification steps a temperature of 4°C was maintained; no precautions were made to exclude O_2. The final preparation was analyzed by means of PAGE and found to be over 95% pure. The A_{280}/A_{344} ratio was 0.90. Molar concentrations of the FeSII protein were determined from the absorbance at 344 nm, using ε_{344} = 33.2 mM^{-1} cm^{-1} for the two [2Fe-2S] clusters in the dimeric protein [27]. The protein concentration was determined with the micro biuret method [28] after precipitation with deoxycholic acid and trichloro-

acetic acid [29], using a molecular mass of 26.28 kDa per dimeric FeSII protein. The results indicated that the purified FeSII protein contained 1.8 [2Fe-2S] clusters per dimer. Earlier preparations of the recombinant FeSII protein yielded 1.9 clusters per dimer [26]. All concentrations of the FeSII protein are expressed here as concentrations of the dimeric protein calculated from the absorbance at 433 nm, i.e. based on the content of two [2Fe-2S] clusters per protein.

Purification of nitrogenase proteins.

A. vinelandii ATCC strain 478 was grown and the nitrogenase MoFe and Fe proteins were isolated as described by Duyvis et al. [9]. Protein concentrations were determined with the micro biuret method, as described above. The molar concentrations of the MoFe and Fe proteins were calculated from their molecular masses of 230 kDa and 63 kDa, respectively. The activities of the purified MoFe and Fe proteins were determined on the basis of the acetylene reduction activity at 30 °C, as described by Braaksma et al. [30]. The specific activity of each of the purified nitrogenase proteins was calculated from the maximum acetylene reduction rate at the optimal MoFe protein : Fe protein ratios, which were 1 μM MoFe protein plus 20 μM Fe protein for the measurement of the specific activity of the MoFe protein and 2 μM MoFe protein plus 1 μM Fe protein for the measurement of the specific activity of the Fe protein. The specific activities for the purified MoFe and Fe proteins were at least 8 and 2 mol ethylene s^{-1} (mol enzyme)$^{-1}$ respectively.

Previous studies have indicated that the FeSII protein does not function as an electron donor to nitrogenase [13, 20, 21]. However, to rule out any effect of the FeSII protein on the nitrogenase activity the activities of the MoFe protein (8 moles Fe protein per mole MoFe protein) and the Fe protein (1 mole Fe protein per mole MoFe protein) were assessed in the presence of FeSII protein concentrations ranging from 1 to 16 moles FeSII protein per mole MoFe protein. No effects of the FeSII protein on the activities were observed (data not shown).

Preparation of the protein mixtures.

In vivo, the Fe protein is not reduced under conditions of oxygen-stress and is predominantly present in the oxidized form with MgADP bound (discussed below). Complex formation between the FeSII protein, the MoFe protein and the Fe protein requires the presence of Mg^{2+} [22]. All protein mixtures were prepared with the same anaerobic standard buffer: 50 mM TES/NaOH, pH 7.4, 5 mM $MgCl_2$, 1 mM MgADP. At the given concentration, MgADP saturates the nucleotide binding sites of the Fe protein. The MoFe and Fe proteins were made dithionite-free by passage through a 1 cm x 10 cm Biogel P6-Fine (Bio-Rad) column, equilibrated with standard buffer, containing

also 150 mM NaCl in the case of the MoFe protein. The Fe protein was oxidized with PMS, while passing through the column, as described earlier [22]. The FeSII protein was purified aerobically; the oxidized FeSII protein was transferred to anaerobic standard buffer, also by passage through a 1 cm x 10 cm Biogel P6-Fine column. Next, protein concentrations were determined as described above.

Samples containing free Fe protein or free FeSII protein were subsequently prepared by dilution with standard buffer to a final protein concentration of 10 μM. The two-component protein mixture was prepared by mixing of the reductant-free MoFe protein and oxidized Fe protein, both in standard buffer, in a fixed molar ratio of 1 : 2. Three-component protein mixtures were prepared by mixing of the reductant-free MoFe protein and oxidized Fe protein in a fixed molar ratio of 1 : 2, followed by addition of the oxidized FeSII protein, all in standard buffer. The molar ratio of FeSII protein : MoFe protein was varied from 0.2 : 1 to 1 : 1 in the different experiments. For determination of the oxygen stability of Av2 in the two-component and three-component protein mixtures, these mixtures were diluted with standard buffer to a final MoFe protein concentration of 5 μM. Three-component protein mixtures used for stopped-flow experiments were diluted similarly to a final MoFe protein concentration of 10 μM. All manipulations during the preparation of the mixtures were done under strictly anaerobic conditions, but without addition of dithionite.

Preparation of the AlF-MgADP stabilized nitrogenase complex.

The AlF-MgADP stabilized nitrogenase complex was prepared by incubating the purified, i.e. dithionite reduced, MoFe and Fe proteins with aluminum fluoride and MgADP essentially as described by Duyvis et al. [24]. $Na_2S_2O_4$ and excess Fe protein were removed by applying the complex preparation onto a 1 x 10 cm DEAE Sephacel ion-exchange column, equilibrated with standard buffer also containing 0.9 mM AlF_3 and 9 mM NaF. The complex was eluted with the same buffer with 250 mM NaCl and next diluted with standard buffer to a final concentration of 5 μM with respect to the MoFe protein. Aluminum and fluoride form compounds of the general composition $AlF_x(OH^-)_y$. In the pH range 5 - 8 and with millimolar fluoride concentrations at least five different mixed OH^- and F^- complexes of Al^{3+} are present [31]. For this reason we use 'AlF' as the general abbreviation for all forms of aluminum, fluoride and OH^- coordination.

Oxygen-inactivation of the protein mixtures.

The two- and three-component protein mixtures (FeSII protein variable from 0 to 5 μM; 5 μM MoFe protein; 10 μM Fe protein; in standard buffer) were incubated under argon in a 7.5 ml closed vial at room temperature. A 100 μl sample (t = 0 min) was taken and added to 400 μl assay mixture containing 25 mM $Na_2S_2O_4$ to assess the nitrogenase

activity with the acetylene reduction assay at 30 °C, as described by Braaksma et al. [30]. Next the vial was opened and air was blown in while stirring the solution gently. This procedure allows exposure of the proteins to a constant O_2 concentration of 240 μM. Further 100 μl samples were taken and tested for nitrogenase activity at 3, 6 and 10 min after the start of the exposure to oxygen. The oxygen-inactivation of 10 μM free Fe protein, in standard buffer, was determined similarly. To assess the activity of the free Fe protein, two molar equivalents of MoFe protein were added to the assay mixture.

To determine the oxygen-inactivation of the AlF-MgADP stabilized nitrogenase complex 500 μl of the mixture (5 μM with respect to the MoFe protein, in standard buffer) was exposed to air as described above. Samples of 200 μl, taken at 0, 3, 6 and 10 min, were injected into an anaerobic vial containing 20 μl 200 mM $Na_2S_2O_4$ in standard buffer. After flushing the vial with argon for 2 min, 20 μl of 500 mM KP_i, pH 7.4, was added and the complex was reactivated by incubating the mixture anaerobically for 45 min at 50 °C. When incubated at this temperature the phosphate replaces the aluminum fluoride, allowing the dissociation of the complex [24]. The nitrogenase activity was determined, as described above, using 100 μl of the reactivated nitrogenase.

Reduction of the protein mixtures.

The kinetics of the reduction of the three-component protein mixtures was determined by rapid mixing of the samples with $Na_2S_2O_4$ in a Hi-Tech SF-51 stopped-flow spectrophotometer (Salisbury, Wiltshire, UK) equipped with an anaerobic kit and a data acquisition and analysis system. One syringe contained mixtures of 5 or 10 μM FeSII protein, 10 μM MoFe protein and 20 μM Fe protein, in standard buffer. The other syringe of the stopped-flow spectrophotometer contained 16 mM $Na_2S_2O_4$ in the same buffer. The mixing ratio was 1 : 1. Absorbance changes at 430 and 550 nm were recorded on different time-scales. The reduction of free FeSII protein was investigated similarly, with in the one syringe 10 μM of the oxidized protein, and in the other syringe 16 mM $Na_2S_2O_4$, both in standard buffer.

The change in molar extinction upon reduction of the three-component protein mixtures, required for the simulations, were derived directly from the experimental stopped-flow traces: $\Delta\varepsilon_{430}$ = 10.6 and $\Delta\varepsilon_{550}$ = 4.2 mM^{-1} cm^{-1} for the free FeSII protein; $\Delta\varepsilon_{430}$ = 11.2 and $\Delta\varepsilon_{550}$ = 3.3 mM^{-1} cm^{-1} for MoFe protein plus Fe protein (with MgADP bound) in a 1 : 2 ratio. Reduction of the FeSII protein showed a lower molar extinction change than calculated from the spectra determined previously [20]. This is a result of the bandwidth of the spectrophotometer used in the stopped-flow experiments. The values for the incubations of Fe protein plus MoFe protein include a minor effect of the MoFe protein in molar extinction change upon reduction (about 10%).

Terminology of proteins, complexes and kinetic species.

The MoFe and Fe proteins from *A. vinelandii* are generally abbreviated as Av1 and Av2, respectively. Hereafter the heterotetrameric ($\alpha_2\beta_2$) MoFe protein and the homodimeric (δ_2) FeSII protein will be referred to as 'Av1' and 'FeSII', respectively. In vivo, Av2 is not reduced under conditions of oxygen-stress and MgADP, bound to the oxidized Fe protein, is only very slowly replaced by MgATP [32]. As a consequence Av2 is predominantly present as oxidized Av2(MgADP)$_2$. To approximate to the physiological conditions all experiments were performed in the presence of saturating MgADP concentrations. As a shorthand notation, 'Av2' will be used hereafter to refer to the dimeric (γ_2) Fe protein with MgADP bound. At the cellular protein concentrations in vivo (Av1≈50 μM, Av2≈80 μM, FeSII≈50 μM [33]) and with a dissociation constant of about 1 μM [10] almost all Av2 is bound to Av1. The complex formed by one Av1 and two Av2, with MgADP bound, will be indicated as the Av1·[Av2]$_2$ complex. It must be noted, however, that the presence of a nucleotide (MgADP or MgATP) is not required for the formation of a three-component complex by FeSII, Av1 and Av2 [22]. The oxygen-inactivated form of Av2 will be indicated as Av2$_{inact}$. The suffix 'red' is used for the dithionite reduced form of a protein or species (e.g. FeSII$_{red}$, Av2$_{red}$). The kinetic species Av1αβ, FeSIIδ and Av2 are used to describe the kinetics of inactivation, complex formation and reduction of the proteins in the various experiments. It is generally accepted that the two Av2 binding sites on Av1 are independent. Such an independent functioning αβ-subunit pair of Av1 is referred to as the Av1αβ species. We assumed that the δ subunits of FeSII each have two different binding sites for Av1αβ; the independently functioning half of FeSII is referred to as the FeSIIδ species. Shorthand notations are used in the Results section only.

Results

Av1 protects Av2 from inactivation by oxygen.

The residual activity of free Av2 after exposure to oxygen is shown in Fig. 1 (trace 'Av2'). The inactivation of Av2 is rapid and can be described by single exponential decay with $k_{obs} = 2 \times 10^{-2}$ s^{-1} (pseudo first-order reaction at 240 μM O_2). However, when Av1 is present during exposure to oxygen the decay is considerably slower (Fig. 1, trace 'Av2 + Av1'), indicating that Av1 protects Av2 against oxygen-inactivation. When approximated by single exponential decay the 'overall' rate constant for inactivation of Av2 in the presence of Av1 is 5×10^{-3} s^{-1}, i.e. four times slower than for free Av2. From the rate constants for the reversible association of Av1 with Av2 (k_2 and k_{-2}, Table I) it

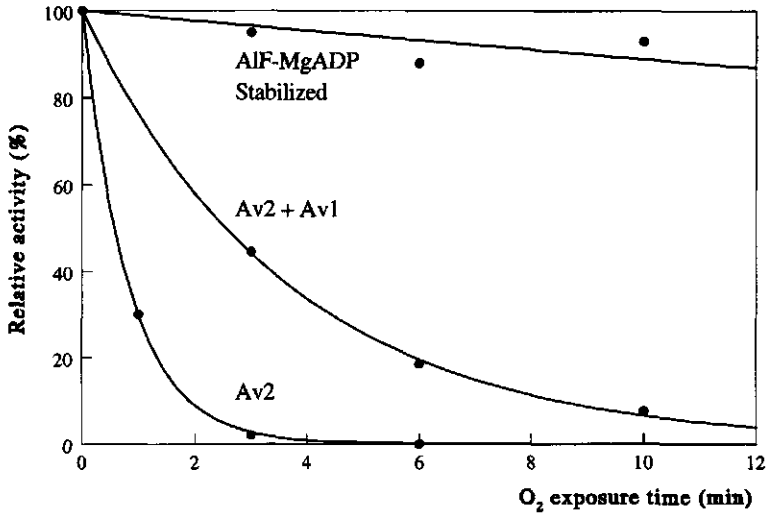

Figure 1

Inactivation of nitrogenase by oxygen. Relative residual activity as a function of the time of exposure to 240 μM oxygen. 'Av2': 10 μM free Av2. 'Av2 + Av1': 10 μM Av2, 5 μM Av1. 'AlF-MgADP Stabilized': 5 μM of the AlF-MgADP stabilized two-component nitrogenase complex. All in standard buffer. The lines drawn through the data-points are single-exponential decay curves with rate constants $k = 2 \times 10^{-2}$ s^{-1} for free Av2, $k = 5 \times 10^{-3}$ s^{-1} for Av2 in the presence of Av1 and $k = 2 \times 10^{-4}$ s^{-1} for the AlF-MgADP stabilized complex.

follows that, at the given concentrations of Av1 and Av2, approximately 75% of Av2 is bound to Av1, in an Av1·$[Av2]_2$ complex, at the start of the exposure to oxygen. The fourfold decrease in the rate of inactivation that is observed when Av1 is added to Av2 indicates that free Av2 is inactivated much more rapidly than Av2 associated with Av1. Apparently, the rate of inactivation of Av2 in the presence of Av1 depends on the dissociation constant of the Av1·$[Av2]_2$ complex.

A stable, but enzymatically inactive protein complex can be prepared by incubating the Fe and MoFe proteins with MgADP, AlF_3 and NaF. This stabilized two-component protein complex was isolated and also exposed to oxygen. After exposure the complex was dissociated at 50°C in the presence of phosphate to restore the activity, as described before [24]. As shown in Fig. 1 (trace 'AlF-MgADP stabilized'), this sample retained 95% of its activity after a 10 min exposure to oxygen. This result confirms the conclusion, drawn above, that the association with Av1 protects Av2 against inactivation by oxygen.

Protection against oxygen-inactivation by the FeSII protein.

Oxidized A. *vinelandii* nitrogenase proteins associate with FeSII to form a three-component protein complex in which nitrogenase is protected from inactivation by oxygen. This FeSII-mediated protection was investigated in vitro with incubations containing FeSII (0-5 μM), reductant-free Av1 (5 μM) and oxidized Av2 (10 μM) in the presence of MgADP and $MgCl_2$.

Fig. 2A shows the residual nitrogenase activity of the three-component protein mixtures after exposure to oxygen for 0, 3, 6 and 10 min (fitted curves are discussed below). As is obvious from this figure, increasing the FeSII : Av1 ratio from 0 to 1 results in a considerable increase of the residual nitrogenase activity, which indicates that FeSII offers protection against oxygen-inactivation. At the highest FeSII : Av1 ratio over 80% of the nitrogenase was still active after 10 min of exposure to oxygen, whereas, at that time, the activity of the sample that did not contain FeSII (ratio = 0) was reduced to less than 10% of the initial activity.

Fig. 2B shows the protection, caused by FeSII (defined in the legend), as a function of the molar FeSII : Av1 ratio (for simplicity, only the data-points for exposure times of 3 and 6 min are shown). This figure indicates that the protection increases linearly with the FeSII : Av1 ratio until this ratio is about 0.5 FeSII molecule per Av1 molecule. At higher FeSII : Av1 ratios the protection increases only slightly. Since previous studies have shown that FeSII is a homo-dimer both in vitro and in vivo [26], the conclusion that can be drawn from these results is that one FeSII dimer suffices for the almost optimal protection of two Av1 and four Av2 molecules.

The stoichiometry of the three-component protein complex as isolated from *A. vinelandii* [20], or prepared in vitro from purified proteins [22] has been analyzed before and revealed a FeSII : Av1 : Av2 molar ratio of approximately 1 : 1 : 2, i.e. a twofold higher FeSII content than required for the almost optimal protection against oxygen-inactivation. This suggests that, depending on the available amount FeSII, two forms of the three-component protein complex, with different stoichiometries, can exist that both offer protection for the nitrogenase Fe protein against oxygen-inactivation. Evidence for the existence of both types of three-component protein complexes is given below.

Figure 2

Inactivation of nitrogenase in the three-component protein mixtures. A: relative residual nitrogenase activity as a function of the time of exposure to 240 μM oxygen. 5 μM Av1, 10 μM Av2; FeSII : Av1 molar ratios as indicated in the figure (ratios 0.3 and 0.75, shown in Fig. B, are omitted in Fig. A). All in standard buffer. The simulated curves are based on the model in Fig. 4 and the kinetic constants from Table I. B: relative protection against inactivation of the samples in A as a function of the FeSII : Av1 ratio after 3 (•) or 6 (o) min exposure to oxygen. 100% protection corresponds to the activity before exposure to oxygen. 0% protection corresponds to the activity of the sample without FeSII ('0') observed after either 3 or 6 min exposure to oxygen.

Figs. 2A and 2B show that in the three-component protein mixtures, even at the highest FeSII : Av1 ratios, nitrogenase is slowly inactivated by oxygen. Also, previous investigations showed that the three-component protein complex is by no means totally stable [14, 21, 22]. In the presence of only Av1, Av2 is inactivated quite rapidly (appr. 90% inactivation after 10 min exposure to oxygen). This inactivation was ascribed to the dissociation of Av2 from Av1. On the other hand, the Fe protein in the AlF-MgADP stabilized protein complex (Fig.1) is very resistant to oxygen-inactivation (appr. 5%

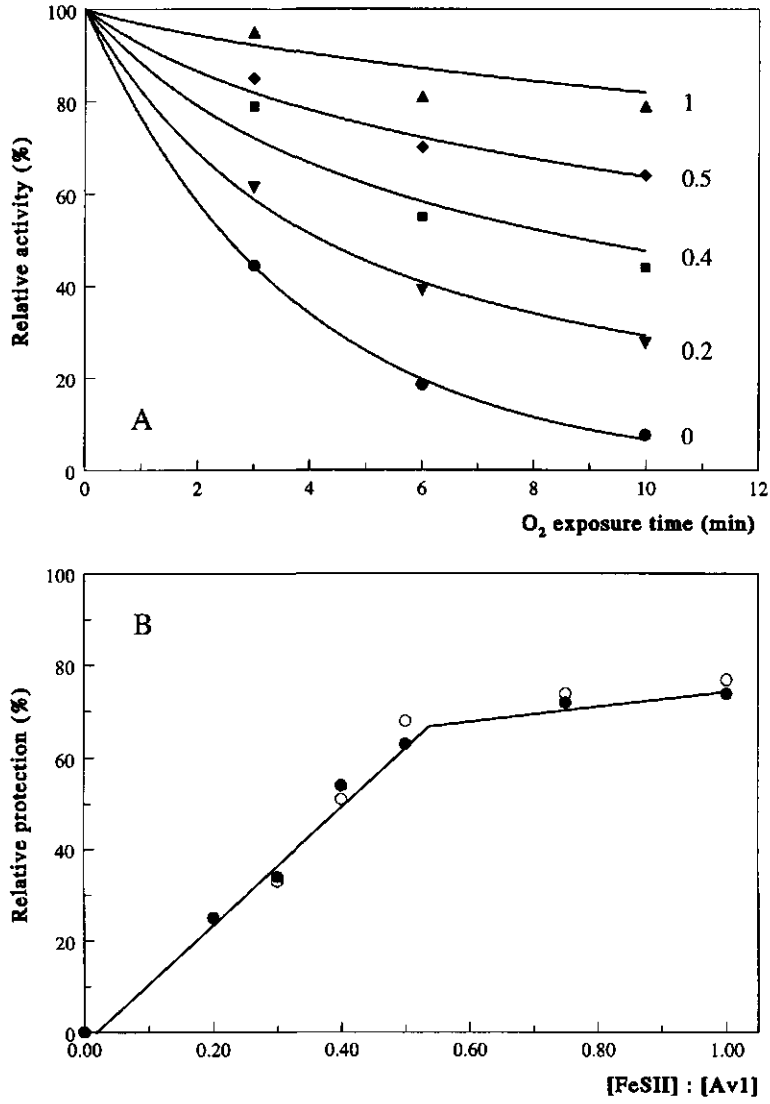

inactivation after 10 min exposure to oxygen). Since Av2 can not dissociate from this AlF-MgADP stabilized complex, this slow inactivation must take place while Av2 is bound to Av1. The rate of inactivation of the three-component protein mixtures at the highest FeSII : Av1 ratios is intermediate between these extremes (appr. 20% inactivation after 10 min exposure to oxygen). It is possible that the rate of inactivation observed for the three-component protein mixtures is determined by the rate of dissociation of FeSII from the three-component protein complex and subsequent dissociation of Av2 from Av1·$[Av2]_2$, and that, similar to the AlF-MgADP stabilized complex, also in the three-component protein complex protection against oxygen-inactivation is based on stabilization of the Av1·$[Av2]_2$ complex.

Reduction of free FeSII and the three-component protein mixtures.

Fig. 3 shows the reduction with 8 mM $Na_2S_2O_4$ (actual reductant 3.35 μM $SO_2^{\bullet-}$) of protein mixtures containing FeSII, Av1 and Av2 in a 1 : 1 : 2 ratio (I) and a 0.5 : 1 : 2 ratio (II), respectively. Reduction of these mixtures by $Na_2S_2O_4$ was followed in a stopped-flow spectrophotometer observing the decrease in absorbance at 430 and 550 nm. The data of both traces I and II can be approximated by single exponential decay with k_{obs} = 0.13 s^{-1} (not shown; the fitted curves in Fig. 3 are discussed below). Free Av2 is reduced, under exactly the same conditions, with k_{obs} = 6.8 s^{-1} [10]. In the presence of excess Av1 reduction of Av2 takes place with k_{obs} = 1.5 s^{-1}; this observed rate is a combination of the rate of dissociation (2.8 μM^{-1} s^{-1}) and association (3.3 μM^{-1} s^{-1}) of the Av1αβ·Av2 species, reduction of free Av2 (k_{obs} = 6.8 s^{-1}) and reduction of Av2 in the Av1αβ·Av2 species (k_{obs} = 0.5 s^{-1}) [10]. The inset in Fig. 3 shows the reduction of purified, free FeSII. The observed rate constant for this process is k_{obs} = 0.39 s^{-1}.

The rate constant observed for the reduction of both the three-component protein mixtures is significantly slower than those observed for the reduction of free FeSII, of free Av2 and of Av2 in the presence of Av1. This means that no significant amounts of free FeSII, free Av2, or Av2 in a Av1·$[Av2]_2$ complex, are present in either of these mixtures. Consequently, when FeSII, Av1 and Av2 are present in a 1 : 1 : 2 ratio (I) practically all of the proteins must be incorporated into a three-component protein complex. This is consistent with the stoichiometry (1.1 : 1 : 2) that was found by Scherings et al. [22]. Apparently, under these conditions one FeSII binds one Av1 plus two Av2 molecules, presumably as one Av1·$[Av2]_2$ complex. Also when FeSII, Av1 and Av2 are present in a 0.5 : 1 : 2 ratio (II) practically all of the proteins must be incorporated into a three-component protein complex. This is in agreement with the data shown in Fig. 2: at the protein ratios used here nitrogenase was almost optimally protected against oxygen-inactivation. Apparently, at relatively low FeSII concentrations, one FeSII is capable of binding two Av1 plus four Av2 molecules, presumably as two Av1·$[Av2]_2$ complexes.

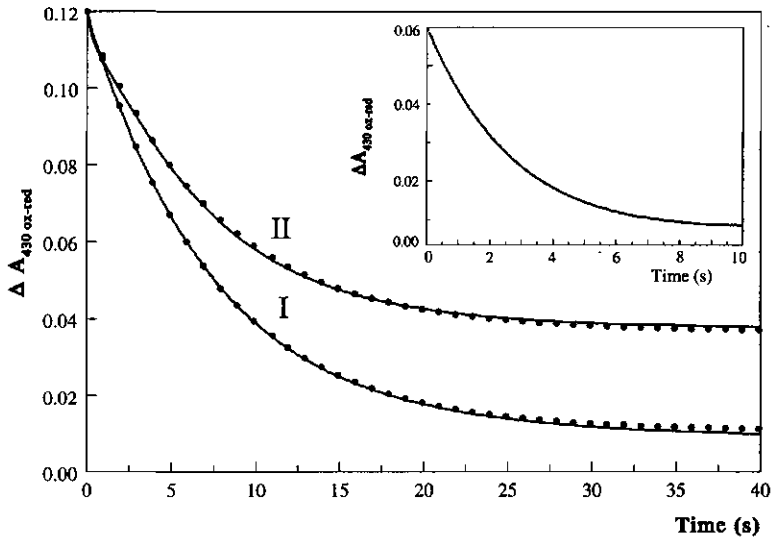

Figure 3

Reduction of free FeSII and the three-component protein mixtures. Stopped-flow traces, recorded at 430 nm, of the reduction, with 8 mM $Na_2S_2O_4$, of the three-component protein mixtures. I: 5 μM FeSII; 5 μM Av1; 10 μM Av2. II: 2.5 μM FeSII; 5μM Av1; 10 μM Av2. Inset: 5 μM FeSII. All in standard buffer. The simulated curves for traces I and II (•marks), are based on the model presented in Fig. 4, the kinetic constants from Table I and the molar extinction coefficients from Materials and Methods.

Computer simulation and fitting of the experimental data.

The proposed mechanism, based on the results described above, is that one FeSII can bind one or two Av1·$[Av2]_2$ complexes, which suppresses the dissociation of Av2 from Av1. If this hypothesis is true, reduction of oxidized Av2 in these complexes must be slow compared to the reduction of the free protein: it is known that the Fe protein from *K. pneumoniae* is not [11] and Av2 only slowly [10] reduced by dithionite when it is bound to the MoFe protein. A kinetic analysis of the reduction of the different mixtures can therefore provide evidence for complex formation as a mechanism of protection against oxygen-inactivation.

Based on the experiments a model (Fig. 4) was set up to describe the reactions involved in the oxygen-inactivation, reduction and complex formation of the proteins in the different mixtures. The possible association of FeSIIδ with Av1αβ·$Av2_{inact}$ (oxygen inactivated Av2 bound to Av1) is not considered in this model. The simulation program Fitsim [34, 35] was used to obtain kinetic constants. The reactions involved, with the values for the rate constants obtained in the present study and by Duyvis et al. [10], are also presented in Table I.

Simulation of the oxygen-inactivation data (Fig. 2A shows the simulated curves together with the corresponding experimental data), which will be discussed first, was done in consecutive steps. An initial value for the rate of inactivation of free Av2 could be determined directly from the data presented in Fig. 1 (trace 'Av2'). The same k_{obs} for the inactivation of Av2 thus obtained and the rate constants for the reversible association

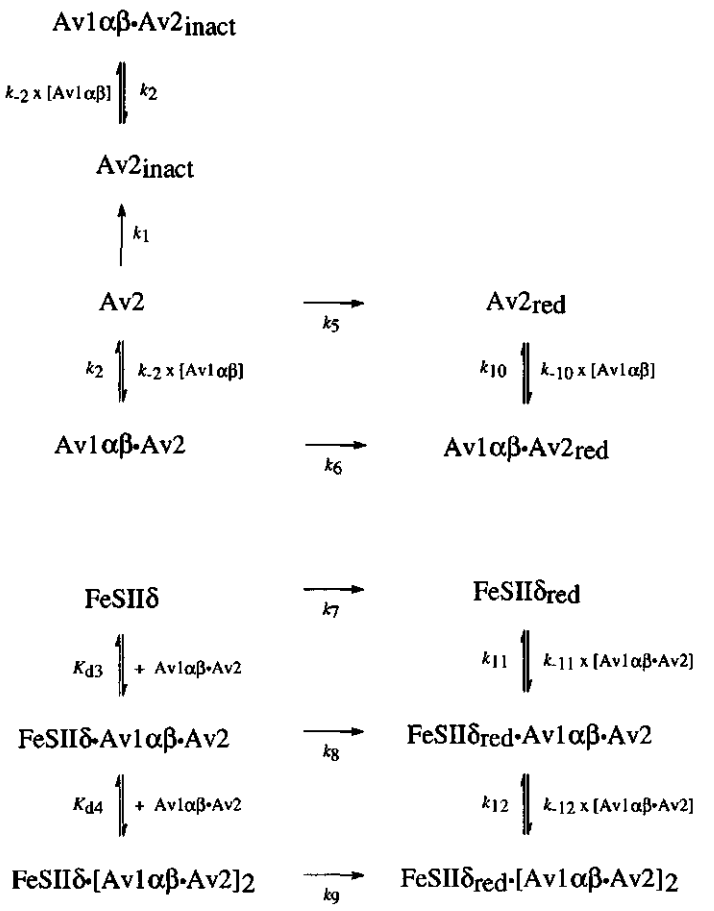

Figure 4

Reactions involved in the model proposed for the oxidative inactivation, complex formation and reduction of FeSII, Av1, Av2. The reactions are also presented, with values for the kinetic parameters, in table I. Reactions 1 and 5-9 are pseudo first-order reactions. Av1αβ represents one of two independently functioning halves of the tetrameric ($\alpha_2\beta_2$) MoFe protein. Each Av1αβ species is assumed to have one binding site for Av2 (γ_2) and one binding site for FeSIIδ. FeSIIδ represents one independently functioning half of the dimeric (δ_2) FeSII protein. Each FeSIIδ species is assumed to have two different binding sites for Av1αβ·Av2.

of Av2 with Av1αβ [10] have been used to describe the inactivation of Av2 in the presence of Av1 (Fig. 2A, trace '0'). The experimental data could be simulated best when both the oxidized and inactivated forms of Av2 were allowed to associate with Av1αβ, thus forming Av1αβ·Av2 and Av1αβ·$Av2_{inact}$ species, respectively, and the rate constants for both interactions were identical. The value for the rate of inactivation of free Av2 by oxygen that resulted from these simulations was $k_1 = 1.8 \times 10^{-2}$ s^{-1}. As is obvious from Fig. 2A the inactivation of Av2 in the presence of Av1 can be simulated quite accurately with this simple and logical model.

Finally, using the values mentioned for the different rate constants, the oxygen-inactivation of the mixtures containing Av1, Av2 and various concentrations FeSII were analyzed. The experimental data obtained for all the FeSII : Av1 ratios used in the oxygen-inactivation assays were fitted simultaneously (only fits and experimental data for the FeSII : Av1 ratios 0, 0.2, 0.4, 0.5 and 1 are shown in Fig. 2A; ratios 0.3 and 0.75 were also investigated and consistent with the presented data). The simulations were relatively insensitive to the actual *k*-values for the rate of association and dissociation of the FeSIIδ·Av1αβ·Av2 and FeSIIδ·$[Av1\alpha\beta \cdot Av2]_2$ species, but did depend on the K_d values. The best fit of the dissociation constant of the FeSIIδ·Av1αβ·Av2 species was found to be $K_{d3} = 95 \pm 44$ nM. Only a minimum value could be determined for the dissociation constant of the FeSIIδ·$[Av1\alpha\beta \cdot Av2]_2$ species, since in the simulations the rate constant for association of the complex (k_{-4}) inclined towards zero. Setting a limit of $k_{-4} = 10^{-3}$ s^{-1}, resulted in $K_{d4} > 2$ μM. Although these are only rough approximations of the dissociation constants of these complexes, the results do suggest that the species FeSIIδ·$[Av1\alpha\beta \cdot Av2]_2$ is not very stable, i.e. the second Av1αβ·Av2 is not bound very firmly to FeSIIδ. When Av1αβ·$Av2_{inact}$ was allowed to participate in the formation of the three-component complexes, the second Av1αβ·Av2 or Av1αβ·$Av2_{inact}$ was bound more firmly than the first one, but the fitting of the experimental data was worse. Also a model that did not take the formation of a FeSIIδ·$[Av1\alpha\beta \cdot Av2]_2$ species into account resulted in simulations that deviated much from the experimental data: both parameters that are indicative for the quality of the fit (the R-squared value and the mean-squared error [35]) become worse. Therefore, the FeSIIδ·$[Av1\alpha\beta \cdot Av2]_2$ species, whether unstable or not, plays an important role in the mechanism by which FeSII protects nitrogenase against oxygen-inactivation. This importance is even more significant in vivo since nitrogenase concentrations in *A. vinelandii* cells are over 50 μM [33], i.e. more than ten times higher than in the in vitro experiments discussed here. Fig. 2 shows that, allowing both the formation of the FeSIIδ·Av1αβ·Av2 and the FeSIIδ·$[Av1\alpha\beta \cdot Av2]_2$ species, and using the obtained kinetic parameters, also the experimental data for the inactivation of the three-component protein mixtures can be simulated quite accurately.

Reaction	Rate constants	Source
$Av2 \xrightarrow{k_1} Av2_{inact}$	$k_1 = 1.8\ 10^{-2}\ s^{-1}$	Present work
$Av1o\beta \bullet Av2_{inact} \underset{k_{-2i}}{\overset{k_{2i}}{\rightleftharpoons}} Av1o\beta + Av2_{inact}$	$k_{2i} = 2.8\ s^{-1}$ $k_{-2i} = 3.3\ \mu M^{-1}\ s^{-1}$	Present work
$Av1o\beta \bullet Av2 \underset{k_{-2}}{\overset{k_2}{\rightleftharpoons}} Av1o\beta + Av2$	$k_2 = 2.8\ s^{-1}$ $k_{-2} = 3.3\ \mu M^{-1}\ s^{-1}$	Duyvis [10]
$FeSII\delta \bullet Av1o\beta \bullet Av2 \underset{k_{-3}}{\overset{k_3}{\rightleftharpoons}} Av1o\beta \bullet Av2 + FeSII\delta$	$K_{d3} = 95$ nM	Present work
$FeSII\delta \bullet [Av1o\beta \bullet Av2]_2 \underset{k_{-4}}{\overset{k_4}{\rightleftharpoons}} Av1o\beta \bullet Av2 + FeSII\delta \bullet Av1o\beta \bullet Av2$	$K_{d4} > 2\ \mu M$	Present work
$Av2 \xrightarrow{k_5} Av2_{red}$	$k_5 = 6.8\ s^{-1}$	Duyvis [10]
$Av1o\beta \bullet Av2 \xrightarrow{k_6} Av1o\beta \bullet Av2_{red}$	$k_6 = 0.5\ s^{-1}$	Duyvis [10]
$FeSII\delta \xrightarrow{k_7} FeSII\delta_{red}$	$k_7 = 0.39\ s^{-1}$	Present work
$FeSII\delta \bullet Av1o\beta \bullet Av2 \xrightarrow{k_8} FeSII\delta_{red} \bullet Av1o\beta \bullet Av2$	$k_8 = 9.8\ 10^{-2}\ s^{-1}$	Present work
$FeSII\delta \bullet [Av1o\beta \bullet Av2]_2 \xrightarrow{k_9} FeSII\delta_{red} \bullet [Av1o\beta \bullet Av2]_2$	$k_9 = 14.8\ 10^{-2}\ s^{-1}$	Present work
$Av1o\beta \bullet Av2_{red} \underset{k_{-10}}{\overset{k_{10}}{\rightleftharpoons}} Av2_{red} + Av1o\beta$	$k_{10} = 25\ s^{-1}$ $k_{-10} = 26\ \mu M^{-1}\ s^{-1}$	Duyvis [10]
$FeSII\delta_{red} \bullet Av1o\beta \bullet Av2 \underset{k_{-11}}{\overset{k_{11}}{\rightleftharpoons}} FeSII\delta_{red} + Av1o\beta \bullet Av2$	Rate constants could not be determined from experimental data.	
$FeSII\delta_{red} \bullet [Av1o\beta \bullet Av2]_2 \underset{k_{-12}}{\overset{k_{12}}{\rightleftharpoons}} FeSII\delta_{red} \bullet Av1o\beta \bullet Av2 + Av1o\beta \bullet Av2$	Rate constants could not be determined from experimental data.	

Table I

Reactions involved in the oxidative inactivation, reduction and complex formation of nitrogenase from *A. vinelandii*. These reactions are also shown in a scheme in Fig. 4. The rate constants related to oxygen-inactivation (reaction 1) and reduction (reactions 5 to 9) are pseudo first-order rate constants measured with 240 μM oxygen and 8 mM $Na_2S_2O_4$ (actual reductant 3.3 μM $SO2^{\bullet-}$) respectively. Shorthand notations are explained in the legend of Fig. 4 and in the Materials and Methods section.

Further kinetic parameters were obtained by simulating the reduction of the three-component protein mixtures, using the kinetic parameters determined so far. The relevant reactions are shown in Fig. 4. The rate of reduction of free FeSII was determined experimentally: this process could be analyzed directly, i.e. without data simulation, by fitting a single exponential decay curve with k_{obs} = 0.38 s^{-1} to the experimental trace (Fig. 3, inset). This curve fitted the experimental data closely, both at 430 nm and at 550 nm. The rates of reduction of free Av2 and of Av2 in the presence of Av1 are known from literature; a detailed kinetic analysis of the rate of reduction of the Av1αβ·Av2 species, of the dissociation of this species, both in the reduced and oxidized form, and of the reduction of free Av2 will be published elsewhere [10].

Using all the kinetic parameters and extinction coefficients thus obtained, curves based on the kinetic model shown in Fig. 4 were fitted, simultaneously, to the experimental data obtained for the reduction of the three-component protein mixtures at both 430 and 550 nm. This yielded the pseudo first-order rate constants for the reduction of FeSIIδ in the FeSIIδ·Av1αβ·Av2 species (k_8 = 9.8 (± 0.1) 10^{-2} s^{-1}) and for the reduction of FeSIIδ in the FeSIIδ·[Av1αβ·Av2]$_2$ species (k_9 = 14.8 (± 0.03) 10^{-2} s^{-1}). The standard errors for the rate constants for the dissociation and association of the reduced FeSIIδ_{red}·Av1αβ·Av2 species and for the reduced FeSIIδ_{red}·[Av1αβ·Av2]$_2$ species were relatively large, indicating that the simulation is not very dependent on these parameters. This is a consequence of the fact that the rate of dissociation of these reduced species is relatively fast compared to the rate of reduction of FeSIIδ in the FeSIIδ·Av1αβ·Av2 and FeSIIδ·[Av1αβ·Av2]$_2$ species. The kinetic parameters for dissociation and association of these reduced species were therefore left out of further consideration. Experimental data for the reduction of the three-component protein mixtures, at 430 nm, are compared with the simulations in fig. 3. As is obvious from this figure the experimental data can be explained adequately with the presented model.

Discussion

The [4Fe-4S] cluster in the Fe protein is located at the surface of the dimeric protein, exposed to the solvent [1]. Although the three dimensional structure of the Fe protein-MoFe protein complex has not yet been solved, results obtained by the study of altered proteins prepared by site-directed mutagenesis have indicated that amino acid residues surrounding the [4Fe-4S] cluster in the Fe protein interact with the MoFe protein when these proteins are associated [36-38]. A docking model based on the crystal structures of the Fe and MoFe proteins and these amino-acid substitution studies

[39-41], suggests that when the Fe protein is bound to the MoFe protein its [4Fe-4S] cluster is no longer exposed to the solvent, but is buried in the Fe protein-MoFe protein interface. The crystal structure of the AlF-MgADP stabilized nitrogenase complex shows that also in this complex the [4Fe-4S] clusters are buried in the Fe protein-MoFe protein interface [25]. We propose that this buried position prevents the disintegration of the cluster upon oxidation.

Some interesting similarities exist between the AlF-MgADP stabilized two-component protein complex and the FeSII stabilized three-component protein complex. Formation of the three-component protein complex requires that the Fe and FeSII proteins involved are oxidized; the [4Fe-4S] cluster of the Fe protein in this complex is in the oxidized state [22, 42]. Duyvis et al. [8] demonstrated that in the AlF-MgADP stabilized complex the [4Fe-4S] cluster of the Fe protein is also in the oxidized state, even though this complex was prepared in the presence of the reducing agent dithionite. In addition, both these complexes are relatively resistant to oxygen-inactivation. These similarities suggest that protection against oxygen-inactivation by these protein complexes is based on the same principle: stabilization of the Fe protein-MoFe protein complex.

Since no structure is available for the three-component protein complex one can only speculate on its configuration and spatial organization. The FeSII protein may link Fe protein-MoFe protein complexes to form polymers, in which case the observed stoichiometry of one FeSII protein per Fe protein-MoFe protein complex would allow interaction of the FeSII protein with either the Fe protein or the MoFe protein. It is very unlikely, however, that the FeSII protein interacts directly with the Fe protein in a complex in which the FeSII protein binds only one or two Fe protein-MoFe protein complexes. First, the minimal stoichiometry of the three-component protein complex determined in this study (one dimeric FeSII protein per two Fe protein-MoFe protein complexes, i.e. per four Fe proteins) makes direct interaction of the FeSII protein with the Fe protein improbable. Furthermore, earlier studies have indicated that the FeSII protein has only a small effect on the stability of the Fe protein in the absence of the MoFe protein; also no fixed Fe protein : FeSII protein stoichiometry was found in the absence of the MoFe protein [13]. We therefore propose that the FeSII protein interacts with the MoFe protein in the Fe protein-MoFe protein complex, resulting in stabilization of the Fe protein-MoFe protein complex.

The kinetics of the reduction of the three-component protein mixtures indicate that the FeSII and Fe proteins, at both stoichiometries investigated, are incorporated in a three-component protein complex, which points at the existence of two different forms of three-component protein complexes. Size-exclusion chromatography and analytical ultracentrifugation of the in vitro prepared three-component protein complex already

demonstrated that this complex exists in more than one form [22]. In the model presented here one form has a stoichiometry of one dimeric FeSII protein per Fe protein-MoFe protein complex, which is in agreement with the stoichiometry of the complex as isolated from *A. vinelandii* [20], the other form has a stoichiometry of one dimeric FeSII protein per two Fe protein-MoFe protein complexes, which is in agreement with the minimal stoichiometry that is required to obtain almost optimal protection against oxygen-inactivation. The simulations of the oxygen-inactivation assays showed that complex formation of the FeSII protein with two Fe-protein-MoFe protein complexes plays an important role in the protection against oxygen-inactivation.

Fig. 5 shows a schematic drawing of one of the possible spatial organizations of the three-component protein complexes, taking into account the considerations about the interaction of the FeSII protein with the MoFe protein and the model that was used to simulate the experimental data.

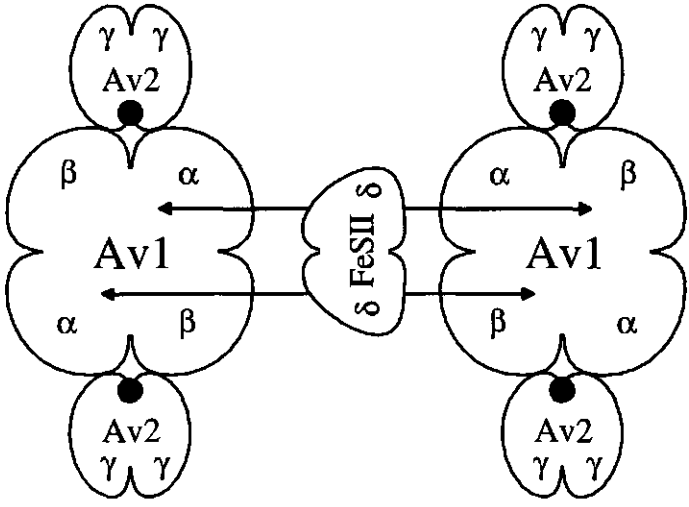

Figure 5

Schematic representation of one of the possible spatial organizations of the three-component protein complexes. FeSII binds Av1 perpendicular to both the Av1·[Av2]$_2$ complexes, i.e. these complexes must be considered to be rotated, facing FeSII. Black dots indicate the [4Fe-4S] cluster in the Fe protein. Kinetic species, used for data simulation, are the top or bottom halves of the physical complexes depicted here. Arrows indicate sites on the independent Av1αβ·Av2 species where the independent FeSIIδ species can bind. Such binding sites may be located on one α or β subunit or on both the subunits.

Acknowledgments

We thank F. Moshiri and R. Maier from the John Hopkins University in Baltimore, USA, for providing us with the plasmid pAVFeSII, harboring the structural gene for the FeSII protein, and professor C. Veeger for his continuous support and interest. This investigation was supported by the Netherlands Foundation for Chemical Research (SON) with financial aid from the Netherlands Organization for Scientific Research (NWO).

References

1 Georgiades, M.M., Komiya, H., Chakrabarti, P., Woo, D., Kornuc, J.J. and Rees, D.C. (1992) *Science 257*, 1653 - 1859
2 Kim, J. and Rees, D.C. (1992) *Nature 360*, 553 - 560
3 Shah, V.K. and Brill, W.J. (1977) *Proc. Natl. Acad. Sci. USA 74*, 3249 - 3253
4 Hawkes, T.R., McLean, P.A. and Smith, B.E. (1984) *Biochem. J. 217*, 317 - 321
5 Bolin, J.T., Ronco, A., Morgan, T.V., Morteson, L.E. and Xuong, N.H. (1993) *Proc. Natl. Acad. Sci. USA 90*, 1078 - 1082
6 Peters, J.W., Stowell, M.H.B., Soltis, M., Finnegan, M.G., Johnson, M.K. and Rees, D.C. (1997) *Biochemistry 36*, 1181 - 1187
7 Lowe, D.J. and Thorneley, R.N.F. (1984) *Biochem. J. 224*, 877 - 886
8 Duyvis, M.G., Wassink, H. and Haaker, H. (1994) *Eur. J. Biochem 225*, 881 - 890.
9 Duyvis, M.G., Wassink, H. and Haaker, H. (1996) *J. Biol. Chem. 47*, 29632 - 29636.
10 Duyvis, M.G., Wassink, H. and Haaker, H. (1997) *Biochemistry*, submitted
11 Lowe, D.J., Ashby, G.A., Brune, M., Knights, H., Webb, M.R. and Thorneley, R.N.F. (1995) in: *Nitrogen fixation: fundamentals and applications* (Tikhonovich I.A., Romanov V.F. and Provorov N.A., Eds.) pp. 103 - 108, Kluwer Academic Publications, Dordrecht.
12 Thorneley, R.N.F. and Lowe, D.J. (1983) *Biochem. J. 215*, 393 - 403
13 Veeger, C., Laane, G., Scherings, G., Matz, L, Haaker, H. and Van Zeeland-Wolbers, L. (1980) in: *Nitrogen Fixation* (Newton W.E. and Orme-Johnson W.H. Eds.) vol. I, pp. 111 - 137, University Park Press, Baltimore.
14 Wang, Z.C., Burns, A. and Watt, G.D. (1985) *Biochemistry 24*, 214 - 221.
15 Robson, R.L. (1979) *Biochem. J. 181*, 569 - 575.
16 Yates, M.G. (1988) in: *The Nitrogen and Sulphur Cycles* (Cole J.A. and Ferguson S.J.. Eds.) pp. 383 - 416, Cambridge University Press, Cambridge.
17 Gallon, J.R. (1992) *New Phytol. 122*, 571 - 609.
18 Kelly, M.J.S., Poole, R.K., Yates, M.G. and Kennedy, G. (1990) *J. Bacteriol. 172*, 6010 - 6019.
19 Shethna, Y.I, DerVartanian, D.V. and Beinert, H. (1968) *Biochem. Biophys. Res. Comm. 31*, 862 - 867.
20 Scherings, G., Haaker, H. and Veeger, C. (1977) *Eur. J. Biochem. 77*, 621 - 630.
21 Moshiri, F, Kim, J.W., Fu, C. and Maier, R.J. (1994) *Mol. Microbiol. 14*, 101 - 114.

22 Scherings, G., Haaker, H., Wassink, H. and Veeger, C. (1983) *Eur. J. Biochem. 135*, 591 - 599.
23 Renner, K.A. and Howard, J.B. (1996) *Biochemistry 35*, 5353 - 5358.
24 Duyvis, M.G., Wassink, H. and Haaker, H. (1996) *FEBS Lett. 380*, 233 - 236.
25 Schindelin, H., Kisker, C., Schlessman, J.L., Howard, J.B. and Rees, D.C. (1997) *Nature 387*, 370 - 376
26 Moshiri, F., Course, B. R., Johnson, M.K. and Maier, R.J. (1995) *Biochemistry 34*, 12973 - 12982.
27 DerVartanian, D.V., Shethna, Y.I. and Beinert, H. (1969) *Biochim. Biophys. Acta 194*, 548 - 563.
28 Goa, J. (1953) *Scand. J. Clin. Lab. Invest. 5*, 218 - 222.
29 Bensadoun, A., and Weinstein, D. (1976) *Anal. Biochem. 70*, 241 - 250.
30 Braaksma, A., Haaker, H., Grande, H.J. and Veeger, C. (1982) *Eur. J. Biochem. 121*, 483 - 491.
31 Martin, R.B. (1988) *Biochem. Biophys. Res. Com. 155*, 1194 - 1280
32 Ashby, G.A. and Thorneley, R.N.F. (1987) *Biochem. J. 246*, 455 - 465
33 Klugkist, J., Haaker, H., Wassink, H. and Veeger, C. (1985) *Eur. J. Biochem. 146*, 509 - 515
34 Barshop, B.A., Wrenn, R.F. and Frieden, C. (1983) *Anal. Biochem. 130*, 134 - 145.
35 Zimmerle, C.T. and Frieden, C. (1989) *Biochem. J. 258*, 381 - 387
36 Lowery, R.G., Chang, C.L., Davis, L.C., McKenna, M.C., Stephens, P.J. and Ludden, P.W. (1989) *Biochemistry 28*, 1206 - 1212.
37 Seefeldt, L.C. (1994) *Protein Sci. 3*, 2073 - 2081.
38 Wolle, D., Kim, C.H., Dean, D.R. and Howard, J.B. (1992) *J. Biol. Chem. 267*, 3667 - 3673.
39 Howard, J.B. and Rees, D.C. (1994) *Annu. Rev. Biochem. 63*, 235 - 264.
40 Howard, J.B. (1993) in: *Molybdenum enzymes* (Stiefel E.L., Coucouvanis D. and Newton W.E., Eds.) pp. 271 - 289, Chapman and Hall, New York.
41 Peters, J.W., Fisher, K. and Dean, D.R. (1995) *Annu. Rev. Microbiol. 49*, 335 - 366.
42 Simpson, F. and Burris, R.H. (1984) in: *Advances in nitrogen fixation research* (Veeger C. and Newton W.E., eds.) p. 243, Nijhoff and Junk Publishers, The Hague, The Netherlands.

Chapter 4

Redox properties and electron paramagnetic resonance spectroscopy of the transition state complex of *Azotobacter vinelandii* nitrogenase

Johan H. SPEE, Alexander F. ARENDSEN, Hans WASSINK, Sophie J. MARRITT, Wilfred R. HAGEN and Huub HAAKER

Abstract

Substrate reduction catalyzed by nitrogenase requires the association of the iron (Fe) protein and the molybdenum-iron (MoFe) protein, MgATP-dependent electron transfer from the Fe protein to the MoFe protein, and on-enzyme MgATP hydrolysis, followed by protein-protein complex dissociation. Aluminum fluoride (AlF) plus MgATP or MgADP inhibit nitrogenase by stabilizing the protein-protein complex of an intermediate of the on-enzyme MgATP hydrolysis reaction. We report here the redox properties and electron paramagnetic resonance (EPR) signals of the AlF-MgADP stabilized transition state complex of *Azotobacter vinelandii* nitrogenase. The midpoint potential of the iron-molybdenum-sulfur-homocitrate cluster in the MoFe protein remains unchanged, but that of the [4Fe-4S] cluster in the Fe protein, and of the unique [8Fe-7S] cluster in the MoFe protein are both lowered. Furthermore a change in spin-state of the EPR signal of the two electrons oxidized [8Fe-7S] cluster was observed. The present results reveal a possible mechanism of MgATP hydrolysis driven electron transport within the nitrogenase protein complex: conformational changes of the protein complex during the on-enzyme MgATP hydrolysis lower the potential of [4Fe-4S] cluster of Fe protein and that of the [8Fe-7S] cluster of MoFe protein. This process turns both clusters into effective reductants for substrate reduction at the iron-molybdenum-sulfur-homocitrate cluster, the putative substrate-binding site of nitrogenase.

Introduction

Nitrogenase catalyzes the biological reduction of N_2 to NH_3. The enzyme complex consists of two dissociable metalloproteins: the molybdenum-iron (MoFe) protein, an $\alpha_2\beta_2$ tetramer which contains two unique [8Fe-7S] clusters (P-cluster) plus two iron-molybdenum-sulfur-homocitrate clusters (FeMoco) [1], and the Fe protein, a γ_2 dimer that contains a single [4Fe-4S] cluster [9]. Substrate-binding, activation and reduction take place on the MoFe protein, presumably on FeMoco. The Fe protein provides the MoFe protein with the required electrons and couples ATP-hydrolysis to the substrate reduction (see [2] for a review). A kinetic mechanism for nitrogenase catalysis has been described by Lowe and Thorneley [3] and was recently modified [4-6]. The Fe protein associates with the MoFe protein; each $\alpha\beta$-half of the MoFe protein has an independent binding site for one Fe protein. Binding of MgATP to the Fe protein induces a conformational change in the Fe protein-MoFe protein complex that is necessary for

electron transfer from the Fe protein to the MoFe protein; this reaction is followed by hydrolysis of MgATP after which the oxidized Fe protein, with MgADP bound, dissociates from MoFe protein [4]. With dithionite as the reductant, this dissociation is the rate-limiting step [7, 8]. Next, the oxidized Fe protein is reduced and two MgADP molecules are replaced by two MgATP molecules preparing the Fe protein for a second round of docking to the MoFe protein and subsequent electron transfer. This cycle is repeated until sufficient electrons have accumulated to reduce N_2 bound to FeMoco.

The association of the MoFe protein with the Fe protein and the interaction with MgATP has a central role in this process. A clue to how the hydrolysis of MgATP facilitates electron transfer within nitrogenase came from the crystal structure of the Fe protein. A close structural similarity was observed between the nucleotide-binding sites of the Fe protein from *A. vinelandii* and the molecular switch protooncogenic *ras* protein p21 [9]. This similarity suggested that MgATP-binding and hydrolysis might switch nitrogenase between different conformations. Evidence for this hypothesis was presented by Lanzilotta et al. [10]. By using the altered Fe protein, L127Δ, that resembles the Fe protein in the MgATP-bound conformation without MgATP bound, Lanzilotta et al. showed that only the ATP-bound conformation is necessary for electron transfer from the Fe- to the MoFe protein and that the two proteins form a tight complex in this conformation. By using an other altered Fe protein (D39N), it was shown that after electron transfer and MgATP hydrolysis, the protein-protein complex could not change to its MgADP-bound conformation, which completely prevented dissociation of the protein-protein complex [11]. Additional evidence for the MgATP hydrolysis driven conformational changes of the protein-protein complex came from inhibition of nitrogenase by aluminum fluoride. It was shown that aluminum fluoride in the presence of MgATP or MgADP inhibits nitrogenase by stabilization of the protein-protein complex [12, 13]. From solution X-ray scattering, a low resolution structure of the *Klebsiella pneumoniae* AlF-inhibited nitrogenase was obtained [14]. The agreement between the docking model constructed from the crystal structures of the separate proteins [2] and the solution X-ray scattering structure is good except for flexible, solvent exposed loop sections of the MoFe protein and parts of the Fe protein. The data suggest that the conformation of the AlF-MgADP stabilized nitrogenase is more compact than that of the separate proteins. Nitrogenase and protooncogenic *ras* proteins have similar aluminum fluoride-binding characteristics. The Fe protein and Ras alone do not bind or become (in)activated by aluminum fluoride alone; only in the presence of the nucleotide diphosphate and their physiological partner (the MoFe protein or the guanosine triphosphatase activating protein, respectively) a stable complex was formed [12, 13, 15]. Crystal structures of GDP or ADP and aluminum fluoride-binding proteins revealed that aluminum fluoride binds with a geometry resembling that of the putative transition

state of the G(A)TPase mechanism: an octahedrally coordinated Al ion with four F ligands, one O from the ß phosphate of G(A)DP and one from a water molecule [16-18]. It is therefore very likely that the AlF-MgADP inhibited nitrogenase represent the transition state for the S_N2 on-enzyme ATPase reaction of nitrogenase. The redox properties and the EPR signals of both the purified Fe- and the MoFe proteins have been investigated extensively. In the present paper we report on the redox properties and EPR signals of the putative transition state analogue of the on-enzyme ATPase reaction of nitrogenase. The mechanistic significance of the data is discussed.

Materials and methods

Preparation of the aluminum fluoride-MgADP inhibited nitrogenase.

Azotobacter vinelandii ATCC strain 478 was grown and the nitrogenase MoFe- and Fe proteins were isolated and characterized as described elsewhere [4]. The molar concentrations of the MoFe- and Fe protein were calculated from their molecular masses of 230 kDa and 63 kDa, respectively. Aluminum fluoride MgADP inhibited nitrogenase (transition state complex) was prepared as described by Duyvis et al. [12]. The specific activity of this complex, as detected by the acetylene reduction assay, was less than 0.06 mol ethylene s^{-1} (mol MoFe)$^{-1}$, (less than 1% of the maximal MoFe protein activity). Aluminum and fluoride form compounds of the general composition $AlF_x(OH^-)_y$. In the pH range 5 - 8 and with millimolar fluoride concentrations at least five different mixed OH^- and F^- complexes of Al^{3+} are present [19]. Consequently we use 'aluminum fluoride' or 'AlF' as the general abbreviation for all forms of aluminum, fluoride and OH^- coordination.

Redox titration and EPR spectroscopy of the transition state complex.

Dye mediated redox titrations of the transition state complex of nitrogenase were done in an anaerobic cell under purified argon. The protein / mediator mixture was in 50 mM Tris/HCl, pH 8.0. The final complex concentration was 56 µM with respect to the MoFe protein. Methyl- and benzyl-viologen, 2,2'-Bipyridinium-N,N'-di-propylsulfonate, neutral red, safranin-O, phenosafranin, anthraquinone-2-sulfonate, phenazine ethosulfate, 2,6 dichlorophenol-indophenol, resorufin, tetramethyl-p-phenylenediamine, 2-hydroxy 1,4-napthoquinone, indigo disulfonate and methylene blue mediators were used at a final concentration of 40 µM. The redox potential was adjusted with freshly prepared $Na_2S_2O_4$, and potassium ferricyanide solutions in 0.5 M Tris/HCl, pH 8.0. Potentials reported in this paper are relative to the normal hydrogen electrode (NHE) and were

obtained by using a potential of + 246 mV (vs. NHE) for the saturated calomel electrode at 22 °C [20]. EPR spectra were taken on a Bruker ER 200D spectrometer with peripheral equipment, as described in [21]. Parallel mode spectra were taken with the ER4116 dual-mode resonator. Spectra were simulated as multicomponent effective S=1/2 powder patterns broadened by g-strain collinear with the Zeeman interaction [22].

Stopped-flow analysis of the formation of the transition state complex.

The kinetics of the formation of the AlF-MgADP stabilized transition state complex was analyzed by rapid mixing of the nitrogenase proteins with MgATP and aluminum fluoride in a Hi-Tech SF-51 stopped-flow spectrophotometer (Salisbury, Wilts, UK) equipped with an anaerobic kit and a data acquisition and analysis system. One syringe of the stopped-flow spectrophotometer contained 20 μM MoFe protein, 120 μM Fe protein and 10 mM $Na_2S_2O_4$ in 50 mM TES/NaOH, pH 7.4 and 5 mM $MgCl_2$. The other syringe contained 10 mM MgATP, 0.8 mM $AlF_3 \cdot H_2O$, 8.0 mM KF and 10 mM $Na_2S_2O_4$ in the same buffer. The mixing ratio was 1:1. Absorbance changes, for detection of oxidation and reduction of the Fe protein, were recorded at 430 nm.

Results and discussion

Stopped-flow analysis of the formation of the transition state complex.

Fig. 1 shows the changes in absorbance (ΔA_{430}) of the dithionite-reduced Fe protein upon addition of aluminum fluoride and / or MgATP. The observations can be explained with the current model for the interaction of the nitrogenase proteins, described in the Introduction. In the presence of dithionite the Fe protein is reduced and under the experimental conditions both binding sites on the MoFe protein will be occupied by Fe protein with MgATP bound within the the mixing time of the stopped-flow apparatus [3]. Within 0.1 s after mixing with MgATP the bound Fe protein is oxidized (Fig 1, inset): binding of MgATP induces a structural change in the protein-protein complex that allows the transfer of one electron from the Fe protein to the MoFe protein. Oxidation of the Fe protein is followed by on-enzyme ATP hydrolysis and dissociation of the oxidized Fe protein from the MoFe protein. With dithionite as the reductant, this dissociation is the rate limiting step in the catalytic cycle (2.8 s^{-1} at 20 °C); after dissociation, the Fe protein is reduced at 6.8 s^{-1} [34]. Since the Fe protein is present in excess, the docking sites on the MoFe protein are rapidly reoccupied by reduced Fe protein. These kinetics result in the oxidation of 30% of Fe protein, mainly bound to the MoFe protein (the inset of Fig. 1 shows a ΔA_{430} of about 0.1, which corresponds to oxidation of approximately

20 μM Fe protein, whereas 60 μM was present in the sample). After a few seconds, the MgADP concentration increases and, consequently, increasing amounts of reduced Fe protein with MgADP bound will occupy the Fe protein-binding sites on the MoFe protein. This is observed as a decrease of the absorbance at 430 nm: the Fe protein is not oxidized since MgADP inhibits electron transfer to the MoFe protein. Because dithionite is present in excess, MgADP inhibition results in a steady increase of the amount of reduced Fe protein. When no aluminum fluoride is added (trace 'ATP') the ADP inhibition and reduction of the Fe protein are completed within 50 s.

When aluminum fluoride is present, however, the system does not reach this redox state (trace 'ATP + AlF'). Initially there is no significant difference between the two samples (Fig. 1, inset): the maximal amount of Fe protein is oxidized upon the addition of ATP, resulting in a rapid increase of the absorbance, and the subsequent re-reduction of the protein results in a decrease. In time, however, the absorbance increases again, suggesting oxidation of Fe-S clusters. After 250 s this oxidation reaches its

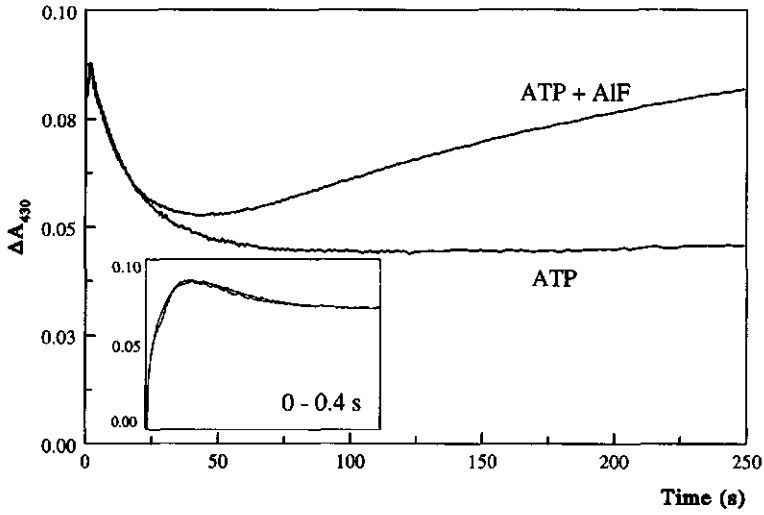

Figure 1

Stopped-flow spectroscopy of the formation of the AlF-MgADP stabilized transition state complex. Changes in absorbance were measured at 430 nm. At this wavelength, the absorbance is largely determined by the oxidation state of the [4Fe-4S] clusters of the Fe protein; contributions of the clusters of the MoFe protein are negligible. 'ATP': dithionite reduced MoFe protein and Fe protein were mixed with MgATP. 'ATP + AlF': dithionite reduced MoFe protein and Fe protein were mixed with MgATP and AlF. Inset: the 'ATP' and 'ATP + AlF' traces, as defined above, during the first 0.4 s. Final concentrations: MoFe protein 10 μM; Fe protein 60 μM; $Na_2S_2O_4$ 10 mM; AlF_3 0.4 mM; KF 4 mM; MgATP 5 mM.

maximal value. Complex formation with AlF and MgADP was confirmed by parallel experiments: samples of the incubations were taken and after dilution the activity of the MoFe protein was tested. It was found that after an incubation time of 250 s all MoFe protein activity was inhibited by complex formation (data not shown). The redox changes occurring during the formation of the AlF-MgADP stabilized transition state complex were confirmed by redox titration and EPR spectroscopy.

Redox titration and EPR spectroscopy: the [4Fe-4S] cluster.

The [4Fe-4S] cluster of the Fe protein is a one-electron donor that operates between the +1 and +2 oxidation levels. There has been one report that the hydroquinone form of methylviologen can reduce the [4Fe-4S] cluster to its all ferrous state [23]. The cluster is diamagnetic in the oxidized state. Reduced by dithionite, in a one-electron process with E_m = -473 mV for the Fe protein with MgADP bound, or E_m = -435 mV for the Fe protein with MgATP bound [24], the cluster exhibits EPR spectra from non-interacting mixtures of S=3/2 and S=1/2 spin states [25]. However, no significant S=3/2 or S=1/2 EPR signals with g-values characteristic for the Fe protein could be detected in the samples containing the AlF-MgADP stabilized transition state complex at redox potentials between -500 and +100 mV. The very weak signal that is observed is probably caused by a small amount of free Fe protein. This suggests that the Fe protein in the AlF-MgADP stabilized transition state complex is diamagnetic, and therefore oxidized, within this potential range. We do not think that the absence of an EPR signal of the Fe protein is caused by the formation of the all ferrous state of the [4Fe-4S] cluster. If this is the case, the cluster must stay in its all ferrous state from -500 to +100 mV, which is very unlikely. In addition to this, we found that, under the conditions used, the free Fe protein could not be reduced to its all ferrous state: the intensity of the S=3/2 and S=1/2 signals did not change when the protein was incubated with 10 mM dithionite at pH values between 7.5 and 10 (under these conditions the E_h changes from approximately -550 to -700 mV, respectively). The conclusion must be that the specific conformation of the transition state complex lowers the midpoint potential of the Fe protein to a value significantly less than -500 mV, thus inducing the transfer of one electron to the MoFe protein and disabling the re-reduction of the Fe protein by dithionite.

Redox titration and EPR spectroscopy: FeMoco.

Previous studies have shown that the purified, dithionite-reduced MoFe protein exhibits only an S=3/2 EPR signal that is assigned to the iron-molybdenum-sulfur-homocitrate cofactor (FeMoco) [26]. Under turnover conditions, i.e. in the presence of reduced Fe protein and MgATP, the S=3/2 FeMoco signal disappears, presumably because of so-called super-reduction of the cofactor: the Fe protein transfers at least one

electron to the dithionite-reduced FeMoco [27, 28]. The dithionite-reduced FeMoco can also be oxidized to a diamagnetic redox state [29]. For this one-electron process, midpoint potentials of -100 mV [30] and -42 mV [31] have been reported. Fig. 2. shows that the EPR spectrum observed for the AlF-MgADP stabilized transition state complex is in good agreement with this. At low redox potentials an S=3/2 signal is observed with g = 3.7 that changes into S=0 (diamagnetic) with a midpoint potential of about -100 mV. Super-reduction of FeMoco was not observed within the given potential range (-500 to +100 mV). In conclusion, redox properties and EPR spectra of the FeMoco in the AlF-MgADP stabilized transition state complex are not different from those observed for the purified MoFe protein.

Redox titration and EPR spectroscopy: the P-cluster.

Different from FeMoco, the P-cluster is diamagnetic in the presence of dithionite [26, 31]. This situation has been proposed by Münck et al. [26] to correspond to the all-ferrous, uncharged cluster, which is therefore designated P^0. Upon oxidation of P^0, in a two-electron process with E_m = -307 mV, an S=3 signal appears in the EPR spectrum [31]. However, the existence of a one-electron oxidized P-cluster, P^{1+}, has also been

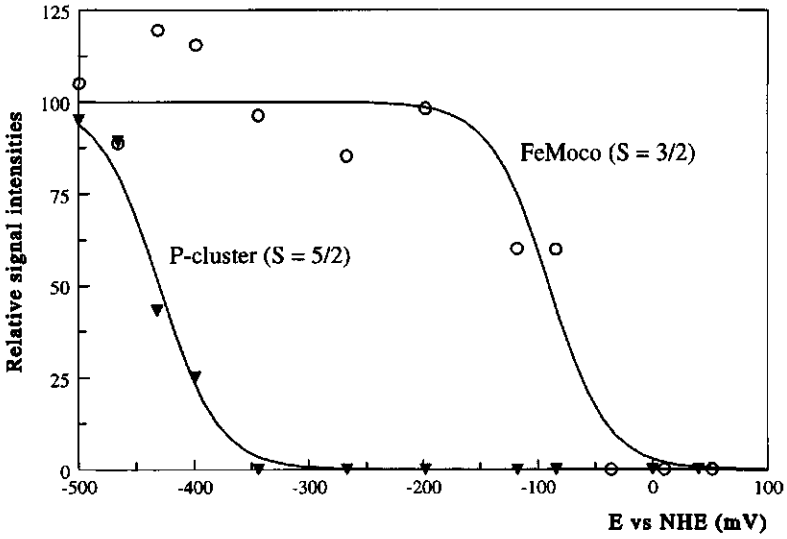

Figure 2

Redox titration of the AlF-MgADP stabilized transition state complex.
The solid lines are least-squares fits to the n = 1 Nernst equation with E_m = -90 mV for the iron-molybdenum cofactor (S=3/2) and E_m = -430 mV for the P-cluster (S=5/2) of the MoFe protein.

proposed and is associated with a physical, i.e. non-interacting, mixture of S=5/2 and S=1/2 signals [32]. The midpoint-potential for abstraction of the first electron, $P^0 \rightarrow P^{1+}$, is believed to be close to that for abstraction of the second electron, $P^{1+} \rightarrow P^{2+}$. The P^{2+} clusters can be oxidized further to form P^{3+} clusters in a one-electron process with a midpoint potential of +90 mV, resulting in S=7/2 and S=1/2 signals [31]. As for the purified protein, the S=5/2 signal is difficult to detect in the AlF-MgADP stabilized transition state complex because the coefficient D of the zero-field interaction is negative: the S=5/2 multiplet is inverted and the EPR detected $|\pm 1/2\rangle$ doublet is an excited state. At low temperatures the signals are too weak for detection by depopulation of the $|\pm 1/2\rangle$ doublet, at higher temperatures the signals are broadened by spin-lattice relaxation.

Fig. 3 shows the S=5/2 P-cluster signal and S=3/2 FeMoco signal at 23 K. At low temperature (4.2 K) the S=5/2 signal disappears and the two samples (A and B) give identical FeMoco S=3/2 spectra (not shown).

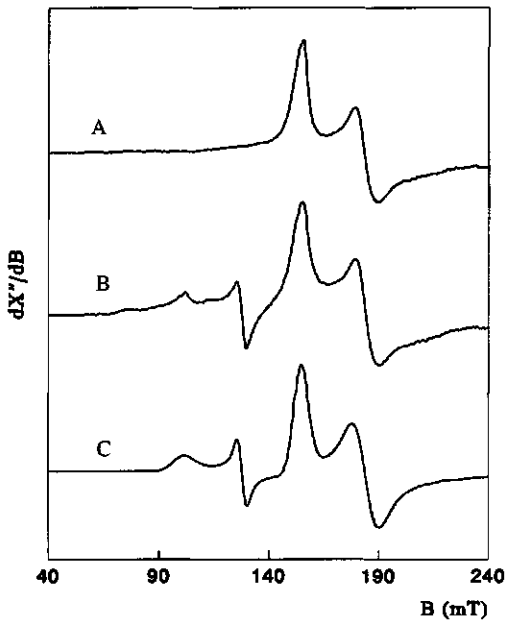

Figure 3

Low-field EPR spectra of the AlF-MgADP stabilized transition state complex poised at different redox potentials. The samples were 56 μM with respect to the MoFe protein in 50 mM Tris/HCl, pH 8.0. Trace A: complex poised at -287 mV (FeMoco S=3/2 signal). Trace B: complex poised at -462 mV (FeMoco S=3/2 and P-cluster S=5/2 signals). Trace C: simulation of trace B (see Table I). EPR conditions: microwave frequency, 9.41 GHz; microwave power, 200 mW; modulation frequency, 100 kHz; modulation amplitude, 0.8 mT; temperature 23 K.

Fig. 4 shows the dependence of the S=5/2 signal intensity on temperature, both experimental and theoretical. The dependence of the S=5/2 signal on the redox potential is shown in Fig. 2. Not only the negative zero-field interaction, but also the fact that the midpoint-potential for the transition of P^0 to P^{1+} is close to that for P^{1+} to P^{2+}, makes the S=5/2 signal difficult to detect in the free MoFe protein. In the AlF-MgADP stabilized transition state complex, however, these potentials are further apart and the S=5/2 signal can be discerned more easily. The signal appears (upon oxidation of P^0 to P^{1+}) at a potential < -500 mV, out of the range of these experiments. The midpoint potential associated with the disappearance of the S=5/2 signal at increasing redox potentials, i.e. the oxidation of P^{1+} to P^{2+}, is about -430 mV. Since, in the purified MoFe protein, this value is about -310 mV [31] the midpoint potential for abstraction of the second electron from the P-cluster is lowered in the transition state complex. The S=3 signal, that is exhibited by P^{2+} in the purified MoFe protein [31, 32], was hardly detectable in the AlF-MgADP stabilized transition state complex. Possibly S=0 for P^{2+} in this complex; the weak S=3 signal that was detectable at E_h = -250 mV may be caused by a small amount of free MoFe protein in the sample. Whatever the spin-state of P^{2+} in the transition state

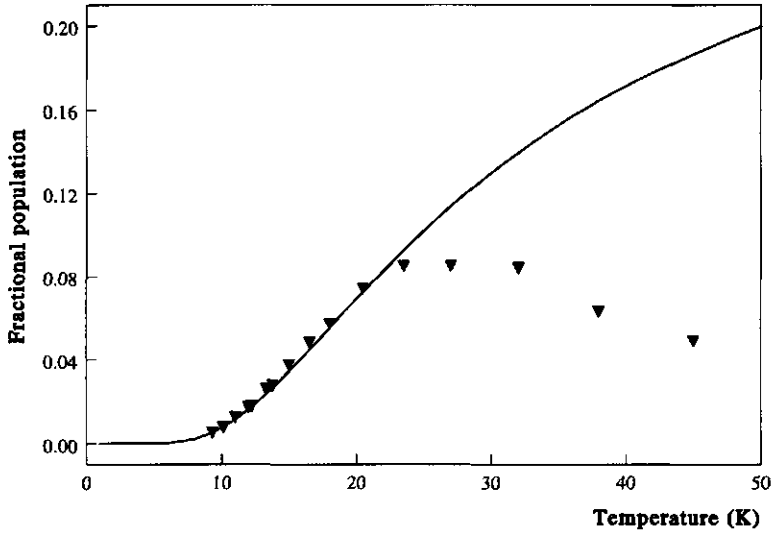

Figure 4

Thermal (de)population of the highest doublet ($m_S = \pm 1/2$) of the inverted (D<0) S=5/2 multiplet from the P^{1+} clusters in the AlF-MgADP stabilized transition state complex. The datapoints are the amplitude at g = 5.27 multiplied by the detection temperature (i.e. corrected for Curie-law temperature dependence). The solid line is a fit of the data to a Boltzmann distribution over the sub-levels of an S=5/2 system with D = -8.11 cm^{-1}. The deviation above T ≈ 25 K reflects lifetime broadening.

complex may be, it is different from that found for the purified protein. Apparently, the exchange-coupling is different in the AlF-MgADP stabilized transition state complex, which points at a different conformation of the P-cluster.

In the simulation of trace C, Fig. 3, the ratio of S=3/2 (FeMoco) over S=5/2 (P^{1+}) is 1 : 0.14. In Fig. 4 it is shown that the population of the measured doublet is 0.085 at T=23 K. For FeMoco the population of the measured doublet is 0.65 at this temperature. This can be calculated from $D \approx 5$ cm^{-1} [26]. Thus, for equal amounts of S=3/2 (FeMoco) and S=5/2 (P^{1+}), the ratio should be 0.085 : 0.65 = 0.13. The value of 0.14 found in the simulation is very close to this, so the two signals are essentially stoichiometric, i.e. the S=5/2 signal accounts for 100% of the P-clusters in the sample. Consequently this is not a matter of a physical mixture of S=5/2 and S=1/2 spin states, as was previously observed for the purified MoFe protein. Fig. 5 shows the S=1/2 spectra from the AlF-MgADP stabilized transition state complex. At E_h = -462 mV (trace A) only a weak S=1/2 signal from Fe protein is detected. At E_h = -287 mV (trace B) two S=1/2 species are present in equal amounts (α and β in the simulation parameters in Table I).

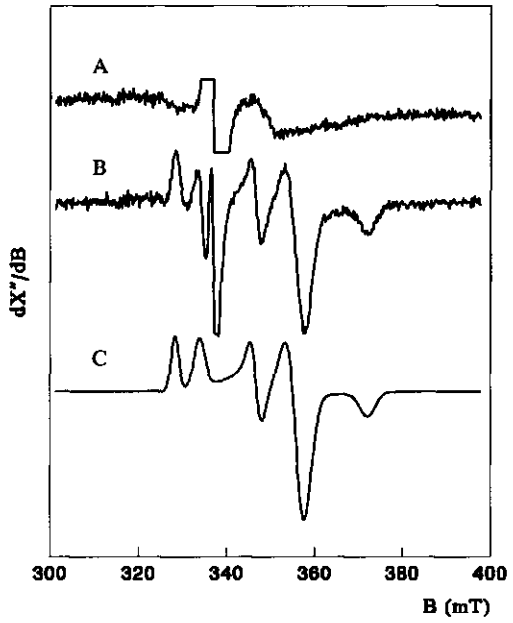

Figure 5

S=1/2 spectra from the AlF-MgADP stabilized transition state complex poised at different redox potentials. Trace A: complex at -462 mV. Trace B: complex at -287 mV. Trace C: simulation of trace B (see Table I). The (partially) truncated radical signal in traces A and B is from the redox mediators. EPR conditions: microwave frequency, 9.416 GHz; microwave power, 0.8 mW; modulation frequency, 100 kHz; modulation amplitude, 0.8 mT; temperature, 13 K.

One peak in trace B (the second one from low field) is deformed by the radical and by the negative g_z peak (g = 2.0) of the S=3/2 signal from FeMoco.

These results show that the S=1/2 and S=5/2 signals do not have a parallel redox behavior, which is in contradiction with what was found previously for free MoFe protein [32], but it does agree with the observation above that the S=5/2 signal accounts for all of the P-clusters in the sample. Possibly this condition is specific for the AlF-MgADP stabilized transition state complex. The nature of these two S=1/2 signals present in the AlF-MgADP stabilized transition state complex and in the purified MoFe protein, remains to be established.

Mechanistic implications.

Our data suggest a possible mechanism for the electron-transfer from the Fe protein to the FeMoco in the MoFe protein, the putative substrate-binding site of nitrogenase. After binding and on-enzyme hydrolysis of MgATP, the protein-protein complex changes its conformation to the MgADP-bound conformation. The AlF-MgADP stabilized protein-protein complex is suggested to be part of this reaction coordinate. In this transition state the redox potentials of the [4Fe-4S] cluster of the Fe protein and of the P-cluster of the MoFe protein are lowered and both clusters become one electron oxidized. The electron acceptor is FeMoco. Changes in redox properties are probably caused by conformational changes of the protein-protein complex. The disappearance of the S=3 signal of the P-clusters, in the range between -500 and +50 mV, shows that such conformational changes indeed take place in the MoFe protein when the protein-protein complex assumes the transition state. Furthermore, the recent publication of the crystal structure of the AlF-MgADP stabilized complex reveals that also the dimeric Fe protein has undergone substantial conformational changes in this complex [33].

Table 1 **Parameters used for the simulation of EPR spectra.**

	Low-field spectra (Fig. 3)		High-field spectra (Fig. 5)	
	S=3/2	S=5/2	S=1/2 (α)	S=1/2 (β)
g_x	4.35	6.64	1.808	1.887
g_y	3.65	5.27	1.941	1.887
g_z	2	2	2.016	2.050
Δ_{xx}	0.11	0.4	0.010	0.012
Δ_{yy}	0.11	0.08	0.007	0.012
Δ_{zz}	0.11	0.1	0.009	0.007
ratio	1	0.14	1	1

Acknowledgments

This research was supported by the Netherlands Foundation for Chemical Research (SON) with financial aid from the Netherlands Organization for Scientific Research (NWO). We thank Professor C. Veeger and Dr. W.M.A.M. van Dongen for their continuous support and interest.

References

1 Peters, J.W., Stowell, M.H.B., Soltis, S.M., Finnegan, M.G., Johnson, M.K., and Rees, D.C. (1997) *Biochemistry 36*, 1180 - 1187
2 Howard, J.B. and Rees, D.C. (1994) *Annu. Rev. Biochem. 63*, 235 - 264
3 Lowe, D.J. and Thorneley, R.N.F. (1984) *Biochem. J. 224*, 877 - 886
4 Duyvis, M.G., Wassink, H. and Haaker, H. (1994) *Eur. J. Biochem 225*, 881 - 890
5 Lowe, D.J., Ashby, G.A., Brune, M., Knights, H., Webb, M.R. and Thorneley, R.N.F. (1995) in: *Nitrogen fixation: fundamentals and applications* (Tikhonovich I.A., Romanov V.F. and Provorov N.A., Eds.) pp. 103 - 108, Kluwer Academic Publications, Dordrecht
6 Duyvis, M.G., Wassink, H. and Haaker, H. (1996) *J. Biol. Chem. 47*, 29632 - 29636
7 Hageman, R.H., and Burris, R.H. (1978) *Proc. Natl. Acad. Sci. U.S.A. 75*, 2699 - 2702
8 Thorneley, R.N.F. and Lowe, D.J. (1983) *Biochem. J. 215*, 393 - 403
9 Georgiadis, M.M., Komiya, H., Chakrabarti, P., Woo, D., Kornuc, J.J. and Rees, D.C. (1992) *Science 257*, 1653 - 1659
10 Lanzilotta, W.N., Fisher, K. and Seefeldt, L.C. (1996) *Biochemistry 35*, 7188 - 7196
11 Lanzilotta, W.N., Fisher, K. and Seefeldt, L.C. (1997) *J. Biol. Chem. 272*, 4157 - 4165
12 Duyvis, M.G., Wassink, H. and Haaker, H. (1996) *FEBS Lett. 380*, 233 - 236
13 Renner, K.A. and Howard, J.B. (1996) *Biochemistry 35*, 5353 - 5358
14 Grossman, J.G., Hasnain, S.S., Yousafzai, F.K., Smith, B.E., and Eady, R.R. (1997) *J. Mol. Biol. 266*, 642 - 648
15 Mittal, R., Ahmadian, M.R., Goody, R.S., and Wittinghofer, A. (1996) *Science 273*, 115 - 117
16 Sondek, J., Lambright, D.G., Noel, J.P., Hamm, H.E. and Sigler, P.B. (1994) *Nature 372*, 276 - 279
17 Coleman, D.E., Berghuis, A.M., Lee, E., Linder, M.E., Gilman, A.G. and Sprang, S.R. (1994) *Science 265*, 1405 - 1412
18 Fisher, A.J., Smith, C.A., Thoden, J., Smith, R., Sutoh, K., Holden, H.M. and Rayment, I. (1995) *Biophys. J. 68*, 19s - 28s
19 Martin, R.B. (1988) *Biochem. Biophys. Res. Com. 155*, 1194 - 1280
20 Dutton, P.L. (1978) *Meth. Enzymol. 54*, 411 - 435
21 Pierik, A.J. and Hagen, W.R. (1991) *Eur. J. Biochem. 195*, 505 - 516
22 Hagen, W.R., Hearshen, D.O., Harding, L.J. and Dunham, W.R. (1985) *J. Mag. Reson. 61*, 233 - 244

23 Watt, G.D., and Reddy, K.R.N. (1994) *J. Inorg. Biochem. 53*, 281 - 294
24 Braaksma, A., Haaker, H., Grande, H.J. and Veeger, C. (1982) *Eur. J. Biochem. 121*, 483 - 491
25 Hagen, W.R., Eady, R.R., Dunham, W.R. and Haaker H. (1985) *FEBS Lett. 189*, 250 - 254
26 Münck, E., Rhodes, H., Orme-Johnson, H., Davis, L.C., Brill, W.J. and Shah, V.K. (1975) *Biochim. Biophys. Acta 400*, 32 - 53
27 Orme-Johnson, W.H., Hamilton, W.D., Jones, T.L., Tso, M.-Y.W., Burris, R.H., Shah, V.K., and Brill, W.J. (1972) *Proc. Natl. Acad. Sci. USA 69*, 3142 - 3145
28 Mortenson, L.E., Zumft, W.G., and Palmer, G. (1973) *Biochim. Biophys. Acta 292*, 422 - 435
29 Zimmermann, R., Münck, E., Brill, W.J., Shah, V.K., Henzl, M.T., Rawlings, J. and Orme-Johnson, H. (1978) *Biochim. Biophys. Acta 537*, 185 - 207
30 O'Donnell, M.J., and Smith, B.E. (1978) *Biochem. J. 173*, 831 - 839
31 Pierik, A.J., Wassink, H., Haaker, H. and Hagen, W.F. (1993) *Eur. J. Biochem. 212*, 51 - 61
32 Tittsworth, R.J. and Hales, B.J. (1993) *J. Am. Chem. Soc. 115*, 9763 - 9767
33 Schindelin, H., Kisker, C., Schlessman, J.L., Howard, J.B. and Rees, D.C. (1997) *Nature 387*, 370 - 376
34 Chapter 3, page 68 (Duyvis, M.G., Wassink, H. and Haaker, H. (1997) *Biochemistry*, submitted)

Chapter 5

The role of NifM in the maturation of the nitrogenase Fe protein from *Azotobacter vinelandii*.

Karel VAN DER HEIJDEN, Johan H. SPEE, Bas VAN DER BAAN, Wilfred IJKEL, Jos SCHALK, Yvonne B.M. BULSINK and Walter M.A.M. VAN DONGEN

Abstract

The *nifM* gene in the *Azotobacter vinelandii nif*-gene cluster encodes a 30 kDa protein. The role of NifM in the maturation of the nitrogenase Fe protein was investigated. Comparison of the nucleotide- and derived amino acid sequence of *nifM* with sequences in several nucleotide- and protein sequence databases reveals a high homology between NifM and proteins involved in protein folding, especially *E. coli* parvulin, a peptidylprolyl *cis-trans* isomerase (PPIase). Deletion of *nifM* from the *A. vinelandii* genome resulted in accumulation of inactive, precipitated nitrogenase Fe protein, indicating that NifM might be required for proper folding of the Fe protein.

The NifM protein was purified from an *E. coli* clone containing the *A. vinelandii nifM* gene on a plasmid under control of the T7-ϕ10 promoter and tested for PPIase activity with two artificial substrates. Although activity was observed with one of the substrates, this activity was found to be due to a contamination of the NifM preparation with a small amount of an *E. coli* PPIase.

Introduction

Nitrogenase, the enzyme that catalyzes the reduction of dinitrogen to ammonia (nitrogen fixation) consists of two proteins. The MoFe protein, or Av1, is an $\alpha_2\beta_2$ tetramer containing two [8Fe-7S] clusters (P-clusters) and two [Mo-7Fe-9S-homocitrate] clusters (FeMoco) [1]. The iron-molybdenum clusters probably form the active site of the enzyme. The Fe protein, or Av2, donates the electrons required for nitrogen reduction to the MoFe protein. The Fe protein is a homodimer containing a single [4Fe-4S] cluster between the subunits [2].

Biosynthesis of the Fe protein. Biosynthesis of the nitrogenase proteins requires the concerted activity of the proteins encoded by approximately 20 genes. In *Azotobacter vinelandii*, these *nif* genes are located in 2 clusters [3, 4]. Indications about the functions of these genes in the biosynthesis of nitrogenase have been obtained by investigating *A. vinelandii* mutants in which specific *nif* genes were deleted. These studies indicated that for biosynthesis of active Fe protein an intact copy of the *nifM* gene was absolutely required: no Fe protein activity was detectable in Δ*nifM* mutants [5]. Deletion of two other genes, *nifS* and *nifU* resulted in a considerable decrease of Fe protein activity in *Azotobacter* cells. The *nifS* gene encodes a pyridoxalphosphate-dependent cysteine desulfurase, which catalyzes, under reducing conditions, the conversion of cysteine into alanine and sulfide [6, 7]. The sulfide produced in this reaction can be used for the biosynthesis

of iron-sulfur clusters: in the presence of Fe-ions and cysteine NifS catalyzes the biosynthesis of the [4Fe-4S] cluster in the apoprotein of the nitrogenase Fe protein [8]. Genes encoding proteins with high sequence similarity to *A. vinelandii nifS* have been found recently in several non-diazotrophic organisms, including *E. coli* and *B. subtilis* [9, 10], suggesting that the role of this protein in biosynthesis of Fe-S clusters is not limited to the nitrogenase Fe protein; indeed, in vitro NifS catalyzed biosynthesis of Fe-S clusters in several other apo-Fe-S proteins has been demonstrated now [10, 11, 12]. The role of NifU, a protein with a [2Fe-2S] cluster [13], in the biosynthesis of the nitrogenase Fe protein is not yet clear. Also the Fe protein of *Klebsiella pneumoniae* nitrogenase requires NifM for biosynthesis. Experiments in which *K. pneumoniae nifH*, the gene encoding the subunit of the Fe protein, was introduced in *E. coli* cells together with different sets of other *nif* genes indicated that coexpression of *nifH* and *nifM* was sufficient to produce active Fe protein [14].

Several functions for NifM have been suggested, among these insertion of the [4Fe-4S] cluster, conformational isomerization of the cluster in a post-insertional event and promotion of proper assembly of the two subunits of the Fe protein for appropriate positioning of the ligands of the Fe-S cluster (reviewed by Dean et al., [15]). Recently it was proposed that NifM might be a peptidylprolyl *cis-trans* isomerase (PPIase) [16].

Peptidylprolyl cis-trans isomerases. PPIases are enzymes found both in prokaryotes and in eukaryotes (see [17] and [18] for reviews). They catalyze the interconversion of the *trans*-isomer of proline into the *cis*-isomer. During protein synthesis, peptide bonds formed by the proline residues are in the *trans* conformation, but in folded proteins appr. 15% of the residues have a *cis* conformation. Although *cis-trans* isomerization occurs spontaneously, PPIases considerably increase the rate of this process. A mechanism involving stabilization of a transition state that is characterized by partial rotation around the C-N amide bond, for which the enzymes use free energy released from favorable noncovalent interactions with the substrate ('catalysis by distortion') has been proposed. [19, 20].

Together with the protein disulfide isomerases (which catalyze the formation of disulfide bridges), PPIases enhance the rate of one of the two slow steps in protein folding in vitro. Acceleration of in vitro refolding of a series of proteins by PPIases has been demonstrated (reviewed in [17]). Although definitive proof for their function in vivo is still lacking, it is generally believed now that these enzymes, together with the chaperone systems, are required for fast and accurate protein folding. PPIases are subdivided into three classes: FK506-binding proteins or FKBP's, which are inhibited by immunosuppressive macrolides (FK506, rapamycin), cyclophilins (inhibited by the immunosuppressive peptide cyclosporin A) and parvulins, which are neither inhibited by macrolides nor by cyclosporin. PPIases belonging to the different classes have a different specificity for the synthetic substrates that are used to test their activity [21, 22]. There is

no sequence similarity between FKBP's, cyclophilins and parvulins, but extensive sequence homology exists between different PPIases within each class. On the basis of this homology NifM is believed to be a parvulin-type PPIase. Besides the prototype PPIases (which usually consist of 90 - 170 residues) PPIase-like domains and PPIase activities are also found in larger proteins, which might have other functions as well.

Materials and methods

Plasmids.

A summary of the plasmids and recombinant *A. vinelandii* strains used in this study is given in Table I. Plasmids pDB527, pDB559, pDB551 and pDB525 were gifts of Dr. D. Dean (Virginia Polytech and State University, Blacksburg, Virginia, USA). Plasmid pDB527 contains the *A. vinelandii nifH* gene, amplified with PCR from start- to stopcodon and inserted downstream of the strong T7-ϕ10 promoter of expression vector pET-5a [23]. Plasmids pDB559, pDB551 and pDB525 contain the *A. vinelandii nifM*, *nifS* and *nifU* genes, respectively, downstream of the T7-ϕ10 promoter of pT7-7 [24]. Expression of genes under control of the T7-ϕ10 promoter was in *E. coli* BL21[DE3] [25]; *E. coli* TG2 [26] was used as a host-strain for the construction of plasmids.

Plasmid pAV41 was constructed as follows: first, *orf9* (the gene downstream of *nifM* and in the same operon) was isolated on a 2.0 kb *Sph*I/*Stu*I restriction fragment (see Jacobson, [3], for restriction sites used) and inserted into *Sph*I/*Hin*dIII digested pDB559. Next, the resulting plasmid, pAV40, was digested with *Xba*I and *Cla*I. The resulting 2.2 kb fragment, i.e. the entire insert with *nifM* and *orf9* downstream the vector encoded T7-ϕ10 ribosome-binding site (RBS), was made blunt-ended with Klenow-polymerase and S1-nuclease and inserted into *Bam*HI-digested pDB527 (the *Bam*HI ends made blunt with Klenow-polymerase). The resulting plasmid, pAV41, contains, in this order, the T7-ϕ10 promoter and RBS of vector pET5a, followed by the *nifH* gene, a second copy of the T7-ϕ10 RBS and the *nifM* and *orf9* genes; *orf9* is preceded by its natural RBS.

Plasmid pAV49 was made in the following way: first, a 3.1 kb *Sph*I fragment containing *nifU*, *nifS* and part of *nifV* was inserted into pUC19. The resulting plasmid, pAV13, was digested with *Sst*I and *Hin*dIII. The 2.1 kb fragment containing the 3' end of *nifU*, the entire *nifS* and the 5' end of *nifV* was inserted into *Sst*I/*Hin*dIII digested pDB525, placing *nifU*, *nifS* and the truncated *nifV* gene under control of the vector-encoded T7-ϕ10 promoter. Finally, the insert of the resulting plasmid (pAV48), including the vector encoded promoter and RBS, was isolated on a 3.1 kb *Bgl*II/*Sph*I restriction fragment and inserted into *Bam*HI/*Sph*I digested pACYC184, resulting in recombinant

***E. coli* strains:**	
E. coli TG2	*thi, supE, hsdS$_K$* (r_K^-, m_K^-), *recA::Tn10* (Tc^R), Δ(*lac-pro*), F'(*traD36, proA$^+$B$^+$ lacI^{q}ZΔM15*) [26]
E. coli BL21[DE3]	F$^-$, *ompT, hsdS$_B$* (r_B^-, m_B^-), *dcm, gal*, (DE3) [25]
***A. vinelandii* strains:**	
A. vin. ATCC478	wild-type *A. vinelandii*
A. vin. DJ67	Δ*nifZM* strain of *A. vinelandii* OP (in-frame deletion); *nif*$^-$ [5]
A. vin. DJ136	Δ*nifM* strain of *A. vinelandii* OP (frameshift deletion); *nif*$^-$ [5]
A. vin. BB1	*nifM* revertant of *A. vinelandii* DJ136, containing the modified *nifM* gene with a 6 x His-tag from pAV42; *nif*$^+$ (this study)
Vectors / plasmids:	
pUC18/19	general cloning vectors, Ap^R, pMB1 origin [39]
pACYC184	general cloning vector, Cm^R, Tc^R, p15A origin [40]
pT7-7	expression vector: T7-ϕ10 promoter and RBS, Ap^R, pMB1 origin [24]
pET-5a	expression vector: T7-ϕ10 promoter and RBS, Ap^R, pMB1 origin [23]
pDB525	*nifU* gene of *A. vinelandii* OP, amplified from start- to stopcodon with PCR and inserted into pT7-7 (gift of Dr. D. Dean)
pDB527	*nifH* gene of *A. vinelandii* OP (encoding the Fe protein), amplified from start- to stopcodon with PCR and inserted into pET-5a (gift of Dr. Dean)
pDB551	*nifS* gene of *A. vinelandii* OP, amplified from start- to stopcodon with PCR and inserted into pT7-7 (gift of Dr. D. Dean)
pDB559	*nifM* gene of *A. vinelandii* OP, amplified from start- to stopcodon with PCR and inserted into pT7-7 (gift of Dr. D. Dean)
pAV13	3.2 kb *Sph*I fragment with *A. vinelandii* ATCC478 *nifU*, *nifS* and the 5'-end of *nifV* inserted into the *Sph*I site of pUC19 (this study)
pAV40	2.0 kb *Sph*I/*Stu*I fragment with *A. vinelandii* ATCC478 *nifM* (3'-end) and *orf9* inserted into *Sph*I/*Hin*dIII digested pBD559 (→ T7-ϕ10 promoter + RBS - *nifM* - *orf9* (this study))
pAV41	2.2 kb *Xba*I/*Cla*I fragment of pAV40 (made blunt with Klenow polymerase and S1 nuclease) inserted into *Bam*HI digested pBD527 (→ T7-ϕ10 promoter + RBS - *nifH* -T7-ϕ10 RBS- *nifM* - *orf9* (this study))
pAV42	2.2 kb *Hin*cII/*Kpn*I fragment with *A. vinelandii* ATCC478 *nifM* and *orf9*, inserted into *Hin*cII/*Kpn*I digested pUC19, with the sequence GCA CAT CAC CAT CAC CAT CAC, encoding Ala-6xHis, inserted into the *Nco*I site of *nifM* (this study)
pAV48	2.1 kb *Sst*I/*Hin*dIII fragment of pAV13 inserted into *Sst*I/*Hin*dIII digested pDB525 (→ T7-ϕ10 promoter + RBS - *nifU* - *nifS* - *nifV* (5'-end) (this study))
pAV49	3.1 kb *Bgl*II/*Sph*I fragment of pAV48 inserted into *Bam*HI/*Sph*I digested pACYC184 (→ T7-ϕ10 promoter + RBS - *nifU* - *nifS* - *nifV* (5'-end) (this study))

Table I **Bacterial strains and plasmids.**

plasmid pAV49. pAV49 contains the T7-ϕ10 promoter and RBS, followed by *nifU*, *nifS* and the truncated *nifV*. The vector of pAV49 (pACYC184) is compatible with the pET-vector in pDB527 and pAV41, allowing coexpression of *nifH*, *nifM*, *nifU*, *nifS* and *orf9* in different combinations of the respective plasmids.

A *nifM* gene with 6 extra codons for a C-terminal histidine-tag was constructed as follows: A 2.0 kb *Hin*cII/*Kpn*I fragment containing the *nifM* and *orf9* genes was inserted into *Hin*cII/*Kpn*I digested pUC19. The resulting plasmid contains a single *Nco*I site overlapping with the codons for the three C-terminal amino acids of NifM. After digestion of this plasmid with *Nco*I, the following synthetic double stranded DNA fragment was ligated into the *Nco*I site:

```
5' CAT GCA CAT CAC CAT CAC CAT CAC GGA TAA TCGAT     3'
3'      GT GTA GTG GTA GTG GTA GTG CCT ATT AGCTAGTAC 5'
   His Ala His His His His His His Gly ***
```

This insertion places an extra Ala-residue and a 6 x His-tag in the correct reading frame in-between the two C-terminal amino acids of wild-type NifM. The *Nco*I site is removed by the mutation. A plasmid (pAV42) with the insertion in the proper orientation was selected by double-stranded plasmid sequencing. pAV42 was introduced into the Δ*nifM*, *nif*$^-$ strain *A. vinelandii* DJ136 by transformation (Dr. D. Dean). 130 transformants showing restoration of diazotrophic growth on plates containing Burk's agar without added nitrogen source were selected. In order to check if the mutated *nifM* gene was properly inserted into the bacterial chromosome by double cross-over, chromosomal DNA of 12 of these transformants was isolated after growth in liquid Burk's medium and digested with *Nco*I. After electrophoresis in a 0.6% agarose gel and transfer to nitrocellulose membrane, the digested DNA was hybridized with the insert of pAV40, labeled by nick-translation with [α^{32}P]dATP as a radioactive precursor. Hybridizing bands of 2.9 and 2.1 kb were detected in the chromosomal DNA of 11 of 12 transformants (2.9, 1.7 and 0.4 kb in the DNA of wild-type *A. vinelandii*). This indicates, that a: proper double cross-over has occurred in these transformants and b: the *Nco*I site at the 3'-end of wild-type *nifM* is lost, as expected for the mutated gene. One of the transformants, *A. vinelandii* BB1, was used for further study.

Bacterial strains and growth conditions.

Wild-type *A. vinelandii* ATCC 478 and *A. vinelandii* BB1 were grown under nitrogen-fixing conditions in a 200 l fermentor containing Burk's medium without added ammonium salts, essentially as described before [27]. The *A. vinelandii* Δ*nifM* mutant DJ67 [5] was grown in a 200 l fermentor containing Burk's medium limited in ammonia

[$(NH_4)_2SO_4$, 5.7 mM]. This allowed this *nif*⁻ mutant to grow to mid-exponential phase on the added nitrogen source. After depletion of the added nitrogen source, the culture was incubated for a further 2 hours at 30 °C in the fermentor causing derepression of the *nif* genes and resulting in expression of the Nif proteins.

E. coli TG2 strains containing recombinant plasmids were grown in TY medium containing the appropriate antibiotics in a thermostatted gyrotory shaker (37 °C, 200 rpm). *E. coli* BL21[DE3] strains containing plasmids used for expression of *nif*-genes from T7-ϕ10 promoters were grown in TY medium, containing 0.2 % sucrose and 100 mg ml^{-1} ampicillin, to mid-exponential phase (OD_{600} = 0.6 - 0.7) in a gyrotory shaker at 37 °C, after which expression was induced by the addition of isopropyl-ß-D-thiogalactopyranoside (IPTG; 0.2 mM final concentration). Different culture conditions were: a: induction at 20 °C (in this case cultures were cooled to 20 °C one hour prior to addition of IPTG), b: induction under anaerobic conditions (in this case culture was in screw-capped bottles which were made anaerobic by tightly closing the screw-caps one hour before induction) and c: combination of a and b.

Purification of NifM from *E. coli* BL21[DE3](pDB559).

A. vinelandii NifM was purified from *E. coli* BL21[DE3] strain harboring recombinant plasmid pDB559. A 6 l culture of *E. coli* BL21[DE3](pDB559) was grown in TY medium containing 100 mg ml^{-1} ampicillin in a thermostatted shaker at 37°C until mid-exponential phase. Induction of expression of *nifM* was either at 37 °C or at 20 °C.

For expression at 37 °C, IPTG (0.2 mM final concentration) was added to the culture when an OD_{600} of 0.6 - 0.7 was reached. Three hours after induction, cells were harvested by centrifugation and broken by passing the cells, resuspended in 100 mM Tris/HCl, 1 mM DTT, pH 8.5, twice through a French pressure cell at 10,000 pounds per square inch. After centrifugation (30 min at 30.000 *g*), almost all (> 90%) NifM produced after induction at 37 °C was found as inclusion bodies in the pelleted cell debris. This pellet was washed twice with 100 mM Tris/HCl, 2% sodium deoxycholate, 10 mM DTT, pH 8.5 and inclusion bodies were solubilized in the same buffer containing 8 M urea. After removal of insoluble material (30 min, 30.000 *g*) the dissolved protein was diluted to appr. 0.15 mg ml^{-1} with urea containing buffer. Next the concentration of urea was first gradually and slowly decreased to 1.8 M by consecutive dialysis steps against equal volumes of 100 mM Tris/HCl, pH 8.5. The remaining urea was removed by 3 consecutive dialysis steps against 5-fold excess 100 mM Tris/HCl, pH 8.5, followed by concentration of the protein by ultra-filtration on an Amicon YM 10 membrane. After removal of precipitated material by centrifugation appr. 20 mg soluble and essentially pure NifM was obtained.

For expression of *nifM* at 20 °C, the mid-exponential phase culture was transferred to a shaker kept at 20 °C. After one hour equilibration at this temperature, IPTG

was added (0.2 mM final concentration). Cells were harvested by centrifugation 7 h later, when the NifM content reached its maximal level. Appr. 75% of NifM accumulates as soluble protein in cells grown at 20°C. The pellet (42 g) was resuspended in 50 ml 100 mM Tris/HCl, pH 8.0, 1 mM DTT. After addition of DNaseI and RNase A, cells were broken by two passages through a French pressure cell at 10,000 psi. Large cell debris was removed by centrifugation at 20,000 *g* for 20 min. This and following steps were performed at 4°C. After dialysis against 2 liters of 100 mM Tris/HCl, pH 7.6, 1 mM DTT (buffer A), the supernatant was loaded onto a DEAE-Sephacel column (25 x 2.6 cm). After application of a linear gradient of 0 - 0.5 M NaCl in buffer A, NifM was found to elute at appr. 0.23 M NaCl. Pooled fractions containing NifM were concentrated by ultra-filtration on an Amicon YM-10 membrane, centrifuged to remove precipitates and applied onto a Superdex 200 gel-filtration column (88 x 2.6 cm) in buffer A + 150 mM NaCl. Pooled fractions from this column were again concentrated by ultra-filtration and centrifuged, followed by a second ion-exchange purification step on Q-Sepharose (15 x 2.6 cm) developed with 0.1 - 0.5 M NaCl in buffer A. Finally, NifM-containing fractions were desalted and applied (without further addition of salt) onto a hydrophobic interaction column (Phenyl-Sepharose, 20 x 2.6 cm). Bound NifM was eluted from this column with a gradient of 0 - 50% (vol./vol.) ethyleneglycol in buffer A. Fractions containing NifM were again concentrated by ultra-filtration and stored in liquid nitrogen.

Assay for measuring PPIase activity of NifM.

The assay for PPIase activity makes use of the selectivity of chymotrypsin for digestion of *p*-nitroaniline esters of tetrapeptides that contain proline in the P_{-2} position [28]. In watery solutions, an equilibrium exists between peptide molecules with proline in the *cis* and *trans* conformations, respectively. Using an excess chymotrypsin, the *trans* conformers are digested very rapidly, while the rate of digestion of the *cis* conformers is dependent on the rate of the *cis-trans* isomerization. Addition of a PPIase to the digestion mixture increases the rate of *cis-trans* isomerization and, therefore, also the rate of digestion of the peptide.

Two peptide substrates were used in this study: *N*-succinyl-Ala-Ala-Pro-Phe-*p*-nitroanilide (suc-AAPF-pNA, Sigma) and *N*-succinyl-Ala-Phe-Pro-Phe-*p*-nitroanilide (suc-AFPF-pNA, Bachem, Switzerland). The assay was performed in a Hi-Tech SF-51 stopped-flow apparatus (Salisbury, Wiltshire, UK). One syringe contained the peptide substrate (6 - 2240 μM, diluted from 1.5 or 50 mg ml^{-1} stock solutions in DMSO) and NifM (0 - 7.2 μM) in 50 mM Hepes/NaOH, 100 mM NaCl, pH 7.5. Prolonged incubation of NifM with the peptide substrate did not influence the ratio of *cis* to *trans* conformers of the peptide. The second syringe contained chymotrypsin (Boehringer), 3.6 mg ml^{-1}, diluted from a 60 mg ml^{-1} stock solution in 1 mM HCl, in 50 mM Hepes/NaOH, 100 mM NaCl, pH 7.5. Both syringes were kept at 20 °C. Directly after filling the syrin-

ges the reaction was started by shooting 0.15 ml of the substrate / NifM mixture against 0.15 ml of the protease solution. The reaction was followed by measuring the increase of the absorbance at 390 nm or at 445 nm (for substrate concentrations above 200 μM.) due to formation of *p*-nitroanilide (ε_{390} = 13,300 M^{-1} cm^{-1}; ε_{445} = 1250 M^{-1} cm^{-1}, [29]). Under these conditions, the *trans* conformer of the substrate is digested by chymotrypsin within the first second after mixing, followed by a slower digestion of the *cis* conformer, the rate being dependent on the activity of PPIase. PPIase activity in NifM preparations was determined as the rate of *p*-nitroanilide production in the slow step of the reaction in the presence of NifM *minus* the rate in its absence due to spontaneous *cis-trans* conversion. Substrate concentrations used for calculation of kinetic parameters were those of the *cis*-conformers; the percentages of *cis*-conformers in watery solutions of the substrates suc-AAPF-pNA and suc-AFPF-pNA were 10% and 25%, respectively.

For inhibition studies rapamycin (Sigma) was added in different concentrations (0-500 nM) to the syringe that contained the substrate and NifM. Use of a stopped-flow apparatus allowed monitoring of the progress of the reaction from 10 ms after mixing. Compared to a conventional spectrophotometer, use of a stopped-flow apparatus has the advantage that variations in mixing times are avoided, which is especially important at high substrate concentrations.

Antibodies against NifM.

Antibodies were raised against NifM purified from inclusion bodies isolated from *E. coli* BL21[DE3] (pDB559) grown at 37 °C. NifM (40 μg in 100 μl buffer) was mixed with 100 μl Freunds complete adjuvans or 100 μl Specoll and injected subcutaneously into BALB/C mice, followed 4 weeks later by a boost with the same amount of NifM. Mice were bleeded one week after the boost. Serum was obtained after centrifugation (10 min, 10,000 *g*) of the clotted blood cells.

Results and discussion

NifM has homology with the peptidylprolyl *cis-trans* isomerase parvulin.

Screening of several nucleotide- and protein sequence databases (EMBL, Genbank, PIR, Swissprot), using a variety of homology search programs (FASTA, TFASTA, BLAST, Smith-Waterman), revealed, apart from NifM proteins from other diazotrophes, only a limited number of other proteins with relevant sequence homology to *A. vinelandii* NifM ([16], our own observations). Among the proteins with homology to NifM (some of these are only putative, as they have not yet been purified, but have only been identified by nucleotide sequencing and other molecular genetic techniques) are the

PPIase parvulin from *E. coli* and proteins encoded by the *prtM* gene of *Lactobaccillus lactis* [30, 31], the *prsA* gene of *Bacillus subtilis* [32] and the *surA* gene of *E. coli* [33]. Genetic and / or biochemical analysis of these genes and / or the proteins they encode suggests that they are all involved in protein folding / maturation. The only one of the proteins for which ample information is available on a genetic level and which has also been characterized biochemically is parvulin, encoded by the *E. coli ppiC* gene [22, 34]. Parvulin has been characterized as a small (10.1 kDa), highly active PPIase with a substrate specificity that is different from the FKBP- and cyclophilin-types of PPIases. Furthermore, its activity is not inhibited by cyclosporin A and FK506.

Indications for involvement in protein folding of the other proteins with sequence similarity to NifM is indirect and stems primarily from genetic experiments: *surA* from *E. coli* was isolated as a locus which upon transposon mutagenesis induced accumulation of misfolded proteins in the periplasm [33]; deletion of *prtM* in *Lactobacillus lactis* results in excretion of the extracellular protease encoded by *prtP* in inactive form [30, 31]; *prsA* is required for biosynthesis of periplasmic α-amylase in *Bacillus subtilis* [32]. Like NifM, also the proteins encoded by *surA, prtM* and *prsA* have a 'domain' with sequence similarity to parvulin (which occurs twice in *surA*) [16]. These proteins are much larger than parvulin (10.1 kDa): NifM, PrtM and PrsA are appr. 33 kDa, SurA 62 kDa. However, outside the region of appr. 100 amino acids with sequence similarity to parvulin and NifM, the sequences of these larger proteins are widely divergent.

Fig. 1 shows a comparison of the amino acid sequence of *A. vinelandii* and *Klebsiella pneumoniae* NifM with parvulin. The sequences of the NifM proteins of *A. vinelandii* and *K. pneumoniae*, which obviously have a similar function in biosynthesis of the nitrogenase Fe proteins in respective species, have hardly any similarity to one another, except for the region where the homology with parvulin is found. Only 70 amino acid residues (24%) of *A. vinelandii* NifM (292 amino acids total) are identical in *K. pneumoniae* NifM (266 amino acids). The conserved residues are primarily clustered in the C-terminal part of NifM: of the 120 N-terminal residues of *A. vinelandii* NifM, only 15 (12.5%) are identical in *K. pneumoniae* NifM, while 55 (32%) are conserved in the 172 C-terminal amino acids.

Maximal conservation is found between residues 182 - 247 of the *A. vinelandii* sequence and residues 160 - 225 of that of *K. pneumoniae nifM* (29 identical residues, i.e. 45%). As shown in the alignment in Fig. 1, the primary structure of parvulin (93 amino acids) is highly similar to the latter regions of both NifM sequences: of the 65 amino acid residues in this region, 20 (19) are identical between parvulin and *A. vinelandii* (*K. pneumoniae*) NifM and another 14 (15) are replaced by residues which are considered to be functionally homologous.

```
NIFMVI          MASERLADGDSRYYLLKVAHEQFGCAPGELSEDQLQQADRIIGRQRHIED  50
PARVULIN
NIFMKL          MNPWQ------RFARQRLARSRWNRDPAALDPADTPAFEQAWQRQCHMEQ  44

NIFMVI          AVLRSPDAIGVVIPPSQLEEAWAHIASRYESPEALQQALDAQALDAAGMR 100
PARVULIN
NIFMKL          TIVARVPEGDIPAALLE-----------NIAASLAIWLDEGDFAPPERA  82

NIFMVI          AMLARELRVEAVLDCVCAGLPEISDTDVSLYYFNHAEQFKVPAQHK--HI 149
PARVULIN                                                MAKTAAALHI  10
NIFMKL          AIVRHHARLELAFADIARQAPQPDLSTVQAWYLRHQTQFMRPEQRLTRHL 132

NIFMVI          LVTINEDFPENTREAARTRIETILKRLRGKPERFAEQAMKHSECPTAMQG 199
PARVULIN        LV-----------KEEKLALDLLEQIKNGAD-FGKLAKKHSICPSGKRG  47
NIFMKL          LLT-----VDNDREAVHQRILGLYRQINASRDAFAPLAQRHSHCPSALEE 177
                *.                    .   .    . *.  * .** **..

NIFMVI          GLLGEVVPGTLYPELDACLFQMARGELSPVLESPIGFHVLYCESVSPARQ 249
PARVULIN        GDLGEFRQGQMVPAFDKVVFSCPVLEPTGPLHTQFGYHIIKVLYRN*     93
NIFMKL          GRLGWISRGLLYPQLETALFSLAENALSLPIASELGWHLLWCEAIRPAAP 227
                * **    * . * ..  .*  .    .  . . .*.*..

NIFMVI          LTLEEILPRLRDRLQLRQRKAYQRKWLVCLLQQNATLENLAHG*       292
PARVULIN
NIFMKL          MEPQQALESARDYLWQQSQQRHQRQWLEQMISRQPGLCG*           266
```

Figure 1

Alignment of the sequences of *A. vinelandii* and *K. pneumoniae* NifM (NIFMVI and NIFMKL, respectively) with *E. coli* parvulin. Amino acid sequences were aligned with the CLUSTAL V program [42] using the PAM250 protein-weight matrix [41]. Identical residues (asterisks) and homologous residues (dots) are only shown in the region where all three sequences overlap. Residues conserved in parvulin and in one or both NifM sequences are shown bold

Deletion of the gene encoding NifM in *A. vinelandii*.

The *A. vinelandii* strain DJ67, in which the *nifM* gene is deleted by genetic modification, was previously shown to accumulate normal amounts of Fe protein. However, the Fe protein was completely inactive in this mutant; also activity of the MoFe protein was very low [5]. We have been able to confirm the results obtained by Jacobson et al. [5] with this strain.

In order to attempt purification of the inactive Fe protein from *A. vinelandii* DJ67, a 200 l culture of this mutant strain was grown under ammonia-limiting conditions. Under these conditions this *nif*$^-$ strain grows to mid-exponential phase on the

added nitrogen source, followed by derepression of the nitrogenase proteins upon exhaustion of the nitrogen source. However, after anaerobic disruption of the *A. vinelandii* DJ67 cells and after removing insoluble material by centrifugation, we noticed that the majority of the Fe protein and large part of the MoFe protein are found in the pellet after the centrifugation step. Fig. 2A shows a Coomassie-stained SDS-polyacrylamide gel containing broken cells of *A. vinelandii* DJ67, fractionated into soluble and insoluble fractions by centrifugation at 20,000 *g* for 30 min. It is apparent from Fig. 2A that, contrary to wild-type *A. vinelandii*, the *ΔnifM* strain DJ67 accumulates the majority of the Fe protein (and also part of the Mo-Fe protein) in the insoluble fraction. Fig. 2B shows an immunoblot of the same fractions of both wild-type and DJ67 *A. vinelandii* cellular proteins incubated with antibodies raised against the Fe protein. The experiment in Fig. 2B confirms the results in Fig. 2A. Further purification of the Fe protein produced by *A. vinelandii* DJ67 was not attempted.

These experiments indicate that deletion of *nifM* results in the accumulation of aggregates of inactive Fe protein in *A. vinelandii* cells that can easily be pelleted by centrifugation, suggesting that the protein is not properly folded. This, and the remarkable sequence homology of NifM with other proteins involved in protein folding / maturation, suggests involvement of NifM in the folding of the Fe protein to its native conformation.

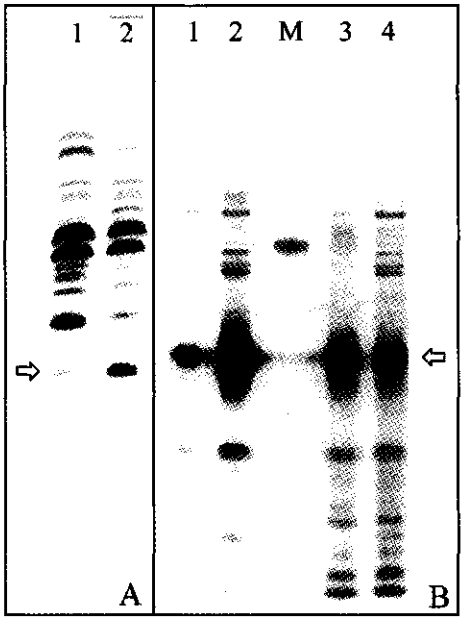

Figure 2

Separation of nitrogenase proteins of wild-type and *ΔnifM A. vinelandii* (strain DJ67) into soluble and insoluble fractions.

A. vinelandii wild-type and DJ67 cells were ruptured in a French-pressure cell, followed by separation of the broken cells into soluble and insoluble fractions by centrifugation. Equivalent amounts of these fractions were analyzed by SDS-PAGE, followed by either (A) staining with Coomassie Brilliant Blue or (B) by immunochemical staining applying antibodies against the nitrogenase Fe protein.
A Lane 1: DJ67, soluble fraction.
A Lane 2: DJ67, insoluble fraction.
B Lane 1: wildtype, insoluble fraction.
B Lane 2: wildtype, soluble fraction.
B Lane 3: DJ67, insoluble fraction.
B Lane 4: DJ67, soluble fraction.
B Lane M: low-molecular-weight markers.
Arrows: position of the Fe protein.

Production of Fe protein in *E. coli*.

Deletion of specific genes in the *A. vinelandii nif* gene clusters gave indications for involvement of four genes in these clusters in the biosynthesis of the Fe protein [3, 5]. *NifH* (the structural gene for the Fe protein) and *nifM* appear absolutely required for synthesis of active Fe protein. Deletion of *nifU* and *nifS* results in mutant strains that accumulate a 15 - 20 fold lower amount of active Fe protein compared to the wild-type strain. This either suggests that *nifU* and *nifS* are not absolutely required for synthesis of active Fe protein, but affect only the efficiency of biosynthesis, or that proteins encoded by genes outside the *nif* gene clusters may (partially) replace *nifU* and *nifS*. In this respect it is interesting to note that the *A. vinelandii* genome contains, outside the *nif* gene clusters, two other copies of *nifS* (Dr. D. Dean, personal communication).

In order to investigate what is the minimum amount of genes required for biosynthesis of active Fe protein, the *nifH* gene was expressed in *E. coli*, alone and in different combinations with *nifM*, *nifU* and *nifS*. Furthermore, the role of *orf9*, an open reading frame encoding a 48 kDa protein which is not required for biosynthesis of active Fe protein in *A. vinelandii* [3], but which is present in the same operon as *nifM*, was investigated.

E. coli BL21[DE3] (pDB527) was used for expression of the *nifH* gene in *E. coli*. Under all conditions tested (induction at 20 °C or 37 °C; aerobic or anaerobic induction) large amounts of Fe protein were produced in *E. coli* BL21[DE3] (pDB527). However, no Fe protein activity was detectable in extracts of these cells. The Fe protein produced in these cells was not soluble and could be easily pelleted in extracts of these cells by low-speed centrifugation (not shown), indicating that it occurred in large aggregates.

Coexpression of *nifH*, *nifU* and *nifS* was done in *E. coli* BL21[DE3] containing both (compatible) plasmids pDB527 and pAV49. Also the Fe protein produced in this doubly transformed expression strain was inactive and insoluble, indicating that NifU and NifS are not sufficient for biosynthesis of active Fe protein.

Also coexpression of *nifH*, *nifM* and *orf9* in *E. coli* BL21[DE3] (pAV41) did not result in production of active and soluble Fe protein. Extracts of *E. coli* BL21[DE3] (pAV41) separated on 15% SDS-polyacrylamide gels clearly showed that the three proteins were produced in high amounts after induction with IPTG. This result does not agree with that obtained by Howard et al. [14]. These authors demonstrated that coexpression of *K. pneumoniae nifH* and *nifM* in *E. coli* was sufficient for production of fully active Fe protein, which was spectroscopically indistinguishable from the Fe protein produced in *Klebsiella*. A difference in the experimental setup between Howard's and our experiments was the use of different expression systems, which yielded high amounts of the recombinant proteins, synthesized in short periods of time, in our case, and only moderate amounts, synthesized over much longer periods of time, in the system used by

Howard. This may be relevant if proteins which are produced in low amounts by the *E. coli* strain itself are involved in maturation of the Fe protein. In this respect, it is interesting that very recently a NifS protein has been purified that is produced in low amounts by *E. coli* (0.15 % of the total cellular protein) [10]. It cannot be excluded that *E. coli* NifS replaces NifS encoded by the *nif* gene cluster in the activation of the Fe protein, but is not able to cope with the high amounts of Fe protein made in the expression system used by us.

Unfortunately, loss of plasmid pAV41 has prevented us till now to investigate if active Fe protein can be produced in *E. coli* by coexpression of all four genes, *nifH*, *nifM*, *nifU* and *nifS*.

Purification of NifM.

A. vinelandii NifM was isolated from an *E. coli* clone, *E. coli* BL21[DE3] (pDB559), that contained the cloned gene in expression vector pT7-7. Induction of gene expression at 37 °C caused NifM to accumulate largely in inclusion bodies. Isolation of the inclusion bodies and refolding from 8 M urea yielded soluble NifM which was purified to homogeneity. However, freezing and thawing caused aggregation of this refolded NifM protein.

Induction at 20 °C resulted in production of NifM as a soluble protein. NifM was purified to high purity with the four-step procedure given in Materials and Methods. Although no purification table is given, as no activity was measured during subsequent steps, it was obvious that considerable loss occurred during purification: high amounts of NifM precipitated during dialysis and especially during the ultra-filtration steps. The final yield of NifM was 46 mg from 23 g of cells. The purified protein was colorless; the UV-visible spectrum gave no evidence for the presence of a cofactor.

Fig. 3 shows a SDS-polyacrylamide gel of four fractions from the final purification step on Phenyl-Sepharose. NifM has an apparent molecular weight of 34 kDa on SDS-polyacrylamide gel, which is close to the molecular weight calculated from the amino acid composition (32.8 kDa, [3]) as derived from the sequence of the gene. The apparent molecular weight of the native protein was determined by chromatography on Superdex 200 with suitable marker proteins. Purified NifM had an apparent molecular weight of 42 kDa on this column; furthermore, a minor peak corresponding with an apparent molecular weight of 71 kDa was detected (Fig. 4). Analysis of the 42 kDa and 71 kDa fractions on SDS-polyacrylamide gel indicated that both peaks contain NifM. Apparently, the majority of NifM is a monomer under these conditions, but a minor fraction runs as a dimer. When NifM is concentrated by ultracentrifugation before application on the Superdex column, a large fraction is present as aggregates with a very high apparent molecular weight.

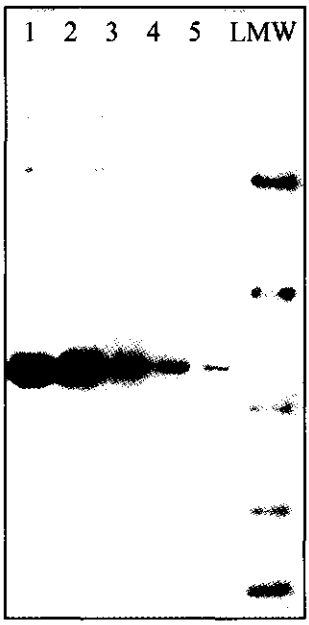

Figure 3

SDS-polyacrylamide gel electrophoresis of NifM purified from *E. coli* BL21[DE3] (pDB559).
Shown are NifM-containing fractions of the final Phenyl Sepharose column (lanes 1-5) and low-molecular-weight marker-proteins (Pharmacia).

The behavior of NifM during hydrophobic interaction chromatography on Phenyl Sepharose, onto which the protein binds without added salts and from which it can only be eluted with high concentrations of ethylene glycol, suggests that NifM is very hydrophobic. We therefore considered the possibility that in *A. vinelandii* NifM is not present as a separate protein, but occurs as a subunit of a larger protein complex. Consequently, purification of NifM (or of the complex) was also attempted from *A. vinelandii*. As indicated by incubation of Western blots of *A. vinelandii* cell extracts with antibodies against NifM, the amount of NifM is very low in *Azotobacter*. In order to allow purification of NifM from *Azotobacter*, 6 codons for His were incorporated into the *nifM* gene, enabling synthesis of NifM with a C-terminal His-tag, and this modified gene was crossed into the *A. vinelandii* Δ*nifM* mutant DJ67. The resulting strain, *A. vinelandii* BB1, was capable of normal diazotrophic growth, indicating that the His-tagged NifM was functional. Purification of the His-tagged NifM was attempted by anaerobic Immobilized Metal Affinity Chromatography of cell-free extract of *A. vinelandii* BB1, grown under diazotrophic conditions. Both zinc-activated iminodiacetic acid Sepharose 6B (Sigma) and nickel-activated nitrillotriacetic acid agarose (Quiagen) were used as chromatographic resin; elution of bound protein was done, subsequently, with increasing concentrations of imidazole (up to 250 mM), followed by EDTA (10 mM) and urea (8 M). Under none of these conditions specific binding and elution of NifM was detected, although cell-free extract of up to 40 g cells was applied to the columns. This suggests that the His-tag on

NifM is not available for binding to the immobilized metal ions, possibly as a result of specific folding or of proteolytic removal.

We also considered the possibility that NifM forms a complex with the protein encoded by *orf9*, which is in the same operon as *nifM*. *Orf9* encodes a homologue of the *E. coli* protein ClpX, an ATP-binding protein which, like certain chaperones, can dissolve protein aggregates and occurs in *E. coli* as a component of the ATP-dependent protease ClpP, [35], However, coexpression of *nifM* and *orf9* in *E. coli* and subsequent purification indicate that NifM and the protein encoded by *orf9* eluted in different fractions of an ion-exchange column.

Is NifM a PPIase?

Based on the homology between NifM and parvulin, we have looked for PPIase activity in NifM isolated from *E. coli* BL21[DE3] (pDB559). The Fe protein from *A. vinelandii* nitrogenase contains 8 proline residues per subunit [36], which are in the folded protein all in the *trans*-conformation ([2], Dr. D. Dean, personal communication), i.e. the same conformation that they have in the unfolded protein as it is synthesized.

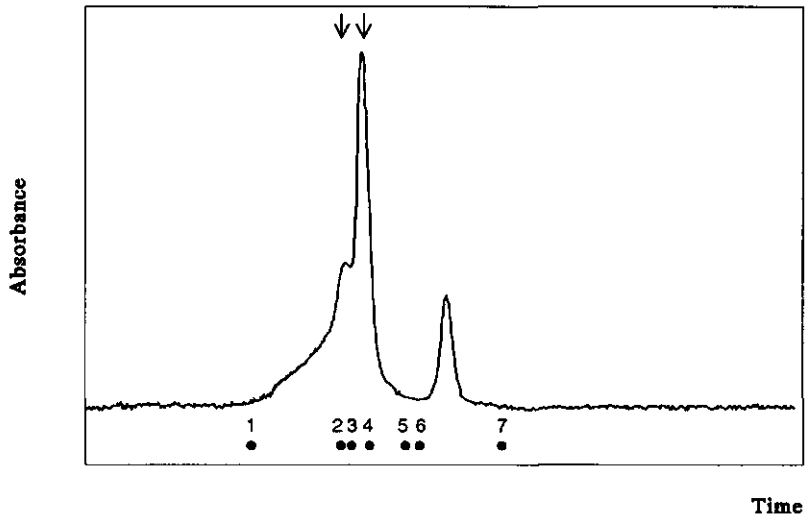

Figure 4

Gel-filtration of purified NifM on Superdex 200. Shown are the two peaks obtained by gel-filtration of the purified NifM (arrows). The position of the following markers (obtained in separate runs) is indicated: 1: Blue dextran, 2: Human transferrin, 3: Bovine serum albumin, 4: Ovalbumin 5: Chymotrypsinogen 6: Cytochrome c_3, 7: $CuSO_4$. The low-molecular-weight peak in the chromatogram is the result of DTT, present in the NifM-sample.

However, it cannot be excluded that some of these residues transiently assume a *cis*-conformation during biosynthesis of the protein, a process which would be facilitated by a PPIase. Three of the prolines in each subunit are close to the Fe-cluster, two of them (Pro-91 and Pro-93) in loops, one from each subunit, that wrap around the [4Fe-4S] cluster and extend over the surface of the other subunit. These loops contain the Cys-97 ligand for the Fe-S cluster. Change of the conformation of these prolines will result in a change of position of the loops (and the cysteine ligands) and may be involved in subunit assembly or cluster incorporation. The involvement of NifM as a PPIase in the maturation of the Fe protein is therefore not inconceivable.

PPIase activity of NifM was determined with two substrates: suc-AAPF-pNA and suc-AFPF-pNA. The side chain of the second amino acid determines the specificity of PPIases belonging to the different classes: cyclophilins have a much higher specificity for suc-AAPF-pNA than for suc-AFPF-pNA; FKBP's, on the other hand, prefer sub-

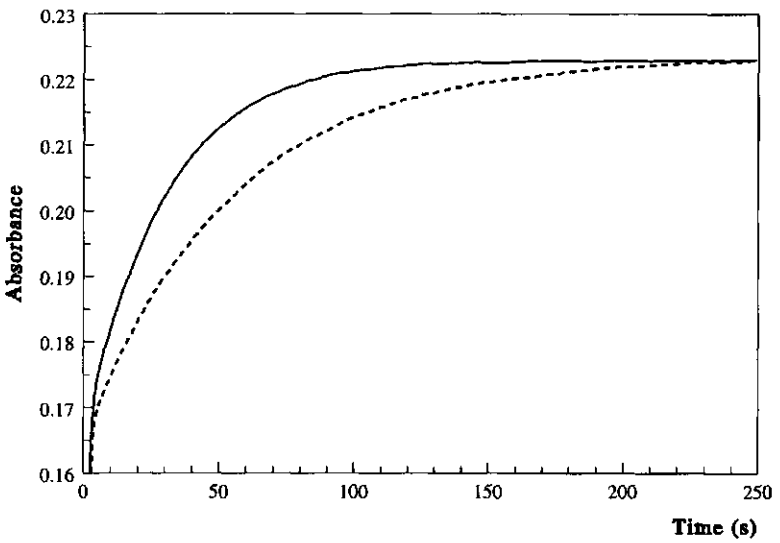

Figure 5

PPIase activity of the purified NifM preparation. Hydrolysis of *cis*-suc-AFPF-pNA by chymotrypsin in the presence (upper curve, continuous line) or absence (lower curve, dotted line) of NifM as measured with a stopped-flow apparatus. 892 μM suc-AFPF-pNA; 3.6 μM NifM; 1.8 mg ml^{-1} chymotrypsin; T = 20 °C. Formation of *p*-nitroaniline was recorded at 395 nm. Note: curves only show the slow step of the PPIase reactions, i.e. the chymotrypsin-catalyzed production of *p*-nitroaniline from the *cis*-conformer of suc-AFPF-pNA after spontaneous (lower curve) and NifM-catalyzed (upper curve) isomerization. Hydrolysis by chymotrypsin of the *trans*-conformer of suc-AFPF-pNA (75% of the total concentration of suc-AFPF-pNA), which occurs within the first second of the reaction, is not shown in this Figure.

strates with a bulky hydrophobic side chain on the second amino acid. Only one parvulin-type PPIase has been isolated until now; it has a slightly higher specificity for suc-AFPF-pNA than for suc-AAPF-pNA [22].

NifM purified and refolded from inclusion bodies had no activity with either substrate. Also NifM isolated as soluble protein had no activity with suc-AAPF-pNA as a substrate, but activity with suc-AFPF-pNA was readily detected (Fig. 5), although at rather high NifM concentrations. Kinetic parameters were determined by measuring the reaction rates at varying substrate concentrations (3 - 1120 μM) and 3.6 μM NifM (Fig. 6). Data-points in Fig. 6 were fitted with the Michaelis-Menten equation, resulting in the following values for the kinetic parameters: k_{cat} = 1.17 s^{-1}; K_M = 0.24 mM; k_{cat} / K_M = 4.8 10^3 M^{-1} s^{-1}. This k_{cat} / K_M value is considerably lower than those measured for prototype PPIases: parvulin and cyclophilins, 1-2 10^7 M^{-1} s^{-1} [29, 22], FKBP's appr. 5 10^6 M^{-1} s^{-1} [29]. Although the K_M-value is in the same range as found for cyclophilins and FKBP's (0.5 - 1 mM), the k_{cat} is 100-1000 fold lower, suggesting that a) NifM has a low activity (as found for some PPIase-domain proteins like FKBP25mem from *Legionella*

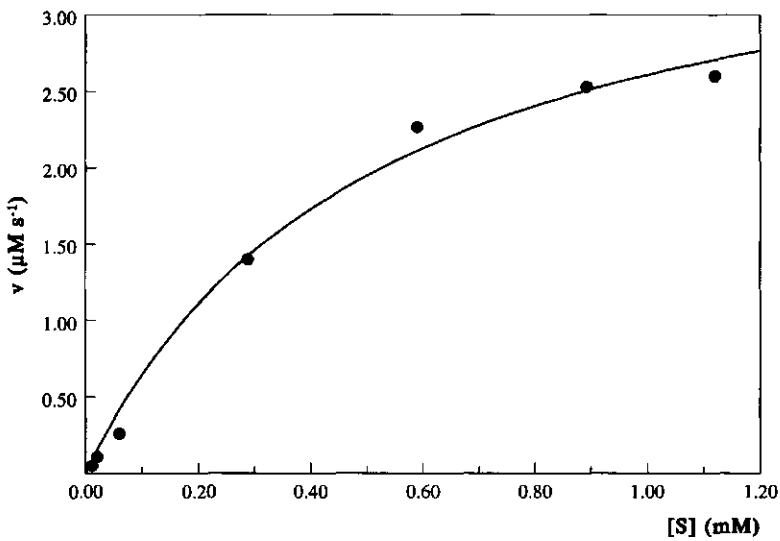

Figure 6

Kinetics of hydrolysis of suc-AFPF-pNA by chymotrypsin in the presence of NifM.
v represents the initial rate of hydrolysis of the *cis*-conformer of suc-AFPF-pNA in the presence of NifM, corrected for the rate of spontaneous hydrolysis in the absence of NifM. Note: [S] is the total concentration of suc-AFPF-pNA in the reaction (*cis*- + *trans*-conformers); the concentration of the *cis*-conformer is 25% of the total concentration. 3.6 μM NifM; T = 20 °C. Data-points were fitted with the Michaelis-Menten equation.

pneumophila, [37] or b) only a small part of the NifM molecules is enzymatically active or c) NifM is contaminated with a small amount of a very active *E. coli* PPIase.

In a first experiment to discriminate between these possibilities the influence of rapamycin on the PPIase activity of NifM was studied. Rapamycin is a competitive inhibitor for FKBP's, but does not inhibit PPIase activity of cyclophilins or parvulin. Fig. 7 shows that 50% of the PPIase activity associated with NifM (concentration NifM in the assay 3.7 μM) was inhibited at a rapamycin concentration of 22 nM. The PPIase activity associated with NifM must therfore be caused by contamination of the NifM preparation with a low amount of a FKBP-type of PPIase.

The conclusion from these experiments must be that, although PPIase activity was found in the NifM preparation, inhibition of this activity with a low concentration of rapamycin indicates that it results from a contamination with a very small amount of an *E. coli* FKBP. Although *E. coli* FKBP's were not known at the time of these experiments, very recently a dimeric FKBP has been isolated from *E. coli* (FKBP22) with similar size and behavior on ion-exchange and hydrophobic interaction columns as NifM [38]. PPIase activity of NifM has, therefore, not been demonstrated.

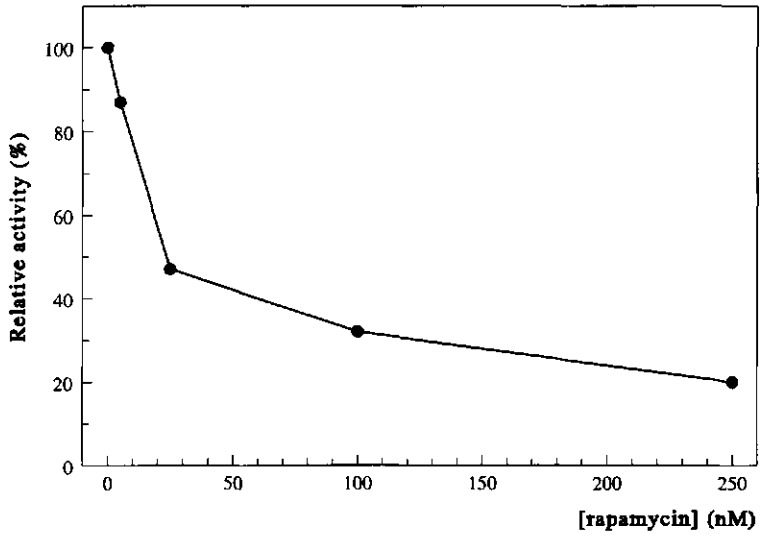

Figure 7

Inhibition of PPIase activity associated with NifM by rapamycin.
Percentual decrease of the initial rate of hydrolysis of the *cis*-conformer of suc-AFPF-pNA with purified NifM (corrected for spontaneous hydrolysis) in the presence of different concentrations of rapamycin. 20 μM suc-AFPF-pNA; 3.6 μM NifM; T = 20 °C. Note: rapamycin did not inhibit spontaneous hydrolysis.

Acknowledgments

Dr. D. Dean (Virginia Polytech and State University, Blacksburg, Virginia, USA) kindly provided us with plasmids pDB525, pDB527, pDB551 and pDB559 and the *A. vinelandii* mutant strain DJ67 and helped with construction of *A. vinelandii* BB1. Dr. J. Kay (University of Sussex, Brighton, UK) did the first PPIase tests with NifM and provided us with information on the assay conditions. Dr. G. Fischer (Max-Planck-Gesellschaft, Arbeitsgruppe 'Enzymologie der Peptidbindung', Halle, Germany) provided us with information about E. coli PPIases prior to publication. We thank professor C. Veeger for his continuous support and interest. This research was supported by the Netherlands Foundation for Chemical Research (SON) with financial aid from the Netherlands Organization for Scientific Research (NWO).

References

1 Kim, J. and Rees, D.C. (1992) *Nature (London) 360*, 553 - 560.
2 Georgiadis, M.M., Komiya, H., Chakrabarti, P., Woo, D., Kornuc, J.J. and Rees, D.C. (1992) *Science 257*, 1653 - 1659.
3 Jacobson, M.R., Brigle, K.E., Bennett, L.T., Setterquist, R.A., Wilson, M.S., Cash, V.L., Beynon, J., Newton, W.E. and Dean, D.R. (1989) *J. Bacteriol. 171*, 1017 - 1027.
4 Joerger, R.D. and Bishop, P.E. (1988) *J. Bacteriol. 170*, 1475 - 1487.
5 Jacobson, M.R., Cash, V.L., Weiss, M.C., Laird, N.F., Newton, W.E. and Dean, D.R. (1989) *Mol. Gen. Genet. 219*, 49 - 57.
6 Zheng, L., White, R.H., Cash, V.L., Jack, R.F. and Dean, D.R. (1993) *Proc. Natl. Acad. Sci. U.S. 90*, 2754 - 2758.
7 Zheng, L., White, R.H., Cash, V.L. and Dean, D.R. (1994) *Biochemistry 33*, 4714 - 4720.
8 Zheng, L. and Dean, D.R. (1994) *J. Biol. Chem. 269*, 18723 - 18726.
9 Sun, D. and Setlow, P. (1993) *J. Bacteriol. 175*, 1423 - 1432.
10 Flint, D.H. (1996) *J. Biol. Chem. 271*, 16068 - 16074.
11 Green, J., Bennett, B., Jordan, P., Ralph, E.T., Thomson, A.J. and Guest, J.R. (1996) *Biochem. J. 316*, 887 - 892.
12 Hidalgo, E. and Demple, B. (1996) *J. Biol. Chem. 271*, 7269 - 7272.
13 Fu, W., Jack, R.F., Morgan, T.V., Dean, D.R. and Johnson, M.K. (1994) *Biochemistry 33*, 13455 - 13463.
14 Howard, K.S., McLean, P.A., Hansen, F.B., Lemley, P.V., Kobaln, K.S. and Orme-Johnson, W.H. (1986) *J. Biol. Chem. 261*, 772 - 778.
15 Dean, D.R., Bolin, J.T. and Zheng, L. (1993) *J. Bacteriol. 175*, 6737 - 6744.
16 Rudd, K.E., Sofia, H.J., Koonin, E.V., Plunkett III, G., Lazar, S. and Rouviere, P.E. (1995) *Trends Biochem. Sci. 20*, 12 - 14.
17 Kay, J.E. (1996) *Biochem. J. 314*, 361 - 385.
18 Galat, A. and Metcalfe, S.M. (1995) *Prog. Biophys. Molec. Biol. 63*, 67 - 118.

19 Harrison, R.K. and Stein, R.L. (1990) *Biochemistry 29*, 1684 - 1689.
20 Harrison, R.K. and Stein, R.L. (1992) *J. Am. Chem. Soc. 114*, 3464 - 3471.
21 Harrison, R.K. and Stein, R.L. (1990) *Biochemistry 29*, 3813 - 3816.
22 Rahfeld, J.U., Schlierhorn, A., Mann, K. and Fischer, G. (1994) *FEBS Lett. 343*, 65 - 69.
23 Rosenberg, A.H., Lade, B.N., Chui, D., Lin, S.-W., Dunn, J.J. and Studier, F.W. (1987) *Gene 56*, 125 - 135.
24 Tabor, S. (1990) in: *Current protocols in molecular biology* (F.A. Ausubel, R. Brent, R.E. Kingston, D.D. Moore, J.G. Seidman, J.A. Smith and K. Struhl, eds.) pp. 16.2.1 - 16.2.11, Greene Publishing and Wiley Interscience, New York, USA.
25 Studier, F.W., Rosenberg, A.H., Dunn, J.J. and Dubendorff, J.W. (1990) *Meth. Enzymol. 185*, 60 - 89.
26 Gibson, T.J. (1984) *Studies of the Epstein-Barr virus genome*. PhD-thesis, University of Cambridge, UK.
27 Duyvis, M.G., Wassink, H. and Haaker, H. (1994) *Eur. J. Biochem 225*, 881 - 890.
28 Fischer, G., Bang, H., Berger, E. and Schellenberger, A. (1984) *Biochim. Biophys. Acta 791*, 87 - 97.
29 Kofron, J.L., Kuzmic, P., Kishore, V., Colón-Bonilla, E. and Rich, D.H. (1991) *Biochemistry 30*, 6127 - 6134.
30 Haandrikman, A.J., Kok, J., Laan, H., Soemitro, S., Ledeboer, A.M., Konings, W.N. and Venema, G. (1989) *J. Bacteriol. 171*, 2789 - 2794.
31 Vos, P., Van Asseldonk, M., Van Jeveren, F., Siezen, R., Simons, G. and De Vos, W.M. (1989) *J. Bacteriol. 171*, 2795 - 2802.
32 Kontinen, V.P., Saris, P. and Sarvas, M. (1991) *Mol. Microbiol. 5*, 1273 - 1283.
33 Missiakas, D., Betton, J.M. and Raina, S. (1996) *Mol. Microbiol. 21*, 871 - 884.
34 Rahfeld, J.U., Rücknagel, K.P., Schelbert, B., Ludwig, B., Hacker, J., Mann, K. and Fischer, G. (1994) *FEBS Lett. 352*, 180 - 184.
35 Wojtkowiak, D., Georgopoulos, C. and Zylicz, M. (1993) *J. Biol. Chem. 268*, 22609 - 22617.
36 Brigle, K.E., Newton, W.E. and Dean, D.R. (1985) *Gene 37*, 37 - 44.
37 Schmidt, B., Rahfeld, U., Schierhorn, A., Ludwig, B, Hacker, J. and Fischer, G. (1994) *FEBS Lett. 352*, 185 - 190.
38 Rahfeld, J.U., Rücknagel, K.P., Stoller, G., Horne, S.M., Schierhorn, A., Young, K.D. and Fischer, G. (1996) *J. Biol. Chem. 271*, 22130 - 22138.
39 Yannisch-Perron, C., Vieira, J and Messing, J. (1985) *Gene 33*, 103 - 119.
40 Chang, A.C.Y. and Cohen, S.N. (1978) *J. Bacteriol. 134*, 1141 - 1156.
41 Dayhoff, M.O., Schwartz, R.M. and Orcutt, B.C. (1978) *Atlas of Protein Sequence and Structure*, Vol.5, Suppl. 3, (Dayhoff, M.O., Ed.) p. 345, NBRF, Washington.
42 Higgins, D.G. and Sharp, P.M. (1988) *Gene 73*, 237 - 244.

Summary

Microperoxidases: kinetics and stability.

Microperoxidases are small enzymes prepared by proteolytic digestion of cytochromes *c*. The proteolytic removal of most of the protein environment allows these enzymes to use a wide variety of substrates in peroxidase- and cytochrome *P*-450-type reactions. A major drawback for the application of microperoxidases, however, is their rapid inactivation. The formation of high valent FeIV-oxo compounds, formed during catalysis, probably plays a key role in this inactivation. Chapter 2 describes the hydrogen peroxide-dependent *para*-hydroxylation of aniline by microperoxidases which have peptides attached to the heme moiety with different chain lengths (microperoxidases 6, 8 and 11, all prepared from horse-heart cytochrome *c*) and composition (microperoxidase 17, prepared from cytochrome c_{550} from *Thiobacillus versutus*).

Investigation of MP6, MP8 and MP11 (with peptide chains of 6, 8 and 11 amino acids, respectively) showed that these microperoxidases have similar V_{max} values, but that the rate of inactivation is dependent on the length of the peptide chain. Inactivation rates (at 0.4 mM aniline) range from 0.141 s^{-1} for MP6 to 0.091 s^{-1} for MP11. Although inactivation is rapid in all cases, a longer peptide chain apparently offers more protection against inactivation. The K_M is also dependent on the length of the peptide chain, ranging from 0.82 mM for MP6 to 0.41 mM for MP11. In addition, the rates of inactivation for these microperoxidases decreases by about 50% when the aniline concentration is increased from 0.4 to 12 mM. This points at a role for the substrate in the inactivation process; possibly binding of aniline to the heme moiety also offers some protection.

MP17 has kinetic properties that are not in line with those of the microperoxidases described above: contrary to what is to be expected on the basis of the length of the attached peptide chain (17 amino acids) the rate of inactivation as well as the K_M and V_{max} values are higher than for the other microperoxidases. Increasing the aniline concentration from 0.4 to 12 mM only decreases the rate of inactivation of MP17 by about 10%. The observed correlation between V_{max} and the rate of inactivation of the microperoxidases confirms the assumption that high valent heme compounds, formed during catalysis, are involved in inactivation. The different catalytic properties of MP17 must be caused by the specific properties of its peptide chain. MP17 does not bind a single peptide chain, as do the other microperoxidases, but two: a short chain (2 amino acids) and a longer chain (15 amino acids), which is the result of proteolytic cleavage between the heme-binding cysteines. Furthermore, the amino acid composition of the (broken) peptide chain is different from that of the other microperoxidases.

The FeSII protein: stabilization of nitrogenase.

The nitrogen fixing soil bacterium *A. vinelandii* produces a small iron-sulfur protein, known as the FeSII protein, that can bind to nitrogenase rendering it temporarily oxygen resistant. In chapter 3 of this thesis evidence is given that FeSII protein offers protection for the nitrogenase Fe protein from *A. vinelandii* against oxygen-inactivation by stabilizing the association of the Fe protein (Av2) with the MoFe protein (Av1).

Av2 was exposed to oxygen (air) in the presence of MgADP under several conditions. Exposure of free Av2, i.e. without adding FeSII or Av1, to oxygen results in rapid inactivation: all activity is lost within 5 minutes. When Av1 is added in a 1 : 2 ratio with Av2 the inactivation is about 4 times slower. Under the experimental conditions approximately 75% of Av2 is associated with Av1, as $Av1[Av2(MgADP)_2]_2$, at the start of the exposure to oxygen, which indicates that Av2 is protected against oxygen-inactivation by association with Av1. Addition of both Av1 and the FeSII protein results in a further decrease of the inactivation. When the FeSII protein, Av1 and Av2 are present in a 1 : 1 : 2 ratio, the rate of inactivation is 8 times slower, as compared to the sample containing only Av2 and Av1. This indicates that the FeSII protein stabilizes the interaction between Av2 and Av1. In the presence of MgADP and aluminum fluoride Av1 and Av2 form a stable $Av1[Av2(AlF/MgADP)_2]_2$ complex, from which Av2 can not dissociate. This nitrogenase complex proved to be the most stable of all investigated samples, which confirms the conclusion that the association of Av2 with Av1 protects Av2 against inactivation by oxygen.

Evidence for the existence of two types of three-component protein complexes, formed by Av2, Av1 and the FeSII protein, was obtained from stopped-flow experiments. It was shown that when Av1 is present in a twofold excess with respect to the FeSII protein, the latter protein binds two $Av1[Av2(MgADP)_2]_2$ nitrogenase complexes, whereas when equimolar amounts of Av1 and FeSII are present in the incubation only one $Av1[Av2(MgADP)_2]_2$ nitrogenase complex is bound by the FeSII protein.

Based on these experiments a model was set up to describe the reactions involved in the oxygen-inactivation and the reduction of the nitrogenase proteins under the various experimental conditions. Using this model and the kinetic parameters obtained from the various experiments, the data could be simulated best when 1: both the active and inactivated forms of Av2 were allowed to associate reversibly with Av1, 2: the rate constants for both interactions were identical and 3: the formation of both types of three-component complexes with the FeSII protein was taken into account. These simulations indicated that the formation of complexes between the FeSII protein and the $Av1[Av2(MgADP)_2]_2$ nitrogenase complex is an adequate explanation for the protection against oxidative inactivation of nitrogenase by the FeSII protein.

The transition state complex of nitrogenase: redox regulation.

Nitrogenase catalyzed reduction of N_2 to NH_3 requires the association of the nitrogenase Fe protein (Av2) with the nitrogenase MoFe protein (Av1), MgATP-dependent electron transfer from Av2 to Av1 and on-enzyme ATP hydrolysis followed by dissociation of Av2, with MgADP bound, from Av1. Aluminum fluoride and MgADP inhibit the dissociation of Av2 from Av1 by stabilizing the protein-protein complex of an intermediate of the on-enzyme MgATP hydrolysis reaction.

Redox titrations and EPR spectroscopy revealed that the redox properties of FeMoco in Av1 remain unchanged in this complex, as compared to the purified, free MoFe protein. The redox properties of the [8Fe-7S] P-clusters in Av1, however, are markedly different. Upon oxidation, in a two-electron process, of the P-clusters in purified Av1 an EPR-signal appears with E_m = -307 mV. In the AlF/MgADP stabilized complex this signal was not observed. Another signal, exhibited by the one electron oxidized P-clusters, appears at a potential lower than -500 mV (out of the range of the experiments). This signal disappears again at E_m = -430 mV, which indicates that in the AlF/MgADP stabilized complex the abstraction of the second electron takes place at this potential. These observations indicate that the P-clusters in the AlF/MgADP stabilized complex have a different conformation, as compared to the P-clusters in free Av1.

The [4Fe-4S] clusters in Av2 operate between the +1 and +2 oxidation levels. Upon reduction of the clusters in purified Av2 EPR-signals appear at E_m = -473 mV when MgADP is bound to the protein or at E_m = -440 mV when MgATP is bound. For the AlF/MgADP stabilized complex, however, no EPR-signals characteristic for reduced Av2 were observed and it was concluded that in the AlF/MgADP stabilized nitrogenase complex the midpoint redox potential of the [4Fe-4S] clusters in Av2 is lowered to less than -500 mV, out of the range of the experiments. This change in redox potential indicates that also the [4Fe-4S] clusters of Av2 in the AlF/MgADP stabilized complex have a different conformation, as compared to the clusters in free Av2.

These results indicate that nitrogenase catalysis involves conformational redox regulation. Free Av2 has a relatively high redox potential which facilitates electron transfer to this protein from reductants (flavodoxin) in the cell. After binding of MgATP, Av2 changes its conformation. These changes in conformation lower the redox potential of the [4Fe-4S] cluster in Av2, thus inducing electron transfer to the P-clusters in Av1. The lowered redox potential of the P-clusters, resulting from conformational changes caused by binding of Av2 to Av1, facilitates electron transfer to FeMoco, the putative substrate-binding site, which has unchanged redox properties. The FeMoco clusters in turn transfer the electrons to the substrate, N_2, to generate ammonia. After on-enzyme hydrolysis of ATP the Fe protein changes to the MgADP-bound conformation and dissociates from the MoFe protein to enter a new cycle of electron transfer.

NifM: its role in the biosynthesis of the Fe protein.

Chapter 5 reports on the investigation of the possible role of NifM in the maturation of the nitrogenase Fe protein from *Azotobacter vinelandii*. NifM was purified from *E. coli* harboring a recombinant plasmid that incorporated the *nifM* gene. The purified protein was colorless: the UV-visible spectrum gave no evidence for the presence of a cofactor. Comparison of the DNA and amino acid sequences of NifM with those of other proteins revealed that NifM has a relevant sequence homology to several proteins that are involved in protein folding / maturation, especially parvulin from *E. coli*. Parvulin is a peptidylprolyl *cis-trans* isomerase, or PPIase. PPIases catalyze the interconversion of the *trans*-isomer of proline into the *cis*-isomer. During protein synthesis, peptide bonds formed by the proline residues are in the *trans* conformation, but in folded proteins, appr. 15% of the residues have a *cis* conformation. In addition, the proper folding of a protein may require the temporary conversion of the *trans* conformation to the *cis* conformation. NifM could therefore be involved, as a PPIase, in the proper folding / maturation of the Fe apoprotein. PPIase activity of NifM could not be demonstrated. The role of NifM in the maturation of the Fe protein, however, was positively demonstrated: deletion of the *nifM* gene from *A. vinelandii* results in the production of inactive, precipitated Fe protein.

Samenvatting

(Summary in Dutch)

IJzer bevattende enzymen en zuurstof.

Enzymen zijn eiwitten die biochemische reacties katalyseren. Deze reacties vormen de basis van het functioneren van het organisme en zijn betrokken bij de afbraak, omzetting en opbouw van de componenten waaruit het organisme bestaat. Zonder enzymen zouden deze reacties niet plaats kunnen vinden en zou leven onmogelijk zijn. IJzer maakt onderdeel uit van veel van deze enzymen en is dan ook onmisbaar voor alle organismen. Het ijzer is meestal opgenomen in een cofactor: een niet door het eiwit gevormd deel van het enzym dat betrokken is bij de katalyse. Veel enzymen met ijzer bevattende cofactoren worden geïnactiveerd door zuurstof of door z.g. geactiveerd zuurstof in de vorm van o.a. waterstofperoxide, superoxide en hydroxyl radicalen. De cofactoren zijn meestal het doelwit van deze oxidatieve afbraak, maar de mechanismen die er aan ten grondslag liggen zijn nog grotendeels onbegrepen. De bestudering van de oxidatieve inactivering van microperoxidases en nitrogenase, met verschillende typen ijzer bevattende cofactoren, vormt een belangrijk deel van dit proefschrift.

Microperoxidases.

In microperoxidases is het ijzer aanwezig in het centrum van de z.g. heem-groep: een cofactor die is opgebouwd uit een ringvormige structuur van, met name, koolstofatomen. De ring is aan de buitenzijde verbonden met twee aminozuren (cysteïnes) in het eiwit; een derde aminozuur (histidine) staat loodrecht op het vlak van de heem-groep en is verbonden met het centrale ijzer-ion. Microperoxidases worden verkregen door het grootste deel van het eiwit van een z.g. cytochroom *c* te verwijderen. Het aantal aminozuren in de resterende eiwitketen geeft het microperoxidase zijn naam. De invloed van de lengte en samenstelling van de eiwitketen van MP6, MP8, MP11 en MP17 voor de katalystische eigenschappen van deze microperoxidases wordt in dit proefschrift beschreven. Microperoxidases worden gebruikt in het biochemisch onderzoek als een modelsysteem voor enzymen die betrokken zijn bij detoxificatie processen, zoals peroxidases en cytochroom *P*-450. Doordat de eiwitomgeving in microperoxidases grotendeels ontbreekt, zijn deze enzymen in staat om de verschillende biochemische reacties waarvoor zij model staan te katalyseren; in de oorspronkelijke cytochromen bepaalt de eiwitomgeving van de heem-groep de reacties die daar plaats kunnen vinden. Een nadelig gevolg is echter dat microperoxidases niet kunnen profiteren van de bescherming tegen oxidatieve inactivering die de eiwitomgeving de heem-groep biedt.

De waterstofperoxide afhankelijke *para*-hydroxylering van aniline door microperoxidases vormt het onderwerp van hoofdstuk 2 van dit proefschrift. Het daar beschreven onderzoek laat zien dat microperoxidases efficiënte katalysatoren zijn, maar dat zij ook snel geïnactiveerd worden tijdens de reacties die zij katalyseren. De vorming van hoog geoxideerde vormen van de heem-groep, die een rol spelen bij de katalyse, ligt waarschijnlijk ten grondslag aan deze inactivering. Onderzoek aan MP6, MP8 en MP11 liet zien dat de V_{max}, de maximale snelheid waarmee het substraat wordt omgezet, voor deze microperoxidases gelijk is, maar dat een langere eiwitketen resulteert in een langzamere inactivering. Dit wijst erop dat inactivering een gevolg is van het grotendeels ontbreken van de eiwitomgeving. Een langere eiwitketen gaat ook gepaard met een lagere K_M, d.w.z. met een hogere affiniteit voor het substraat. Alle onderzochte microperoxidases zijn daarbij enigzins stabieler bij hogere substraat concentraties. Dit kan betekenen dat binding van het substraat aan de heem-groep ook enige bescherming tegen inactivering biedt.

In tegenstelling tot de hiervoor besproken microperoxidases, die gemaakt zijn van paardehart cytochroom *c*, is MP17 gemaakt van cytochroom c_{550} uit de bacterie *Thiobacillus versutus*. MP17 bleek sterk afwijkende eigenschappen te hebben: in tegenstelling tot wat de lengte van de eiwitketen doet vermoeden, verlopen de inactivering en de omzetting van het substraat (V_{max}) sneller dan bij de andere microperoxidases; ook is de affiniteit voor het substraat geringer. De correlatie tussen V_{max} en de snelheid van inactivering bevestigt de veronderstelling dat hoog geoxideerde vormen van de heem-groep, die gevormd worden tijdens de katalyse, betrokken zijn bij de inactivering. MP17 bevat niet één enkele eiwitketen, maar twee: een korte keten (2 aminozuren) en een langere (15 aminozuren) zijn elk middels een cysteïne aan de heem-groep gebonden. Ook de aminozuur samenstelling van deze onderbroken eiwitketen verschilt van die van de andere microperoxidases. De oorzaak van de afwijkende katalytische eigenschappen van MP17 moet dan ook gezocht worden in deze verschillen.

De stabiliteit van nitrogenase.

Nitrogenase speelt een centrale rol in de z.g. stikstof-cyclus: het zet moleculaire stikstof om in ammoniak, een proces dat bekend staat als stikstof-fixatie. Stikstof komt voor in de meeste componenten van de cel. De lucht om ons heen bestaat voor 78% uit moleculaire stikstof (N_2). Dit molecuul is echter zeer stabiel en kan hierdoor niet door organismen gebruikt worden als voedingsbron. Ammoniak kan wel in het metabolisme worden opgenomen; de rol van nitrogenase is dan ook het beschikbaar maken van stikstof in de atmosfeer voor de biosynthese van bijvoorbeeld eiwitten en DNA.

Nitrogenase is een enzym dat is samengesteld uit twee componenten die tesamen een complex kunnen vormen: het ijzer-eiwit (Fe-eiwit) en het molybdeen-ijzer-eiwit

(MoFe-eiwit). Beide delen bevatten z.g. ijzer-zwavel clusters: cofactoren die zijn samengesteld uit ijzer- en sulfide-ionen. Deze ijzer-zwavel clusters zitten vast aan de eiwitketen via bindingen tussen de ijzer-ionen en aminozuren in het eiwit, meestal cysteïnes. Met name het ijzer-zwavel cluster van het Fe-eiwit is erg gevoelig voor oxidatieve afbraak. Dit vormt een probleem voor stikstof-fixerende organismen: enerzijds hebben zij zuurstof nodig om, via biochemische omzetting van voedingsstoffen, energie vrij te maken die nodig is voor de stikstof-fixatie, anderzijds vormt de aanwezigheid van zuurstof een bedreiging voor het nitrogenase enzym dat deze reactie katalyseert. De stikstof-fixerende bodembacterie *Azotobacter vinelandii* heeft twee manieren om dit probleem aan te pakken: het bevat een enzym dat zuurstof in de cel kan omzetten, en het produceert een eiwit, het z.g. FeSII-eiwit, dat nitrogenase tijdelijk kan beschermen tegen inactivering door zuurstof.

In hoofdstuk 3 wordt het onderzoek naar de werking van dit FeSII-eiwit beschreven. Het zuurstof gevoelige Fe-eiwit is hierbij blootgesteld aan zuurstof onder verschillende omstandigheden. In afwezigheid van zowel het MoFe-eiwit als het FeSII-eiwit werd het Fe-eiwit snel geïnactiveerd. Wanneer alleen het MoFe-eiwit aan het Fe-eiwit werd toegevoegd nam de snelheid van inactivering aanzienlijk af. Toevoeging van zowel het MoFe-eiwit als het FeSII-eiwit resulteerde in een nog verdere afname van de inactivering. Dit wordt toegeschreven aan het feit dat het FeSII-eiwit, door aan het Fe-MoFe nitrogenase complex te binden, het Fe-eiwit en MoFe-eiwit bijeen houdt. Twee vormen van het door het FeSII-eiwit gestabiliseerde complex zijn aangetoond: Het FeSII-eiwit bindt bij hogere concentraties een enkel Fe-MoFe nitrogenase complex, bij lagere concentraties kan het twee van deze complexen binden. In aanwezigheid van MgADP en aluminium-fluoride ontstaat een speciale vorm van het Fe-MoFe nitrogenase complex, waarin het Fe-eiwit zeer vast aan het MoFe-eiwit is gebonden; dit complex bleek het beste bestand te zijn tegen inactivering door zuurstof. Uit deze waarnemingen blijkt dat bescherming tegen inactivering van het Fe-eiwit in alle gevallen berust op stabilisatie van het ijzer-zwavel cluster in dit eiwit, of op afscherming van dit cluster van de oplossing en de daarin aanwezige zuurstof, wanneer het Fe-eiwit aan het MoFe-eiwit is gebonden.

Redox regulatie van nitrogenase.

De functie van ijzer in biologische systemen berust op het feit dat dit ijzer-ionen kan vormen met verschillende ladingen: ijzer bevattende cofactoren kunnen electronen opnemen en afstaan. We spreken dan van verschillende redox-toestanden van de cofactor. Een overgang van de ene redox-toestand naar de andere vindt plaats binnen zekere marges rondom een bepaalde redox-potentiaal (de z.g. Nernst curve). Deze potentiaal is mede afhankelijk van de geometrie en eiwitomgeving van de cofactor. Veranderingen in

de conformatie van een eiwit kunnen dan ook de redox-potentiaal van de cofactor in het eiwit veranderen: dit wordt redox-regulatie genoemd.

In hoofdstuk 4 wordt beschreven hoe redox-regulatie een rol speelt in het nitrogenase enzym. Hiertoe is de stabiele vorm van het nitrogenase complex, dat het Fe-eiwit met het MoFe-eiwit vormt in aanwezigheid van MgADP en aluminiumfluoride, onderzocht met behulp van o.a. EPR-spectroscopie. Deze techniek maakt het mogelijk om te zien bij welke potentialen de cofactoren van de ene redox-toestand overgaan in de andere. Het bleek dat de redox-potentiaal van het ijzer-zwavel cluster in het Fe-eiwit en van de P-clusters in het MoFe-eiwit lager waren wanneer deze eiwitten deel uitmaakten van het stabiele complex. De redox-potentiaal van de FeMoco clusters, de veronderstelde de plaats waar in het MoFe-eiwit stikstof wordt omgezet in ammoniak, bleek niet veranderd te zijn in het stabiele complex. Uit deze resultaten blijkt dat het ijzer-zwavel cluster in het vrije Fe-eiwit een relatief hogere potentiaal heeft zodat het een electron op kan nemen van andere componenten in de cel. Door binding aan het MoFe-eiwit verandert de structuur van het Fe-eiwit met als gevolg dat de redox-potentiaal daalt; hierdoor kan het Fe-eiwit zijn electron afstaan aan de P-clusters in het MoFe-eiwit. Structurele veranderingen in het MoFe-eiwit, eveneens het gevolg van de complexvorming met het Fe-eiwit, verlagen de redox-potentiaal van de P-clusters die zodoende hun electronen af kunnen staan aan de FeMoco clusters waar de electronen vervolgens op het substraat (N_2) worden overgedragen en ammoniak wordt gevormd.

Biosynthese van het Fe-eiwit.

In hoofdstuk 5 wordt verslag gedaan van het onderzoek naar de mogelijke rol die het NifM eiwit uit *Azotobacter vinelandii* speelt in de biosynthese van het Fe-eiwit. Vergelijking van het voor NifM coderende gen en de ervan afgeleide aminozuur volgorde met die van andere eiwitten wees op sterke overeenkomsten van NifM met eiwitten die betrokken zijn bij de juiste vouwing van eiwitten; met name met parvuline uit *Escherichia coli*. Parvuline is een z.g. PPIase, een enzym dat het aminozuur proline om kan zetten van de z.g. *cis*-vorm naar de *trans*-vorm, en andersom. Proline heeft als bijzondere eigenschap dat het een knik vormt in de eiwitketen; bij de *cis*-vorm gaat deze knik een andere kant op dan bij de *trans*-vorm. Om een eiwit tijdens de biosynthese in de juiste conformatie te krijgen kan het dus noodzakelijk zijn om een of meerdere prolines (tijdelijk) in de andere vorm om te zetten. Het bleek niet mogelijk om een dergelijke PPIase activiteit ook daadwerkelijk voor het NifM eiwit aan te tonen. Wel is de rol van NifM in de biosynthese van het Fe-eiwit bewezen: wanneer het gen dat NifM codeert uit *A. vinelandii* werd verwijderd, bleek dit organisme niet meer in staat om oplosbaar, actief Fe-eiwit te produceren.

Curriculum vitae

Johannes Hendrikus Spee werd geboren op 14 februari 1958 te Delft. In 1976 deed hij eindexamen atheneum B aan het Sint Stanislascollege, eveneens te Delft. In afwachting van toelating tot een vervolgstudie heeft hij daarna een jaar als uitzendkracht gewerkt bij de gemeente Delft. Vijf jaar later, in 1982, haalde hij de tweede graads akte van bekwaamheid tot het geven van onderwijs in de vakken tekenen en handvaardigheid aan de lerarenopleiding Z.W.N., nog steeds te Delft. De twee daarop volgende jaren studeerde hij aan de Academie voor Beeldende Vorming in Tilburg. Na een roemloze, maar aangename carrière als percussionist in het Brabantse jazz-circuit begon hij in 1987 aan zijn studie biologie aan de Landbouwuniversiteit in Wageningen. In de doctoraalfase deed hij afstudeervakken bij de vakgroep Moleculaire Biologie (Dr. T. Bisseling, Prof. Dr. A. van Kammen) en de vakgroep Biochemie (Dr. A de Kok, Prof. Dr. C. Veeger). In augustus 1992 studeerde hij af.

Van november 1992 tot april 1997 was hij als onderzoeker in opleiding (OIO) verbonden aan de vakgroep Biochemie van de Landbouwuniversiteit te Wageningen, in dienst van de Nederlandse Organisatie voor Wetenschappelijk Onderzoek (NWO). Het onderzoek werd gefinancieerd door NWO, onder toezicht van de Stichting Scheikundig Onderzoek in Nederland (SON). Het onderzoek werd begeleid door Dr. Ir. W.M.A.M. van Dongen en Prof. Dr. C. Veeger. De resultaten van het onderzoek zijn beschreven in dit proefschrift.

Publications

J.H. Spee, H. Wassink, W.M.A.M Van Dongen and H. Haaker (1997) Protection of the nitrogenase Fe protein from *Azotobacter vinelandii* against oxygen-inactivation by complex formation with the MoFe protein, *Biochemistry* (submitted)

J.H. Spee, A.F. Arendsen, H. Wassink, S.J. Marritt, W.R. Hagen and H. Haaker (1997) Redox properties and electron paramagnetic resonance spectroscopy of the transition state complex of *Azotobacter vinelandii* nitrogenase, *J. Biol. Chem.* (submitted)

J.H. Spee, M.G. Boersma, C. Veeger, B. Samyn, J. Van Beeumen, G. Warmerdam, G.W. Canters, W.M.A.M. Van Dongen and I.M.C.M. Rietjens (1996) The influence of the peptide chain on the kinetics and stability of microperoxidases, *Eur. J. Biochem. 241*, 215 - 220

J.H. Spee, W.M. De Vos and O.P. Kuipers (1993) Efficient random mutagenesis method with adjustable mutation frequency by use of PCR and dITP, *Nucleic Acids Res. 3*, 777 - 778

J. Frazzon, J.H. Spee, J. Christiansen and D.R. Dean (1997) Nitrogenase: Two decades of biochemical genetics, in: *Biological fixation of nitrogen for ecology and sustainable agriculture*, (Logocki, A., Bothe, H. And Puhler, A., Eds.) pp. 3 - 8, Springer Verlag, Berlin, Heidelberg, New York

I.M.C.M. Rietjens, J.H. Spee, R. Weiss, A.X. Trautwein, W. Van Dongen, G.W. Canters and C. Veeger (1995) On the role of the axial ligands in heme-based catalysis, *J. Inorg. Chem. 59*, 490

J. Hendle, A. Mattevi, A.H. Westphal, J.H. Spee, A. De Kok, A.Teplyakov, and W.G. Hol (1995) Crystallographic and enzymatic investigations on the role of Ser558, His610 and Asn614 in the catalytic mechanism of *Azotobacter vinelandii* dihydro-lipoamide acetyltransferase (E2p), *Biochemistry 13*, 4278 - 4298

W. Yang, P. Katinakis, P. Hendriks, A. Smolders, F. De Vries, J.H. Spee, A. Van Kammen, T. Bisseling and H. Franssen (1993) Characterization of *GmENOD40*, a gene showing novel patterns of cell-specific expression during soybean nodule formation, *Plant J. 3*, 573 - 585

Slotwoord

Dit boekje is, anders dan de titelpagina doet vermoeden, niet alleen het resultaat van mijn eigen inspanningen. De auteurs die bij de verschillende hoofdstukken staan vermeld hebben ook daadwerkelijk een wezenlijke bijdrage aan het daar beschreven onderzoek geleverd. Daarnaast zijn echter veel personen onvermeld gebleven die een belangrijke rol hebben gespeeld bij de totstandkoming van dit proefschrift. In de wetenschap niet anders dan, helaas, onvolledig te kunnen zijn wil ik een aantal van al deze mensen met name noemen.

Allereerst wil ik Walter van Dongen, mijn co-promotor, bedanken voor zijn deskundige en bereidwillige begeleiding en ondersteuning. Je hebt mijn eigen inbreng in het onderzoek steeds volop de ruimte gegeven en tegelijkertijd altijd, en ogenblikkelijk, klaar gestaan om antwoorden en oplossing te vinden voor de vragen en problemen waar ik mee zat, ook als die geen betrekking hadden op het onderzoek. Zonder ooit de moed te verliezen, of overmoedig te zijn, heb je voor de stabiliteit gezorgd waar het mij vaak aan ontbrak. Het was daarom een geluk om jou als co-promotor te treffen en om onder jouw supervisie het hier beschreven onderzoek uit te kunnen voeren.

In niet mindere mate ben ik mijn promotor, professor Cees Veeger, dankbaar voor zijn voortdurende interesse in mijn onderzoek en zijn opbouwende kritieken bij het schrijven van dit proefschrift. Ik heb me zeer gesterkt gevoeld doordat je bent blijven geloven in het welslagen van mijn promotie, ook wanneer ik daar zelf minder zeker van was. Vooral in de eindfase is jouw inzet, medeleven en begrip van doorslaggevend belang geweest. Ik zal dat niet vergeten.

Ook Ivonne Rietjens ben ik veel dank verschuldigd. Je hebt je ingezet om mij nieuwe kansen te bieden op een moment dat het onderzoek dreigde vast te lopen, zonder dat je daar enige verplichting toe had. Al is het ons niet gelukt om ook al die kansen te benutten, het werk aan microperoxidases dat ik op jouw lab heb verricht en het vertrouwen dat je in mij hebt getoond, heeft mij veel voldoening gegeven.

Huub Haaker wil ik bedanken voor de vruchtbare en plezierige samenwerking. Ik ben erg blij dat je, ondanks de problemen die zich hebben voorgedaan, met veel inzet en zonder scrupules hebt meegewerkt aan een belangrijk deel van dit proefschrift. Je hebt gelijk gekregen: het werk aan 'Pink' en het 'AlF-complex' heeft twee prima hoofdstukken opgeleverd.

EPR is voor veel onderzoekers, en niet in de laatste plaats voor mij, een 'black box'. Wie die doos openmaakt ziet echter dat Fred Hagen erin zit. Fred, bedankt voor je uitleg, je grafieken en je andere bijdragen aan het EPR-hoofdstuk.

Colja Laane wil ik bedanken voor zijn interesse in mijn werk en voor het lezen en van commentaar voorzien van mijn artikelen. Hoewel je niet mijn promotor was, ben je als de nieuwe hoogleraar achter mij gaan staan. Bedankt voor die steun.

Dennis Dean, 'the Great Camel', thanks for your hospitality, advice and friendship. You showed me there's no harm in raising your middle finger to science from time to time, as long as you don't give up. Keep in touch.

Hans Wassink heeft een berg werk voor mij verzet; te veel om op te noemen. Hans, je hebt gelijk: het is dat NWO wil dat er ook promovendi worden aangesteld, maar zonder hen kun je het ook wel af. Bedankt voor je hulp. Marelle Boersma is onmisbaar geweest bij het microperoxidase werk en zowel bij mijn eerste stappen op het gebied van FPLC als SCUBA ben ik bij haar in goed gezelschap geweest. Ik hoop dat we snel weer eens onder kunnen duiken. Willy van den Berg kent alle kneepjes van de moleculaire biologie en beheerst absoluut de beste Freecell strategie van de vakgroep. Bedankt voor alle hulp bij het plakken en knippen van DNA. Wel wil ik me nog excuseren voor de oplossingen, spuiten, naalden, pennen, scharen, linealen, stiften, pipetten en rolletjes plakband die ik misschien wel wat al te vaak van je heb 'geleend'. Adrie Westphal, bij wie ik ook een afstudeervak heb gedaan, heeft aan het roer gestaan bij het navigeren in cyberspace. Adrie, bedankt voor alle online en offline hulp.

Gelukkig heb ik ook het gezelschap gehad van een aantal studenten die veel van het voor hen zo leerzame, saaie werk hebben gedaan. Dat zij bij ons een aftudeervak hebben willen doen bespoedigde het onderzoek en maakte het voor mij een stuk gezelliger. Wilfred IJkel, Bas van de Baan en Jos Schalk, bedankt dat jullie aan NifM hebben willen werken toen ik dat eiwit al aan de wilgen had gehangen. Ook Karel van der Heijden, die als 'nopper' de PPIase activiteit van het NifM eiwit heeft onderzocht, wil ik hier zeker niet onvermeld laten. Ik heb het laatste hoofdstuk voor een groot deel aan jouw inspanningen te danken.

Ik moet ergens stoppen, maar dat wil ik niet doen voordat ik Laura Ausma, Martin Bouwmans en Bery Sachteleben heb bedankt. Wie op de vakgroep Biochemie heeft gewerkt weet waarom.

Het ga jullie goed,

Johan Spee